Dissertation zur Erlangung des Doktorgrades

der Fakultät für Chemie und Pharmazie

der Ludwig-Maximilians-Universität München

Pathophysiology of α-synuclein Spreading Along the Nigrostriatal Dopaminergic Pathway and its Age-dependency

SUN, Fanfan

aus

Jiaozuo, Henan, China

2020

Erklärung

Diese Dissertation wurde im Sinne von § 7 der Promotionsordnung vom 28 November 2011 von Herrn Prof Dr Jochen Herms betreut und von Herrn Prof Dr Stylianos Michalakis von der Fakultät für Chemie und Pharmazie vertreten.

Eidesstattliche Versicherung

Diese Dissertation wurde eigenständig und ohne unerlaubte Hilfe erarbeitet.

München, 29.09.2020

SUN, Fanfan

.....

Dissertation eingereicht am 29.09.2020

1 Gutachter: Prof Dr Stylianos Michalakis

2 Gutachter: Prof Dr Jochen Herms

Mündliche Prüfung am 27.10.2020

Table of Contents

List of Abbreviation

3-OMD	3-O-methyldopa
6-OHDA	6-hydroxydopamine
aa	amino acid
AAVs	adeno-associated virus
AD	Alzheimer`s disease
ALS	amyotrophic lateral sclerosis
APOE	apolipoprotein E
APP	amyloid precursor protein
ATP	adenosine triphosphate
ATP13A2	ATPase cation transporting 13A2
Aβ	amyloid-beta
BAC	bacterial artificial chromosome
BBB	blood-brain barrier
BDNF	brain-derived neurotrophic factor
BMI	body-mass index
BSA	bovine serum albumin
CD200R	cell-surface transmembrane glycoprotein CD200 receptor
CD68	cluster differentiation 68
CNS	central nervous system
COMT	catechol-O-methyl transferase
CSF	cerebrospinal fluid
CSF1R	colony-stimulating factor 1
CX3CR1	C-X3-C motif chemokine receptor 1
DA	dopamine
DAT	dopamine transporter
DBS	deep brain stimulation
DDC	DOPA decarboxylase
DLB	dementia with Lewy bodies
DMEM	Dulbecco`s modified Eagle medium
DNA	deoxyribonucleic acid
DOPAL	3,4-Dihydroxyphenylacetaldehyde
DRs	dopamine receptors
ER	endoplasmic reticulum
FBS	fetal bovine serum
FUS	fused in sarcoma
GABA	gamma-aminobutyric acid
GAK	cyclin-G-associated kinase
GBA	glucosylceramidase beta
GCase	glucocerebrosidase
GCIs	glial cytoplasmic inclusions
GDNF	glial cell line-derived neurotrophic factor
GFP	green fluorescent protein
GI	gastrointestinal
GM1	gangliosidosis 1
GM-CSF	granulocyte-macrophage colony-stimulating factor

GPe	globus pallidus external segment
GPi	globus pallidus internal segment
GWAS	genome-wide association study
HLA-DR	human leukocyte antigen-DR
Hsp70	heat shock protein 70
IBA1	ionized calcium-binding adapter molecule 1
ICAM-1	intercellular adhesion molecule 1
IFN-γ	interferon γ
IFN-γ, - β	Interferon-γ, - β
IHC	immunohistochemistry
IL-1β, -3, -4, -6, -10,-12	interleukin-1β, -3, -4, -6, -10,-12
iNOS	inducible nitric oxide synthase
IRES	internal ribosomal entry sequence
LAG3	lymphocyte-activation gene 3
LAMP2A	lysosomal-associated membrane protein 2A
LBs	Lewy bodies
L-DOPA	L-dihydroxy-phenylalanine
LIMP2	lysosomal integral membrane protein 2
LNs	Lewy neurites
LPS	lipopolysaccharide
LRRK2	leucine-rich repeat kinase 2
MAO	monoamine oxidase
MAPT	microtubule-associated protein tau
MATs	monoamine transporters
MHCII	major histocompatibility complex II
MPP^+	1-methyl-4-phenylpyridinium ion
MPTP	1-methyl-4-phenyl-1,2,3,6-tetrahyopyridine
mRNA	messenger ribonucleic acid
MSA	multiple system atrophy
MSNs	medium spiny neurons
MyD88	myeloid differentiation primary response gene 88
NAc	nucleus accumbens
NAC	non-amyloid β component
NAT2	N-acetyltransferase 2
NFTs	neurofibrillary tangles
NO	nitric oxide
NSCs	neuronal stem cells
OB	olfactory bulb
PBR	peripheral benzodiazepine receptor
PBS	phosphate-buffered saline
PCR	polymerase chain reaction
PD	Parkinson`s disease
PDGF	platelet-derived growth factor
PET	positron emission tomography
PFA	paraformaldehyde
PFFs	pre-formed fibrils
PINK1	PTEN-induced kinase 1
Pitx3	pituitary homeobox 3

PPN	pedunculopontine nucleus
PrP^{c}	cellular prion protein
PrP^{sc}	scrapie isoform of the prion protein
PS1/2	presenilin 1/2
ROS	reactive oxygen species
siRNA	small interfering RNA
Sirp *alpha*	signal regulatory protein *alpha*
SNARE	soluble N-ethylmaleimide-sensitive factor attachment protein receptor
SNpc	substantia nigra pars compacta
SNpr	substantia nigra pars reticulata
SOD1	superoxide dismutase 1
STN	subthalamic nucleus
SV	synaptic vesicles
Syb2/VAMP2	synaptobrevin 2/vesicle associated membrane protein 2
TDP-43	TAR DNA binding protein 43
TFEB	transcription factor EB
TGF-β	transforming growth factor β
TH	tyrosine hydroxylase
TLR-1, -2, -4	toll-like receptor-1, -2, -4
TLR2	toll-like receptor 2
TM9SF2	transmembrane 9 superfamily member 2
TNF-α	tumour necrosis factor α
TNTs	tunneling nanotubes
Trem2	triggering receptor expressed on myeloid cells 2
TSPO	translocator protein (18kDa)
VMAT2	vesicular monoamine transporter 2
VP	ventral pallidum
VTA	ventral tegmental area

List of Figures

List of Tables

List of manuscripts

F. Sun, S. Filser, S. Blumenstock, C. Sgobio, J. Herms. α-synuclein spreading along the nigrostriatal dopaminergic pathway is age-dependent.

S. Blumenstock*, **F. Sun***, P. Marinković, P.M. Goltstein, C. Sgobio, S. Liebscher, J. Herms. Striatal seeding of protofibrillar alpha-synuclein causes cortical hyperreactivity in behaving mice. (*These authors contributed equally)

V. Korzhova, P. Marinković, P. M. Goltstein, **F. Sun**, J. Herms, S. Liebscher. Emergence and fate of aberrant neuronal activity revealed by *in vivo* imaging in awake Alzheimer`s disease transgenic mice.

Manuscripts in preparation

F. Sun, Y. Shi, F. Peters, M. Cui, C. Sgobio, J. Herms. Role of Trem2 dependent microglia in α-synuclein pathology spreading from striatum to cortex.

Y. Shi, **F. Sun**, M. Cui, K. Ochs, M.M. Dorostkar, J. Herms. Targeting translocator protein (18 kDa) alleviates alpha-synuclein-triggered dendritic spine pathology.

Y. Shi, **F. Sun**, F. Peters, K. Ochs. M. Cui, M.M. Dorostkar, M. Brendel, J. Herms. Microglial repopulation restores microglia responsivity in Alzheimer`s disease models.

Scientific poster presentations

F. Sun, C. Sgobio, J. Herms. "Age-dependent effect of chronic exposure of α-synuclein seeding on the nigrostriatal dopaminergic system". Alzheimer`s & Parkinson`s Diseases Congress- AD/PD ™, 2019, Lisbon, Portugal.

C. Sgobio, S. Blumenstock, **F. Sun**, L. Slapakova, M.M. Dorostkar, S. Liebscher, J. Herms. "Altered cortical neuronal activity induced by striatal seeding of prefibrillar alpha-synuclein coincides with reduced GAD67-positive cells in the somatosensory mouse cortex". Alzheimer`s & Parkinson`s Diseases Congress- AD/PD ™, 2019, Lisbon, Portugal.

C. Sgobio, S. Blumenstock, **F. Sun**, M.M. Dorostkar, J. Herms. "Striatal seeding of protofibrillar alpha-synuclein leads to neuronal hyperactivity and coincide with a reduction of GAD67-positive cells in the somatosensory mouse cortex". SfN annual meeting, 2017, Washington DC, USA.

Summary

Parkinson`s disease (PD) is the most common movement disorder that mainly affects the elderly population, featured by several typical motor symptoms due to degeneration of the midbrain neurons and subnormal level of dopamine in the striatum. The role of ageing in neurodegenerative diseases has greatly acknowledged in the last decades, whereas, it remains elusive how ageing contributes to the development of these diseases. In particular, a general mechanistic understanding of the relationship between ageing and PD is yet to be defined.

The α-synuclein protein is the main culprit in PD since one of the main pathology hallmark found in PD brains, the so-called Lewy bodies or Lewy neurites, are primarily consisted of aggregated α-synuclein. Physiologically, α-synuclein is a small, soluble protein and mainly located at the presynapse. Under pathological conditions, α-synuclein adopts an alternative β-sheets enriched conformation and further form into larger and condensed aggregates. Those aggregates are found in the cell soma as well as in proximal dendrites. Misfolded α-synuclein is thought to be a template that recruits endogenous α-synuclein to form pathology and spread throughout the nervous system. These pathological processes can further induce neuroinflammation, neurotransmission failure, oxidative stress and eventually axonal degeneration and cell death.

Studies have shown that the injection of α-synuclein pre-formed fibrils (PFFs) or other pathogenic α-synuclein containing materials into animal brains, also known as “seeding”, can trigger a spreading and LBs-like pathology. However, the age-dependent functional and morphological consequences of PFFs injection are still not investigated yet.

To seek for the underlying causes of PD pathogenesis and progression, I focus my study on the impact of age upon α-synuclein spreading, dopaminergic neurotransmission and neuroinflammation with two types of seeding models. The first model is mice injected with PFFs into the midbrain. I found that the electrically evoked *ex vivo* striatal dopamine release was significantly decreased in adult mice (5-month-old) after 2 months of PFFs

inoculation, but not before. While the dopamine release in young mice (2-month-old) was not affected at each detected time point. To understand why dopamine release was remarkably decreased in older mice, I firstly quantified the number of dopaminergic neurons in the SNpc. Stereological quantification revealed that the number of neuronal cells was not reduced. It suggests that the injection of PFFs into the SNpc rather affects the striatal dopamine release in the adult mice without loss of dopaminergic neurons.

To understand if the injection of PFFs affects the young and adult mice differently, I further analyzed the distribution pattern of α-synuclein aggregates in both SNpc and striatum of each age group. I found that young mice developed a much higher amount of aggregates in the SNpc compared to adult mice. Interestingly, the spreading of pathology from SNpc to striatum was significantly lower in the young mice compared to the adult mice. This suggests that the young mice are probably more efficient in converting misfolded α-synuclein into highly condensed aggregates in the midbrain with lower spreading potency, which restricts its propagation into the striatum.

To understand if the dopaminergic terminals in the striatum are affected by PFFs injection in SNpc, I quantified the volume covered by dopaminergic terminals in the striatum of each age group. I found that dopaminergic innervation tended to be decreased in the mice without evident alteration of dopamine release. While surprisingly, I did not observe a terminal reduction in adult mice with impaired dopamine release. To better understand the terminal alteration, I then analyzed the cumulative frequency distribution of the size of these terminals. Results showed that decreased dopaminergic innervation coincided with an increased proportion of smaller sized terminals. It suggests that the large terminals seem susceptible to the pathology and as compensation, new small terminals might be formed to preserve the normal function of dopamine release.

Considering that neuroinflammation might interfere with the alteration of dopaminergic terminals differently in young and adult mice, I further analyzed the volume covered by microglia in both SNpc and striatum of each age group. Results showed that the young

mice kept a higher microglial coverage in both SNpc and striatum consistently from 1 to 2 months after PFFs injection. However, the adult mice displayed a slightly increased microglial activation after 1 month but lost this property after 2 months of injection. Intriguingly, the observed age-dependent microglial activity coincided with the alteration of dopaminergic terminals and distribution pattern of the aggregates.

To further understand the role of microglia in α-synuclein pathology spreading, I applied another seeding model that displaying a more prominent spreading feature. After the injection of PFFs into dorsal striatum, mice were treated with a CSF1R inhibitor PLX5622 to eliminate microglia from the brain globally. After microglia depletion, α-synuclein pathology in the cortex was significantly enhanced compared to the control mice, which highlights the importance of microglia in the progression of α-synuclein pathology. To explore the potential mechanisms of microglia affecting α-synuclein spreading, I injected PFFs into the dorsal striatum of Trem2 KO mice. Trem2 plays an important role in the proliferation and phagocytic activity of microglia. Similar to the PLX5622 treatment, knock-out of Trem2 also led to a significantly higher amount of α-synuclein aggregates in the cortex. Taken together, it suggests an intriguing role of microglia in the spreading of α-synuclein pathology, probably through a Trem2 dependent manner.

In conclusion, the results of my current study provide new insights into the impact of ageing on α-synuclein spreading, dopaminergic neurotransmission and microglial activation that are linked to the progression of PD. Compared to the adult mice, in the brains of young mice the enhanced formation of aggregates, which reduces the diffusion of the seeding contents, seems to be more efficient and the further pathological propagation is restricted. The preserved striatal dopamine release in the young mice may be attributed to the enhanced microglial activation, probably through terminals pruning. Besides, loss of Trem2 in microglia significantly affects α-synuclein spreading, which supports the notion that microglia phagocytic capability is a critical factor in the pathophysiology of PD.

1. Introduction

1.1 Neurodegenerative diseases

Neurodegenerative diseases are chronic disorders characterized by progressive degeneration (or termed loss) of specific neuronal cell types in selective and distinct brain regions. The gradual loss of neurons alters the structure as well as the function of the brain. Pathological hallmarks of these diseases are defined by abnormal formation of protein-based aggregates. However, the constitution of such aggregates changes within these heterogeneous group of disorders, such as Alzheimer`s disease (AD), Parkinson`s disease (PD), amyotrophic lateral sclerosis (ALS), and up to date, none of these diseases is curable [1]. Among many factors, ageing is considered to be the most important risk factor [2]. However, the ageing population keeps increasing rapidly during the past decades owing to the improvement of the living quality, lifespan, the well-developed hygiene and medical care system, which prominently increase the prevalence of these age-dependent diseases. Nowadays, the clinical intervention is always limited due to the lack of efficient diagnostic tools, and the long term treatment also brings a high financial burden for the family and society as well as emotional stress on patients themselves. Therefore, it is of great importance to improve the diagnostic options and seek effective treatments, but more importantly, to understand the causes and mechanisms underlying each disease.

The onset of the neurodegenerative diseases is mostly sporadic, with only a small portion linking to a genetic aetiology. Both sporadic and familial cases present diverse forms of cognitive decline or behavioural changes, while at the pathological level, they share many features in common. Firstly, neuronal loss and dysfunction are chronic and progressive and usually associated with specific abnormal protein aggregations. Secondly, these diseases start to develop before the onset of clinical symptoms, affecting distinctive vulnerable brain regions [3]. At the molecular level, the disease-related proteins are associated with the pathological hallmarks according to different disease types as summarized in Table 1 [3-5].

Table 1. A brief overview of representative neurodegenerative diseases.

Disease	Key protein(s)	Main pathology	Affected region(s)	Related gene(s)
Alzheimer`s disease	β-amyloid Tau	Amyloid plaques Neurofibrillary tangles (NFTs)	Frontal lobes Basal forebrain Olfactory bulb Locus coeruleus	APP PS1 PS2
Parkinson`s disease	α-synuclein	Lewy bodies(LBs) Lewy neurites(LNs)	Substantial nigra Brainstem Striatum Amygdala Cerebral cortex Hippocampus	SNCA LRRK2 GBA PARK7 PRKN
Multiple system atrophy	α-synuclein	Glial cytoplasmic inclusions (GCIs)	Substantial nigra Putamen Cerebellum	SNCA
Amyotrophic lateral sclerosis	TDP-43 FUS SOD1	TDP-43 inclusions FUS inclusions Hyaline inclusions	Motor cortex Brainstem Spinal cord	TARDBP FUS SOD1
Creutzfeldt-Jakob disease	PrP^{sc}	Protease-resistant PrP^{e}	Cerebral cortex Thalamus Cerebellum	PRNP

1.2 Parkinson`s disease: a common α-synucleinopathy

1.2.1 Epidemiology and clinical symptoms

Parkinson`s disease is one of the most common neurodegenerative diseases second to Alzheimer`s disease as widely known [6]. The aetiology of PD consists of a mixture of factors, such as ageing, genetic risk factors as well as environmental aspects. As an age-related and chronically progressive disease, PD affects about 1% of all people over 60 years of age and is more commonly seen in men compared to women, with a male-to-

female ratio of 1.5 to 1 [7]. And about 90% of the PD cases are sporadic [6].

Motor deficits are the consequences of degeneration in the midbrain (Fig.1 A-B). By describing in the essay titled “An essay on the shaking palsy” in 1817, James Parkinson is the first author who described a series of six patients cases with a particular disorder [8] that included the clinical syndromes of bradykinesia (slowness of movement), akinesia (difficulty in initiating willed movements), rigidity (increased muscle tone), and tremors in hands and jaw. In addition to the motor symptoms, patients also suffer from a large spectrum of non-motor syndromes, such as behavioural changes, sensory abnormalities, autonomic dysfunction, sleep disturbances and even fatigue [9]. Besides, cognitive decline, which ranges from mild deficits to dementia (at end-stage), is another prominent non-motor symptom in PD [10]. A great number of patients suffer from cognition impairments as the disease develops. According to the autopsy series report, 80% of PD patients tend to develop dementia 20 years later after diagnosis [11]. Among PD patients, the mortality rate is approximately three times higher compared to healthy age-matched subjects [12].

1.2.2 Genetic and environmental risk factors

Genetic factors contribute to the aetiology of the familial PD cases, though take a tiny portion among the overall PD patients. As reported in 1997 by Polymeropoulos and co-workers that mutations in SNCA gene (which encodes α-synuclein protein) were identified, suggesting that even a single gene mutant is enough to present PD phenotype at the early onset [13]. Similar to SNCA, the locus property of leucine-rich repeat kinase 2 (LRRK2) is also pleiomorphic and autosomal dominant, and its genetic variants (like p.G2019S) are the major causes for the inherited PD cases [14]. The homozygous mutations of glucosylceramidase beta (GBA) gene have been primarily reported to cause the Gaucher`s disease. However, the heterozygous mutations of GBA are later confirmed to highly correlate to developing PD [15]. There are also some autosomal recessive genes relating to the early onset of PD, such as mutations in PARK2 (also termed Parkin, which

is responsible for nearly 50% recessive cases), PTEN-induced kinase 1 (PINK1), and DJ-1 [14]. Some other related risks factors of PD, including microtubule-associated protein tau (MAPT), cyclin-G-associated kinase (GAK), N-acetyltransferase 2 (NAT2) and apolipoprotein E (APOE), have also been identified by genome-wide association study (GWAS) or other functional assays [16-19].

Ageing may be the most significant risk factor for many neurodegenerative diseases like PD when the function of multiple organelles is compromised with age. For example, the mitochondrial DNA level in the SN neurons gradually decreases with age, which contributes to the dysfunction of mitochondria [20]. Declination of proteasome subunit expression can cause a deficiency in the proteasome system [21]. The efficacy of autophagy is also affected by ageing [22], leading to the uncompleted process of degradation and in turn, results in an increased level of protein accumulations. Moreover, the oxidative stress becomes even more active with age [23], as the nitration of tyrosine residues contribute to the formation of the abnormal α-synuclein protein that involves in PD [24]. Besides, environmental factors like long-term exposure to pesticides or other chemicals may raise the chance of PD onset. Additionally, a high intake of milk and dairy products is also thought to link PD [25]. Other potential risk factors are also listed, such as the traumatic brain injury, diabetes, cancer, body-mass index (BMI), hypotension, fat and alcohol [26], which indicate the importance to conduct a healthy lifestyle including physical exercises.

1.2.3 Pathological hallmarks

Most of the PD cases are sporadic (also called idiopathic), and the inherited cases are less than 10% [16, 27]. For sporadic forms of PD, a critical neuropathological hallmark is Lewy bodies (LBs) (Figure 1 C-E), which was first described as inclusion bodies seen in *paralysis agitans* (p.a.) by Fritz Heinrich Lewy in 1912 [28]. The inclusions are sized 5-25 μm with a dense granular core as well as the radiated filaments halo at the surrounding [29]. Such inclusions also occur in the axonal structures in the form of elongated fibrils,

called Lewy neurites (LNs), which are highly distributed in brain regions like the striatum and amygdala. LNs usually appear at the early stage during the disease progression [30, 31]. Nowadays, it is already known that these inclusions are primarily composed of abnormal aggregates of α-synuclein together with neurofilaments, ubiquitin and other proteins [32, 33]. By sharing the similar neuropathology basis of α-synuclein deposits in different brain-wide areas, PD, dementia with Lewy bodies (DLB) as well as multiple system atrophy (MSA) are generally categorized as α-synucleinopathies [34].

According to the hypothesis by Braak and co-workers, the development of pathology does not follow a random pattern but typically, the inclusions show up along the topographical range and are classified as a six-stage progression (Figure 1 F-G). From the theory, the aggregated depositions initially appear in the brainstem, olfactory bulb and the enteric nervous system, which are the regions that mostly relate to the early onset of PD before clinical symptoms [35]. As pathology develops, lesions form in the midbrain especially in SNpc and are highly related to the motor deficits. At last, the cortical areas are involved at the advanced stage with intracellular α-synuclein inclusions appearing in neurites and glial cells [36]. Whereas, from the gastrointestinal (GI) biopsies of PD patients, α-synuclein accumulates in the stomach, duodenum and the colon [37, 38], which suggests that the pathology probably originates even earlier in the GI tract before further spreading to the brain [39, 40] though the accurate pathway remains unclear. However, instead of a cause for the neurodegeneration, LBs might occur as a final form of the deposits containing cellular damage. Additionally, neuronal degeneration in PD can happen before the formation of LBs, and even present in the cells that are not dead [41].

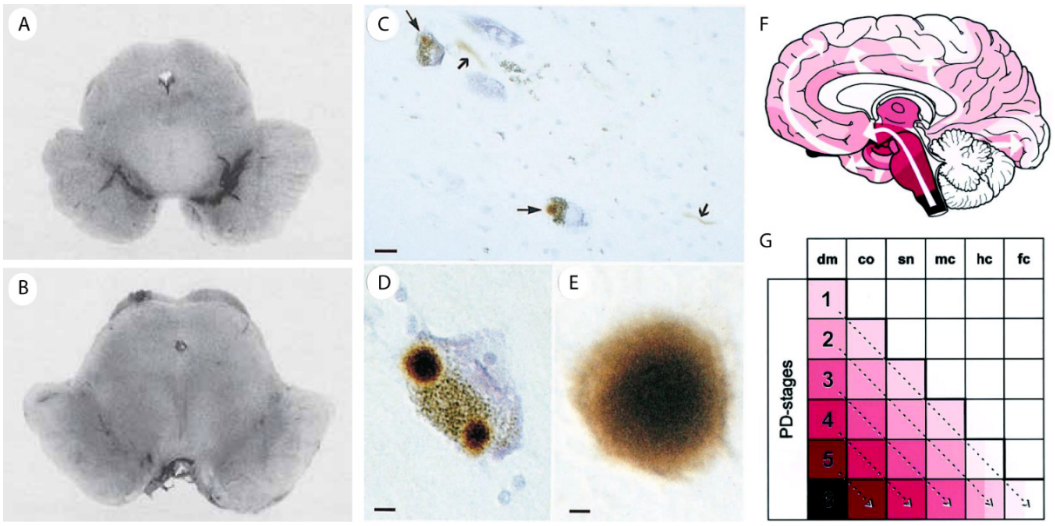

Figure 1. Brain features of Parkinson`s disease. A, the midbrain from a healthy subject with the normal level of pigmentation. **B**, the midbrain from a PD patient with a remarkable decrease of pigmentation in *substatntia nigra pars compacta* [7]. **C-E**, the immunostaining of α-synuclein in *substantial nigra* from PD patients [33]. **C**, α-synuclein positive LBs (long arrows) in the pigmented nerve cells and LNs (short arrows), scale bar 20 µm. **D**, two α-synuclein positive LBs in a pigmented nerve cell, scale bar 8 µm. **E**, an extracellular α-synuclein positive LB, scale bar 4 µm. **F-G**, the staging theory of sporadic PD from Braak [35]. dm, dorsal motor nucleus of the glossopharyngeal and vagal nerves; co, coeruleus-subcoeruleus complex; sn, *substantia nigra*; mc, anteromedial temporal mesocortex; hc, high order sensory association areas and prefrontal fields; fc, first order sensory association areas, premotor areas, primary sensory and motor fields.

1.2.4 Vulnerability of dopaminergic neurons and treatments

Though the pathology distributes and neurodegeneration appears in different brain regions, neurons in the SNpc (*substantia nigra pars compacta*) are the most vulnerable population in PD [42]. Neuronal loss in SNpc can reach a degree of 80% in the patients, which causes a dramatically decreased dopamine (DA) level in striatum and results in severe motor problems. Usually, neuronal loss in SNpc happens mainly in the ventrolateral and the caudal part [43], but the striatal nerve terminals loss seems much severer than the cell loss in SNpc [44].

Though not clearly known, one possible reason for the susceptibility of dopaminergic neurons in PD might be that the waste clearance system of these cells is not efficient enough. Also, mitochondria activity can be compromised due to the interaction with different forms of α-synuclein. As pointed out by Jim Surmeier and collaborators, the

most frequent types of cells that are affected by the inclusions, share similar features: the long and very branchy axons located plenty of synapses, and the constant calcium activity, which is very demanding in ATP production and consumption [45]. These features might partially explain the vulnerability of dopaminergic neurons in PD. Moreover, dopamine is another critical factor that leads to a specific weakness of neurons in SN. The combination of enhanced cytosolic calcium, α-synuclein accumulation, dopamine and its metabolites (like 3,4-Dihydroxyphenylacetaldehyde (DOPAL)) is toxic to the axonal terminals and dendrites [46, 47], which are lost at the early stage even before dopaminergic neuron loss in PD [48]. Pathological processes between neurons and other non-neuronal cells also play a vital role as the disease progresses. Increased gliosis has been observed in the post mortem brains of PD patients [49, 50], suggesting that the population of the microglial cells and astrocytes is dramatically increased at the late stage and most of them stay activated. As the immune cells in the central nervous system (CNS), these glial cells can either alter the morphology or produce inflammation-related cytokines or chemokines to modify the physiological processes as a response to the invasion of pathogens [51, 52]. Thus, exploring the function of glial cells and the relationship between neurons and non-neuronal cells is also very necessary to understand the pathogenesis of PD.

For quite a long time, neuroscientists thought that dopamine only acted as a metabolic precursor of norepinephrine in the brain [53]. It was until several years later that dopamine was identified as an essential neurotransmitter (which is awarded the 2000 Nobel Prize in Medicine) in the CNS according to the studies in 1957-1958 by Carlsson and co-workers [54, 55]. Later on, it was further reported in 1959 by his students Ake Bertler and Evald Rosengren that the bulk location of dopamine was presented in the striatum [56]. Based on this research, dopamine was later found to dramatically decrease in the caudate and putamen in the post-mortem brains of PD patients by Oleh Hornykiewicz and Herbert Ehringer [57, 58]. Then the therapeutic application of the dopamine precursor L-dihydroxy-phenylalanine (L-DOPA) started to develop in 1967.

Orally administration of high-dose L-DOPA in the clinical trial by George Cotzias [59] received wide attention, which is still used as an effective treatment at the early phase of PD today [60]. L-DOPA can cross the blood-brain barrier (BBB), though the cross rate is around 1% via orally delivery [61], it can still enhance the DA synthesis in the living dopaminergic neurons of the midbrain. But for long-term use, most patients suffer from several side effects, such as dyskinesia, which affect their life quality. There are also other therapies for improving the movement deficits in case of the resistance to pharmacological treatments. The deep brain stimulation (DBS) uses thin metal electrodes implantation in specific brain regions is able to alleviate some severe deficits of movement performance, which began from the 1980s and was approved by the Food and Drug Administration of U.S. in 2002. But DBS is still a very tricky tool since the structure and function in the neuronal network are complicated and there are also potential side effects of surgeries [62], especially on immunocompromised patients.

As newly reported, trials of therapy driven by viral vectors also shed light on PD treatment. For example, delivered by adeno-associated virus (AAV), glial cell line-derived neurotrophic factor (GDNF) or NRTN (neuturin, from the same family of GDNF) are driven by different promotors and overexpressed in the brain. These trials show beneficial effects in PD models either on the nigrostriatal system function or the behavioural performance [63-65]. Furthermore, the therapeutic trials that are targeting the protein aggregation process and the transportation of α-synuclein at the cellular level have been put on the stage as well [66].

1.2.5 Experimental animal models of PD

Animal models mimicking the diseases are the vital necessary and best tool to investigate the mechanism of disease pathogenesis and potential treatments. The currently available animal models either lack of pathological features or behavioural deficits, but they can be selected to satisfy the research purposes and answer the scientific questions without invalidating the results by its weakness part.

The first agent used in experimental rodents for modelling PD is the injection of 6-hydroxydopamine (6-OHDA) into SNpc, leads to the selective death of dopaminergic neurons within 24 hours. But this model fails to develop LBs inclusions chronically and sometimes also nonspecifically cause the death of other neuron types [67]. 1-methyl-4-phenyl-1,2,3,6-tetrahyopyridine (MPTP) is another widely used agent for modelling PD, through disrupting the energy system in mitochondria and kills a large number of dopaminergic neurons through ATP depletion [12, 29, 68]. However, the effect of MPTP is so strong and fast that the neurons die irreversibly within a few days. Meanwhile, the lack of LBs pathology—the classical PD hallmark—also limits the application of this toxin-based model [69, 70]. Similar to the MPTP model, rotenone injection induces neuronal degeneration in SNpc. Other phenotypes like the decreased level of tyrosine hydroxylase (TH) and dopamine transporter (DAT), LBs inclusions, and motor deficits are also shown after rotenone injection [71]. Whereas, the low rate (less than 50%) of successful duplication somehow limits its application.

Apart from agent-induced PD models, genetically modified models are also widely used. For example, the expression of mutant and normal α-synuclein in *Drosophila* [72] duplicates the LBs pathology and motor deficits ranging with age. For mutant α-synuclein overexpression model controlled by the TH promoter, the neuronal loss phenotype is rarely shown in the studies [73, 74]. Under the control of pituitary homeobox3 (Pitx3) promoter, mice specifically overexpress α-synuclein A53T in the dopaminergic neurons present remarkable neurodegeneration, motor dysfunction and decreased striatal DA release [75]. Mutations of LRRK2 or parkin in transgenic models are very limited due to the failure either in replicating neurodegeneration or displaying pathological inclusions and related behavioural impairments [76, 77]. There are also some transgenic mouse models overexpressing wild type human α-synuclein, driven by different promoters such as platelet-derived growth factor (PDGF) and Thy-1. These mouse models either display cytoplasmic and nuclear inclusions [78] or chronic motor dysfunction and LBs-like lesions out of SNpc [79], which are not the typical features of PD.

Application of viral vectors mediated overexpression of wild type or mutant α-synuclein in SNpc is also used in modelling PD, which displays a progressive cell loss of DA neurons, motor deficits, and pathological inclusions in striatal terminals or dendrites [80-82]. However, the viability in mice is still a challenge. As reported by several studies during the recent past years, a single injection of pre-formed fibrils (PFFs) of α-synuclein [83, 84] or other materials purified from patient brains [85], can trigger α-synuclein aggregation and conduct a cell-to-cell transmission of pathology throughout the brain. Besides, LBs pathology, progressive neurodegeneration in SNpc, altered DA level in the striatum and significant motor dysfunction have also seen after PFFs inoculation [83]. Furthermore, a combined injection of human α-synuclein PFFs and AAVs-mediated overexpression of human α-synuclein has also been reported. This model can speed up the pathogenic progression with LBs-like pathology, neuronal loss and sustainable neuroinflammation [86]. Considering that human PD cases progress gradually and chronically, animal models with accelerated pathology might not convey several pathological features as presented in human cases.

However, the viral or α-synuclein fibrils based injection models can avoid the high-cost demand of transgenic mouse lines breeding and the time-consuming lines crossing, and with the advantage of controlling the pathology spreading and aggregates formation by injecting materials specifically in the brain regions of interest [87]. In addition, seeding based animal models are very suitable for investigating the physiological mechanism of α-synuclein aggregation and spreading, which are the critical processes of disease initiation. Well-designed animal models can help to understand the mechanisms underlying diseases and the enlarged knowledge of disease pathogenesis, in turn, can contribute to the improvement of currently available animal models that getting closer to mimic the human condition and refine the test of possible treatments to tackle or cure the neurodegenerative diseases.

1.3 The nigrostriatal neurotransmission pathway

1.3.1 Neurotransmission: from substantial nigra to striatum

The *substantia nigra* (SN) is a midbrain structure located in the basal ganglia circuit, which consists of two different segments: the SNpc and SNpr (*substantia nigra pars reticulata*). The SNpc is densely packed with dopaminergic neurons, with the presence of local interneurons and fibres from afferent areas: subthalamic nucleus (STN), cerebral cortex, the superior colliculus, the pedunculopontine nucleus (PPN) [88], medium spiny neurons (MSNs) axons from striatal striosomes [89] and from SNpc itself. The SNpr is composed of dendrites of DA neurons from the SNpc, and it has a strong structural and functional resemblance of the globus pallidus internal segment (GPi). Dopaminergic neurons distribute in many regions throughout the CNS. Such as in the densest midbrain area, the retina, the olfactory bulb (OB) and the hypothalamus. Except for the SNpc cell group, there is another dopaminergic modulatory system in the midbrain. The ventral tegmental area (VTA) is close to SNpc, and they are also similar at the functional level. VTA projects the dopaminergic axons to the nucleus accumbens (NAc) that locating in the ventral striatum, and also innervates brain regions like the frontal cortex and other segments in the limbic system [7]. Dopaminergic neurons population in SNpc can decrease about 4% per decade during the normal ageing [43], but under disease conditions like PD, the decrease is dramatically reaching a 70% rate compared to the age-matched healthy subjects [90].

In dopaminergic neurons, the bio-synthesis of dopamine (Figure 2 A) is directly from tyrosine or indirectly from phenylalanine [91]. Briefly, together with other substances, tyrosine is converted into L-DOPA by the rate-limiting enzyme TH. After reacting with DOPA decarboxylase and pyridoxal phosphate, L-DOPA is further converted to dopamine [92]. Then, the “manufactured” dopamine is loaded into the synaptic vesicles through the “pick-up” process by vesicular monoamine transporter 2 (VMAT2), which provides an acid environment to keep dopamine in stabilization and avoids being oxidized [93]. Upon release to the synaptic cleft (or the extracellular space), dopamine can further bind to

the post-synaptic dopamine receptors (DRs) to promote or prevent an action potential from the postsynaptic neuron. After completing the transmission, dopamine is unbounded from the binding and recycled to the presynaptic neurons through the uptake process by DAT or monoamine transporters (MATs) locating on the pre-synapses [94] [95].

By binding to different striatal DRs that coupled with G-protein, dopamine exerts its facilitation or inhibition effects of signalling cascades via second messenger system to activate associated functions in the connected brain regions. Apart from the wide expression in the CNS, DRs also express in the peripheral system like in the blood vessels, retina, kidney and adrenals [96]. There are at least five subtypes of DRs: D1, D2, D3, D4 and D5. These dopamine receptors are generally divided into two main classes: the D1-like family (including D1 and D5) and the D2-like family (including D2, D3 and D4) [97]. In the CNS, D1-like receptors mostly distribute in the striatum, NAc, SNpr, OB, amygdala and the frontal cortex; the D2-like receptors mainly distribute in the regions like striatum, GP (the lateral part), NAc core, VTA, hypothalamus and hippocampus [98]. To the global level, the expression of D1 receptor is the most dominant throughout the brain. The expression level of D1 and D2 is 10-100 times outweighing the expression of D3, D4 and D5 subtypes [99].

The axonal projections that derive from SNpc neurons to the dorsal striatum are considered as nigrostriatal pathway (Figure 2 B-D), which is responsible for the movement performance and motivated behaviours since the tract goes through and reaches the dorsal domain of the basal ganglia [100]. There are many intrinsic pathways involve different brain structures within the basal ganglia. In general, there exist two distinct working pathways that process dopamine signals and send axonal collateral from the MSNs to the midbrain: the direct pathway and indirect pathway (Figure 2 D), which act as counterparts to each other and achieve a balance within basal ganglia circuits. The nigrostriatal dopaminergic pathway is an important functional network that modulating the direct and indirect pathway.

The direct pathway starts from the striatal MSNs that project inhibitory signals to the cells in GPi and SNpr. Like a relay, the GPi cells create inhibitory contacts to the thalamus cells [101]. When the GPi cells are firing, they inhibit the thalamus function and in this way, the thalamus cannot further excite the neocortex circuits. Thus, when the direct pathway gets excited, the final reactions after the two inhibitory effects on GPi and thalamus is the excitation of the motor cortex, which executes the necessary commands for movements [102]. The indirect pathway also starts in the striatum, but from another distinct group of cells that can inhibit the globus pallidus external segment (GPe), the GPe cells inhibit the activity of STN, which builds excitatory contacts to the GPi cell group. Therefore, when exciting the indirect pathway, the final result after these series of actions is the suppression of thalamocortical circuits that leads to the inhibition of the motor cortex. In a word, when the cortex activates the direct or indirect pathway (through cortico-striatal innervations), the results are further excited or being inhibited respectively, which emphasize that homeostasis of balance through the neural network requires every part of the region to contribute their proper function and regulation. Whereas, decreased level of dopamine leads to an imbalance between the direct and indirect pathway. The reduced activity in the direct pathway or the increased activity in the indirect pathway can result in decreased thalamocortical drive and parkinsonism problems [103].

The striatum is the main gateway structure of the basal ganglia that receives multiple inputs from many brain regions. In the striatum, MSNs population represent almost 95% (in rodents) of the total striatal neurons [104]. By projecting gamma-aminobutyric acid (GABA) transmitter, MSNs make inhibitory connections to the neighbour nucleus in the basal ganglia [105] and receive excitatory inputs from cortex and thalamus at the same time. Moreover, MSNs are also modulated by the dopaminergic inputs from the midbrain and the local striatal interneurons (GABAergic and cholinergic) [106]. The glutamatergic inputs from the cortex (or other areas like hippocampus, amygdala and thalamus) usually project onto the head of the dendritic spine of MSNs, and the

dopamine inputs from the SN create contacts onto the neck, allowing these inputs interact between each other and co-modulate the activity of MSNs [107]. MSNs in the dorsal striatum, receives the dopaminergic signal from the SNpc, with the effect of modulating the initiation of movements controlling the body, limbs and eyes. While, the MSNs in the ventral striatum receive dopamine signal from VTA and exert its effects on reward, motivation, and reinforcement of associative memories [108]. In the dorsal striatum, MSNs are subdivided into two types according to their projection cascades. MSNs in the direct pathway (dMSN) express D1 receptor and command the "go" action to initiate movements, the other type involved in the indirect pathway (iMSNs) express D2 receptor act as the "brake" to suppress movements. However, their projections do not completely differ from each other since some of the dMSNs also innervate their axons to the GPe or ventral pallidum (VP) [109]. Besides, the dorsal striatum is further subdivided into two areas: the dorsolateral and dorsomedial segments. The dorsolateral striatum is mainly involved in regulating the habitual behaviours and the dorsomedial striatum is more important in the goal-directed performance [110, 111].

In PD, the nigrostriatal pathway is the target of L-DOPA treatment, which directly boost the dopamine concentration. Besides, specific subtypes of DRs are also the targets of many other drugs since the functions of DRs and dopamine always go along with each other at the same time. The pharmacological interventions used in PD mainly aim to repair or enhance the dopamine signalling, which can restore the balance between the direct and indirect pathway and finally to alleviate the neurological symptoms of PD. Therefore, investigating the mechanism underlying impairments along the nigrostriatal pathway is of great importance to understand the pathophysiology of PD.

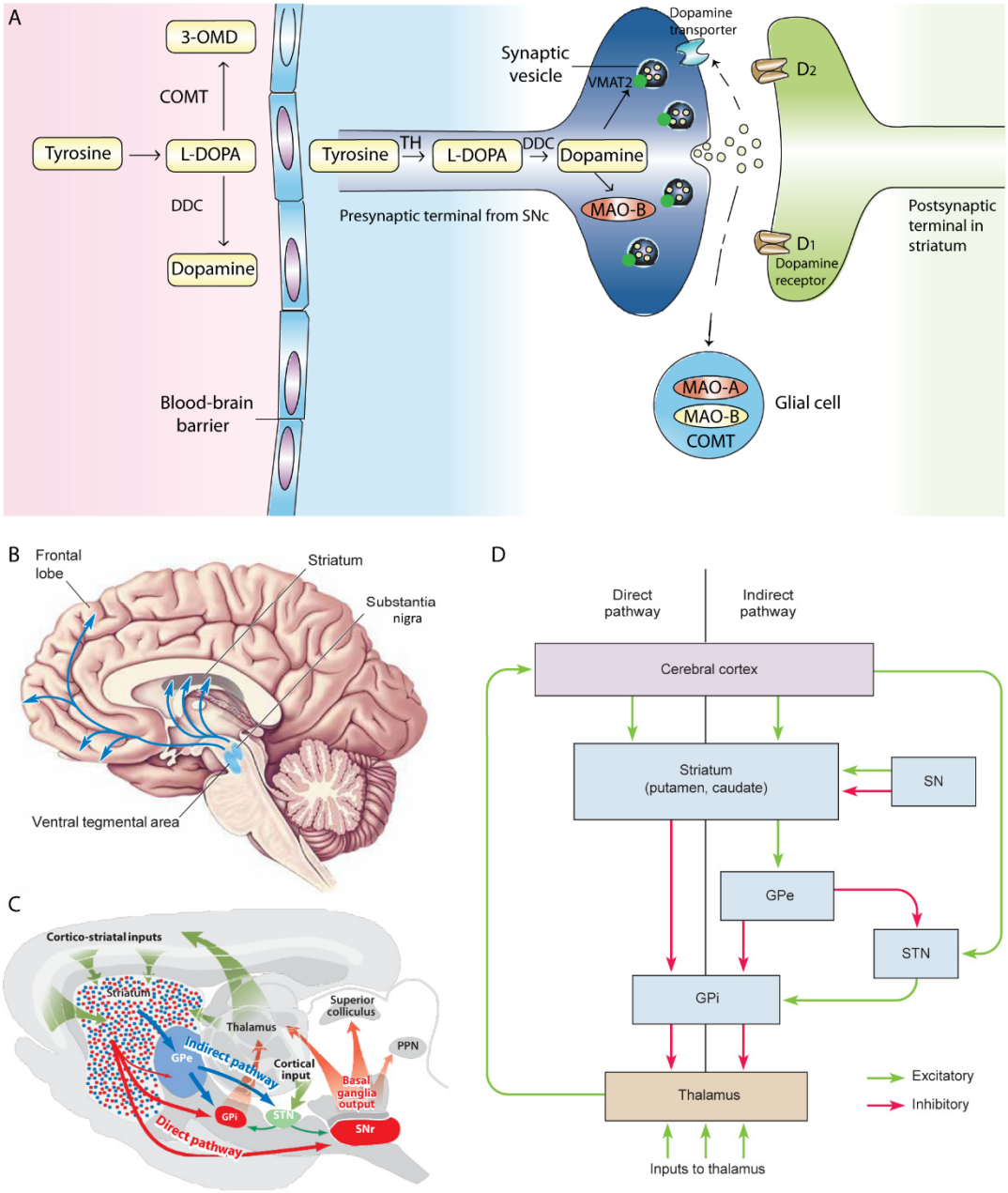

Figure 2. The dopamine system in basal ganglia circuits. A, a schematic diagram of dopamine metabolism (figure adapted from [112]). 3-OMD, 3-*O*-methyldopa; COMT, catechol-*O*-methyl transferase; DDC, DOPA decarboxylase; MAO, monoamine oxidase. **B**, the dopaminergic diffuse modulatory systems arising from the *substantia nigra* and ventral tegmental area, the former projects to the caudate nucleus and putamen (striatum), the latter to the limbic and frontal cortices [7]. **C**, the diagram of representative circuits in the mouse basal ganglia [106]. The striatum receives excitatory inputs from cortices and thalamus, the outputs in basal ganglia starts from the GPi and SNr directing to the thalamus, superior colliculus and PPN. **D**, an illustration of the direct and indirect pathways through the basal ganglia (figure adapted from [7]).

1.3.2 The pre-synaptic protein α-synuclein and dopamine release

Encoded by the SNCA gene, α-synuclein protein consists of 140 amino acid (aa) residues of 14-kDa, and is widely expressed throughout the CNS, especially in the brain regions like neocortex, hippocampus, OB, striatum, thalamus and the cerebellum in rodents [113]. α-synuclein is firstly isolated from the organ of electric ray (the Torpedo) and named according to its presence in the nuclear envelopes and the presynapse [114]. Following the discovery of α-synuclein, its homolog synuclein family members β-synuclein and γ-synuclein have also been identified [115, 116]. Under the normal physiological state, α-synuclein is mostly found in the cytoplasm and a slight amount in the nucleus, mitochondria and endoplasmic reticulum (ER) [117-119].

The amino acid sequence of α-synuclein is divided into 3 domains (Figure 3): the N-terminal domain (aa 1-95), the middle NAC (non-amyloid β component) domain (aa 61-95) and the least conserved C-terminal (aa 96-140) domain [120]. These three domains conformations endow the plasticity features to α-synuclein, which allows its binding to various ligands (like proteins and lipids) and functioning as chaperones [121]. The N-terminus is highly conserved and responsible for interacting with membranes. Moreover, the N-terminus also contains some mutations linked to PD, such as A53T, A30P, A53E and E46K, in addition, G51D and H50Q have also been identified to cluster with this terminal domain [13, 122-124]. The central NAC domain is related to the protein aggregation [125], which is prone to form α-synuclein filaments and trigger pathology [126, 127]. The C-terminus is highly acidic and amphipathic with an almost unfolded conformation [128], which is enriched with a compact monomeric structure that is aggregation resistant. It has also been reported that the C-terminus collaborates with the N-terminus to protect the NAC domain from aggregation [129, 130]. The C-terminus is believed to interact with proteins and modulate the binding property of α-synuclein with membranes. Moreover, post-translational modification of the C-terminal domain may affect the protein interactions. It can induce a tendency to aggregate, the aggregation process can be even more rapid than the full-length α-synuclein once the C-terminus is truncated [131-133].

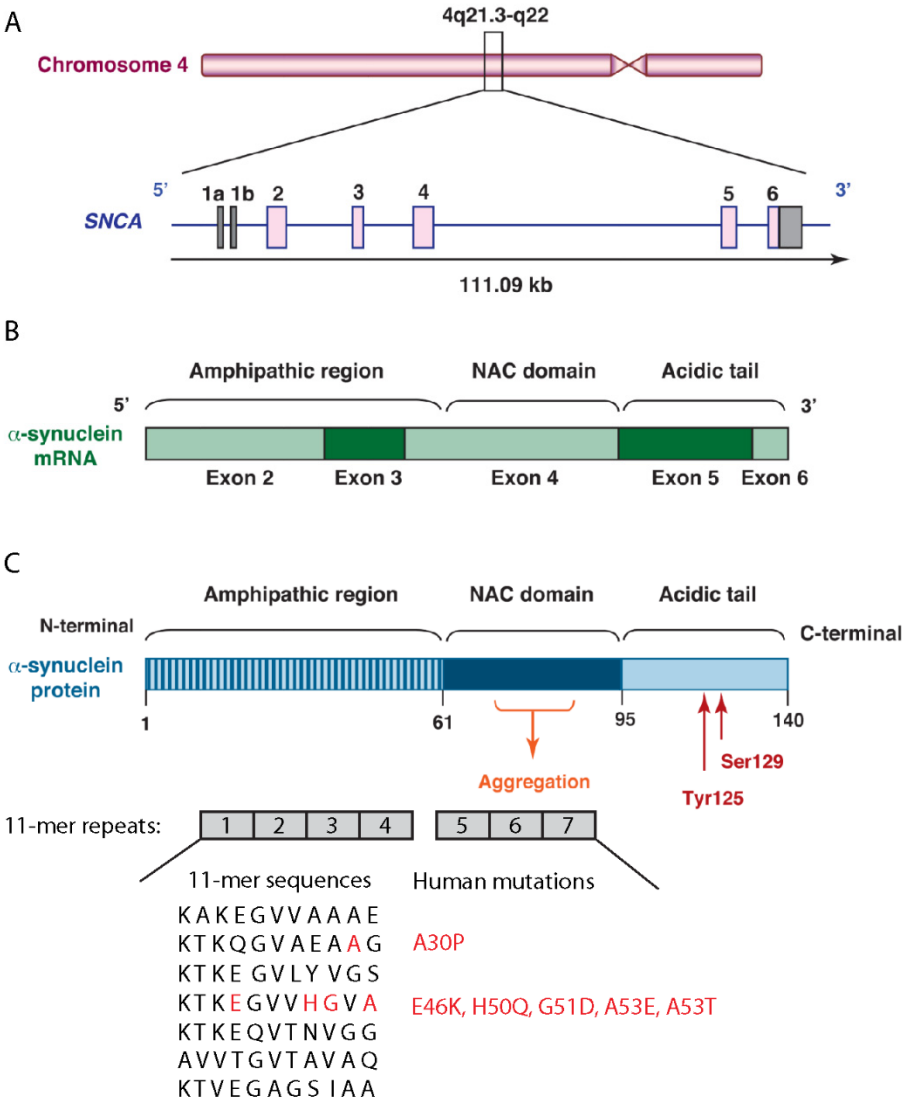

Figure 3. Diagram of α-synuclein gene and protein structure. **A**, the structure of SNCA gene. SNCA encodes α-synuclein, locates on chromosome 4q21.3-q22 and extends a domain of 111kb. **B**, the construction of α-synuclein mRNA. SNCA contains seven exons, five of them correspond to the coding regions. **C**, domains structure of the α-synuclein protein. This 140 amino acid sequence is divided into three distinct domain structures: the N-terminal is highly conserved and amphipathic; the hydrophobic NAC domain locates in the centre and is associated with the formation of fibrils; the C-terminal is acidic and mostly stay unfolded, phosphorylation at serine 129 increases the chance to fibrillation and phosphorylation at tyrosine 125 can prevent fibrillation. N-terminal and NAC domain contribute to the membrane binding, the lipid-binding domain can be divided into seven 11-mer repeats, mutations that are located in the second and fourth stretch link to the disease pathology. (adapted from [134] and [126])

α-synuclein can form an α-helix conformation when binding to the membranes [135], while the *in vitro* recombinant and purified forms are presented as unfolded native proteins [136]. As located mostly at the presynapse, α-synuclein is a very important regulatory factor in the presynaptic function by clustering with different components (Figure 4). Studies have shown that α-synuclein interacts with proteins that are involved in the transportation or fusion of synaptic vesicles (SV). α-synuclein also binds to soluble N-ethylmaleimide-sensitive factor attachment protein receptor (SNARE) complexes to maintain the homeostasis of neurotransmitters release [137, 138], which largely depends on its regulatory effect on the synaptic vesicle recycling. By interacting with the high-curvature membranes, such as the SV, the helix forms of α-synuclein can keep in stabilization [139]. According to the previous research, α-synuclein aggregates take part in the SNARE complex formation, which leads to the reduction of neurotransmitter release and dysfunction in the synapse possibly due to the problems in the docking and fusion of vesicles [137]. Whereas, under physiological condition, α-synuclein binds to the SNARE protein synaptobrevin 2/vesicle associated membrane protein 2 (Syb2/VAMP2) to promote the process of synaptic vesicle fusion [140]. Furthermore, in PD patients, the SNARE complex has been observed to change in the brains [141].

The dopamine signalling is found to be remarkably affected by α-synuclein through different pathways. Physiologically, α-synuclein can bind to DAT, which increases the level of DAT on the plasma membrane and facilitates the uptake of dopamine in the extracellular compart [142], while mutations of α-synuclein decrease this process [143]. Moreover, the α-synuclein-null mice present an impaired DAT function and a decreased level of DAT in the striatum [144, 145]. Upon α-synuclein depletion, the turnover of striatal dopamine uptake is reduced, the striatal dopamine level drops by about 36% and a reduced level of TH and DAT in the striatum [146], which coincides with the neuronal loss in SN [147, 148]. Besides, in the dopamine readily releasing pool, the vesicle refilling rate has been upregulated permanently due to the absence of α-synuclein [149]. Overexpression of α-synuclein inhibits the activity of VMAT2, which in turn leads to the

increased level of cytosolic dopamine that breaks its homeostasis. Whereas, knocking down α-synuclein increases the density of VMAT2 on the vesicles [150]. According to a recent study, mice expressing mutant α-synuclein suffer from degeneration in SN, and a remarkable loss of projecting synapses in the striatum with an elevated dopamine level [151, 152]. Moreover, α-synuclein can inhibit dopamine bio-synthesis process by suppressing the expression and the activity of TH, probably through a decreased phosphorylation effect on TH [153-155]. It has also been reported that with the growing of age, the expression of α-synuclein in SN is increased and the TH expression is decreased [156].

Taken together, dopamine signalling may have a high demand of α-synuclein to function as a regulator during neurotransmission, whereas, at the same time also being very sensitive to the dysfunction of this protein.

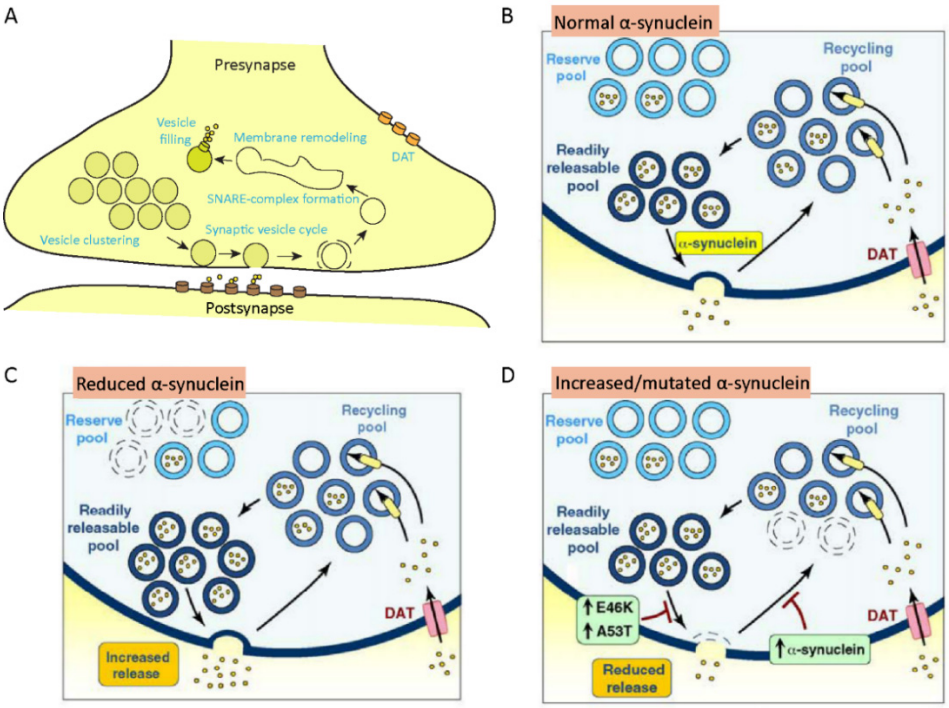

Figure 4. The function of α-synuclein at the synapse and its proposed role in presynaptic vesicle cycling regulation under different α-synuclein levels. **A**, the synaptic function of α-synuclein (adapted from [126]). **B-D**, the proposed role of α-synuclein in presynaptic vesicle cycling regulation (adapted from [134]). **B**, at the physiological level, α-synuclein takes a regulating role in different vesicle pools and in modifying vesicle docking and fusion. **C**, reduced level of α-synuclein down-regulates vesicles availability in reserve pool and promotes vesicles to release more. **D**, increased level or mutation of α-synuclein leads to the decreased vesicles release.

1.4 The misfolding and propagation of α-synuclein in PD

1.4.1 Disease-related forms of α-synuclein

In PD, α-synuclein is the major component of the pathogenic hallmarks LBs and LNs that containing the insoluble and fibrillary form of α-synuclein [157]. α-synuclein possesses the property to transform into different conformations from the physiological native form to the disease-related toxic species (Figure 5). The native monomeric species, including the monomer and tetramer (if it exists) [158, 159], help to shield the central NAC region from a spontaneous aggregation. The tetramer form has been reported to be mediated by the repeats KTKEGV [160], somehow is controversial since other studies doubted its existence [161, 162]. In general, the reported toxic species include the oligomers, fibrils and more condensed aggregates.

The aggregation process of α-synuclein has been intensively studied to clarify the neuronal loss or dysfunction related to toxic α-synuclein species. In the structure of intracellular inclusions, α-synuclein presents as fibrils that are enriched of large β-sheet conformation [33]. This formation process consists of many steps that including small oligomers, large compact oligomers and the proto-fibrils formation, termed nucleation [163, 164]. Following the nucleation, fibrils eventually form through a rapid consumption and addition of monomers, which is thought to be the potential mechanism of α-synuclein pathology spreading [165-167].

For the toxicity of oligomers or fibrils or other highly condensed conformations of α-synuclein (Figure 5), it is still debatable upon which conformation is more toxic. Several studies support the notion that the oligomers are more toxic. It has been observed from the transgenic mouse models and patients with PD that the level of α-synuclein oligomers increases compared to the controls [168]. The soluble oligomers of α-synuclein are thought to be the dominant toxic conformation in α-synucleinopathies though the accurate features need to be further investigated [169, 170]. Before forming the fibrils, oligomers can transform into more compact and stable oligomers that are resistant to proteinase K, and promote severe oxidative stress [171]. Moreover, PD

related mutations of α-synuclein (such as A53T and A30P) in mice increase the formation of oligomers instead of the fibrils [165, 170]. The oligomer toxicity also presents on its permeability through the cell membranes [172], which can form a pore-like conformation allowing the aberrant influx of ions, ultimately leads to the neurodegeneration [173].

Whereas, some other studies argue that the toxicity of α-synuclein fibrils is 1,000 times higher than the oligomers [174]. Early formation of oligomers and an accelerated level of α-synuclein fibrils have been observed under the mutations of A53T, A30P and E46K, which are related to the early-onset of PD [165, 175]. In α-synuclein PFFs injected mouse models, lysosomal fusion and autophagic cargo are impaired, but the formation of the autophagosome is not affected [176]. Moreover, striatal injection of PFFs into wild type mice can induce an abundant pathology in the cortex, impair the dendritic spine plasticity and lead to the cortical dendritic spine loss [177]. Besides, different resources or strains of α-synuclein also present different competent in toxicity and the ability to seed pathology. For example, α-synuclein materials collected from MSA cases are more toxic than that from PD cases in seeding pathology in rodents [178], and the properties of purified α-synuclein materials can be different even within MSA patients [179]. Strains from different species, such as deriving from human or mouse, can also interfere each other in the efficiency of seeding and spreading since they can be mitigated if the injected exogenous α-synuclein is not from the same species as expressed in the host [180, 181].

Factors that trigger the abnormal process can be diverse, like oxidative stress induced by reactive oxygen species (ROS), has been long thought to be a risk factor in PD pathogenesis [182]. The quantity of abnormally oxidized proteins accelerate with age [183] and make neurons more susceptible. Oxidatively modified proteins are more prone to aggregate [24]. Herbicides and pesticides are other factors that can induce α-synuclein misfolding and aggregation, which can damage lysosomes. This further leads to an increased level of ROS, which causes mitochondrial dysfunction and failure in autophagy

[184-187]. In PD patients, the maturation of autophagosomes is delayed, followed by the impairment of the autophagy function [188, 189]. This further alters the mitochondrial respiratory chain function, which eventually results in abnormally accumulated ROS, unstable calcium homeostasis and apoptosis [190, 191].

The abnormal α-synuclein can be processed in the cell through degradation within autophagy or proteasome systems [192, 193]. Autophagic degradation is determined by the activity of lysosomal enzymes. The mutant A53T or A30P of α-synuclein can suppress its degradation and prevent other substrates from being loaded into the lysosomes by tightly binding to the lysosomal-associated membrane protein 2A (LAMP2A) receptor [192]. Interestingly, dopamine can directly modify α-synuclein and further block the chaperone-mediated autophagy, which may partially explain the selective vulnerability of dopaminergic neurons in PD [194]. When the degradation function is impaired, the aberrant proteins can be deposited within the cytosol or released into the extracellular milieu through different pathways. The release of aberrant forms of α-synuclein into the extracellular space can be further promoted by the dysfunction of clearance [195], which contributes to the spreading of α-synuclein pathology throughout the brain.

Given that α-synuclein plays a crucial role in the progression of PD, treatments targeting α-synuclein have been intensively investigated. It has been reported that application of small interfering RNA (siRNA) targeting the mRNA of α-synuclein to reduce its synthesis, does indeed reduce the level of α-synuclein in the hippocampus and the cortex [196]. The aggregation in SNpc is decreased in mice expressing human α-synuclein by an injection of siRNA-containing exosomes [197]. Overexpressing lysosomal transcription factor EB (TFEB) in rat expressing α-synuclein can promote protein degradation, reduce the level of α-synuclein oligomers and prevent lysosomal dysfunction and neurodegeneration [198]. Besides, upregulating the expression of lysosomal proteins, such as lysosomal integral membrane protein 2 (LIMP2) and ATPase cation transporting 13A2 (ATP13A2), also accelerates the degradation of α-synuclein [199-201]. Binding and stabilizing α-synuclein to the vesicle structures is another treatment trial to reduce its

aggregation and misfolding [202]. Other antibodies that are against the C-terminal truncated α-synuclein or monoclonal α-synuclein antibodies can prevent protein propagation and rescue the motor deficits in the rodent models [203, 204]. However, further studies are still needed to understand the α-synuclein pathological process and seek for possible treatments for clinical therapy.

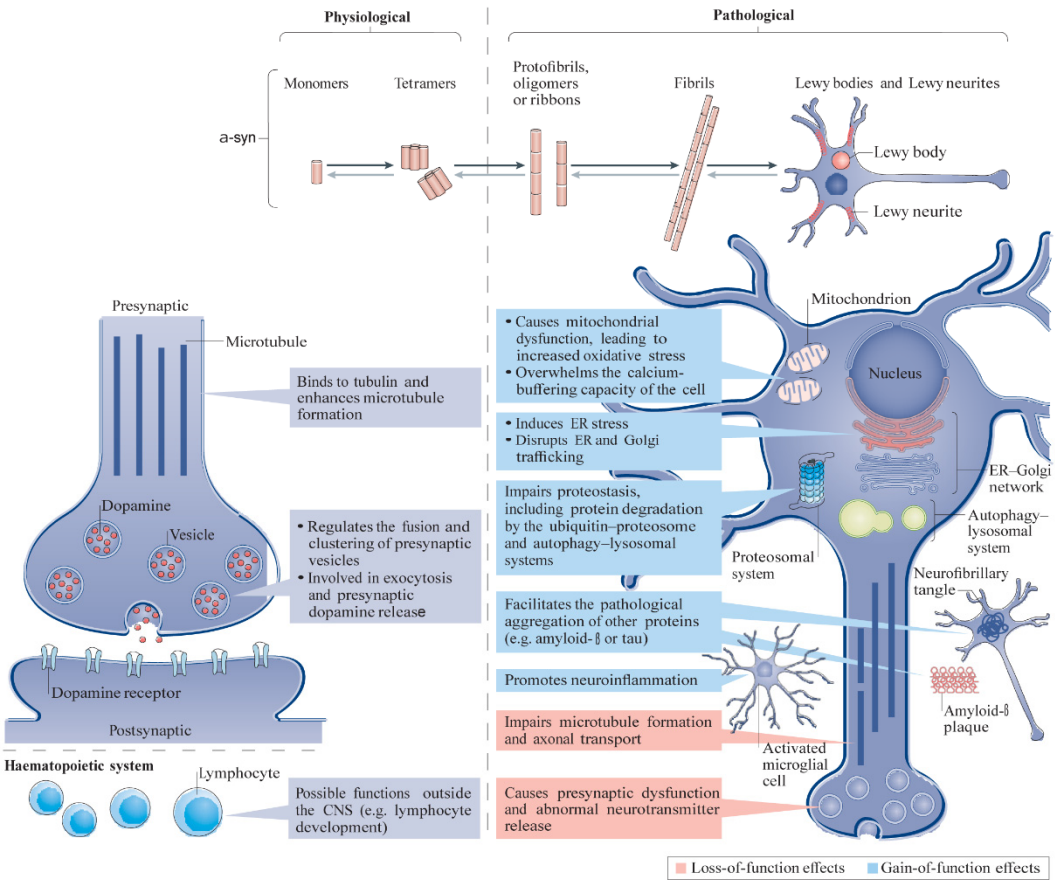

Figure 5. Proposed roles of α-synuclein and its disease-related forms in physiological and pathological processes. The function of α-synuclein depends on its different forms. At physiological level, the monomeric and tetrameric (if exists) forms are thought to be the native state of α-synuclein that regulating the fusion and clustering of presynaptic vesicles, participating in exocytosis and presynaptic dopamine release, binding to tubulin and enhancing microtubule formation. The proposed pathological forms of α-synuclein, like oligomers, protofibrils, ribbons and fibrils, are toxic and cause deficits in neurotransmission and microtubule formation to the loss-of-function level; to the gain-of-function toxic level, they can cause damage to mitochondria and proteostasis process, induce ER stress, neuroinflammation and promote the aggregation of other proteins. (adapted from [205])

1.4.2 Spreading: how α-synuclein pathology develops in the brain

The cellular transmission of α-synuclein was initially described in autopsy tissue from two PD patients, LBs pathology was developed in grafted fetal nigral cells more than a decade after the transplantation procedure [206, 207]. Followed by the initial discovery, the cell to cell pathological α-synuclein transmission was also observed in cell culture and the *in vivo* animal models [208]. The inoculation of exogenous human α-synuclein fibrils in the human cell lines and mouse brains can recruit endogenous α-synuclein to misfold and aggregate into LBs-like structure [209, 210]. The *in vivo* studies by Luk *et al*. have reported that a single injection of mouse α-synuclein fibrils into the striatum of non-transgenic mice cause LBs-like pathology, remarkable neuronal loss in SN and PD-like symptoms [83]. Furthermore, fibrils injection into the OB also causes a progressive LBs-like pathology [211]. Apart from the direct inoculation in the brain, intramuscular injection of α-synuclein materials can cause LBs-like pathology [212], which suggests an efficient penetration of α-synuclein species across the BBB [174]. Besides, the introduction of human LBs enriched fractions into the macaque monkeys and mouse brains can also induce PD-like pathology [213].

Pathological α-synuclein has been reported to be transported to the healthy cells following a prion-like mechanism. During the transmission process, α-synuclein can be released into the extracellular space and taken up by the neighbour cells to contribute to its spreading. However, the accurate routes of α-synuclein secretion and uptake are not yet completely clarified. From several *in vitro* studies, PFFs are transported in both the anterograde and retrograde directions [210, 214]. α-synuclein oligomers that are secreted from the terminals of neuronal cells into the extracellular space can be taken up through retrograde axonal transport to the surrounding cells [215]. Among different conformations of α-synuclein like oligomers, ribbons and fibrils, the *in vivo* inoculation of oligomers presents the most dominant and efficient effect of spreading [174].

Several pathways have been reported to participate in the release and uptake of α-synuclein conformations (Figure 6). For example, the ATP13A2 expression dependent

exosomes [216, 217], clathrin- or lymphocyte-activation gene 3 (LAG3)-mediated endocytosis [218, 219] and tunneling nanotubes (TNTs)-dependent lysosomal vesicles [220].

Exosomes can be released from cells into the extracellular space. This process helps to promote intercellular communication through conveying and sending around specific proteins or RNAs [221-223], which is probably involved in the α-synuclein spreading. Aberrant α-synuclein that contained in the exosomes is more toxic and easy to be taken up by the grafted cells compared to the freely existing α-synuclein oligomers [193, 195, 224]. At the same time, calcium activity also contributes to the increase of exosomal release. According to several *in vitro* studies, clathrin-mediated endocytosis has been found to present in neurons, microglia and oligodendrocytes. Whereas, inhibiting this pathway did not help to completely block the entry of α-synuclein [208, 225, 226]. The leukocyte immunoglobulin protein LAG3 is located on the surface of neurons, which seems to be a specific binding site for α-synuclein since LAG3 helps the fibrillary α-synuclein enter the cell through clathrin-mediated endocytosis [219]. Considering that the endosomes send molecules to lysosomes for degradation, endocytosis of α-synuclein oligomers might contribute to the failure of lysosomal degradation as well. Another specific endocytosis pathway for taking up α-synuclein is phagocytosis, which is an important function of macrophages and microglia. Besides, transport by TNTs is another way for the intercellular spread and transfer of α-synuclein [220]. TNTs contain actin that is interacting with membrane and form protrusions-like bridges, which can last up to hours between cells [227, 228]. The activity of TNTs promotes intercellular communication and the exchange of molecules and organelles [229]. Moreover, TNTs have been found to exist not only between neurons and between astrocytes themselves but also between neurons and astrocytes [230, 231]. It indicates that the usage of TNTs for intercellular information exchange is not only exclusively limited within the same cell type but also between different cell types [232]. Neurons and glial cells are supposed to exchange contents like molecules, exosomes and mitochondria through TNTs [233],

which suggests a possibility of α-synuclein pathology spreading among different cell types in the CNS. Additionally, the interplay of different proteins may also take part in the pathology spreading. For example, the cellular prion protein (PrP^c) has been reported to help internalize α-synuclein fibrils into the cells by enhancing the activity of endocytosis, while less α-synuclein aggregates can be found in mice without PrP^c expression [234].

However, there are still many questions that are needed to be addressed to understand the mechanisms of the pathological α-synuclein spreading. Among many factors, the role of ageing is still not clearly understood in the formation of pathological α-synuclein and its consequences in brain function.

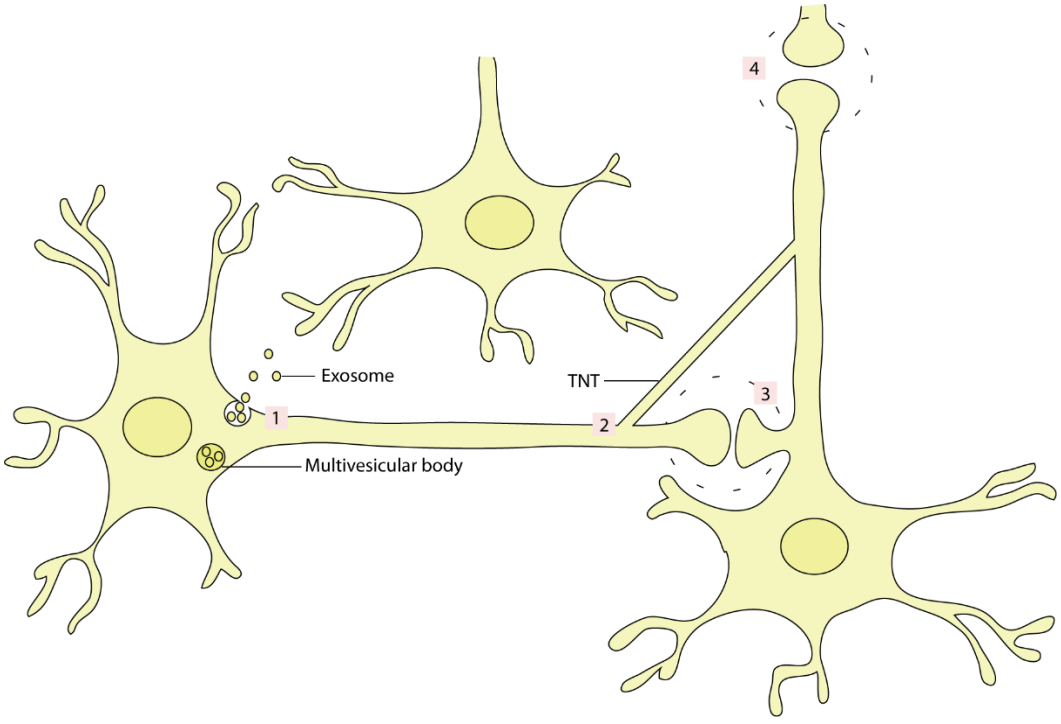

Figure 6. Possible modes of cell-to-cell proteins transfer between neurons. In the diagram, there are two synapse-connected neurons and one separate neuron. Protein like α-synuclein can be released by a small vesicle called exosome (mode 1) as well as the TNTs (mode 2). Exosomes can travel across synapses or even further, to promote the protein transfer to other cell types. TNTs can also trigger communication between different cell types in a long-distance range. As α-synuclein presents at presynapse, it is possible to be released and taken up at the synapse (mode 3) during neurotransmission. Little is known about the possible pathway (mode 4) that proteins are released as a secondary effect of synaptic or cellular compromise. (adapted from [235])

1.5 Neuroinflammation in Parkinson`s disease

1.5.1 Microglia: in rest and activation states

Microglia are the principal immune cells in the CNS and take a crucial role in brain development, maintaining a balance of the neuronal environment, responding to injury and contributing to the tissue repair [236]. The first description as microglia was in 1919, by a Spanish researcher Pio del Rio-Hortega, who also discovered the other glial cell types like astrocytes and oligodendrocytes [237] (Figure 7). In the last two decades, the knowledge of microglia functions (Figure 8) has grown exponentially. Microglia originate from the primitive yolk sac myeloid progenitors that actively seed the brain parenchyma during mid-embryonic development [238, 239]. In the brain parenchyma, microglia take a portion of 10-15% out of the total glial population [240] and present heterogeneity in the morphology across different brain regions [241]. As immune-like cells, microglia become highly mobile once activated [242]. Moreover, microglia can migrate to a focal lesion spot [243], secrete different cytokines as immune response and clear away the pathogens, dying cells, debris as well as abnormal proteins to maintain the innate immune homeostasis environment [244-246]. Microglia can also release neurotrophic factors like brain-derived neurotrophic factor (BDNF) and GDNF, which are vital molecules for neuronal viability [247].

Under physiological condition, microglia stay resting and survey for detrimental changes, this relatively quiescent mode is maintained by several factors. For example, triggering receptor expressed on myeloid cells 2 (Trem2), signal regulatory protein *alpha* (Sirp *alpha*), the C-X3-C motif chemokine receptor 1 (CX3CR1), colony-stimulating factor 1 (CSF1R) and cell-surface transmembrane glycoprotein CD200 receptor (CD200R) [248, 249]. Especially, apart from its strong link in AD, Trem2 is a newly identified risk factor for PD, as its rare missense mutation p.R47H does enhance the susceptibility for the disease [250]. Trem2 is specifically expressed in microglia, acts as a modulator for microglial activation and plays a very important role in microglial phagocytosis function, proliferation and survival [251-254]. Suppressing the expression of Trem2 leads to

microglia activation shifting from the anti-inflammatory state into a pro-inflammatory phenotype [255]. The overexpression of Trem2 in MPTP induced PD mouse model can remarkably prevent dopaminergic neuron loss and neuroinflammation [256]. Another newly reported study suggested that knock-down of Trem2 increases the α-synuclein aggregates induced inflammation and a higher level of neuronal apoptosis *in vitro*, and the knock-out of Trem2 promotes neurodegeneration as well as the microglial inflammatory phenotype [257].

Being activated by different stimuli, microglia can present in different states: the M1 and M2 phenotypes. Generally, the M1 phenotype of activated microglia can be induced by lipopolysaccharide (LPS) or interferon γ (IFN-γ). The M1 phenotype can produce pro-inflammatory cytokines like tumour necrosis factor α (TNF-α), interleukin-1β (IL-1β), IL-6 and IL-12. Besides, cytotoxic molecules like superoxide, NO productions and ROS can also be secreted by M1 phenotype, which enhance the pro-inflammatory effects during injuries and infections [258-262]. Whereas, M2 phenotype exerts an anti-inflammatory and neuroprotective effect [263], by producing IL-4, IL-13, IL-10 and transforming growth factor β (TGF-β) to improve tissue repair.

Microglia activation has been shown in the post-mortem brains of patients with PD as early as reported by McGeer *et al*.[49], since then plenty of studies reported over-activated microglia, termed microgliosis in PD animal models [264, 265]. In PD brains, the long-lasting microglial activation is correlated with increased expression of many cytokines including TNF-α, IL-1β, IL-6 and IFN-γ. And these pro-inflammatory factors are partially responsible for a progressive degeneration of dopaminergic neurons [266, 267]. The application of positron emission tomography (PET) has further been confirmed microglial activation *in vivo*. In brain regions like the midbrain, putamen, pons and cortex in patients with PD, DLB and MSA, α-synuclein deposition and neurodegeneration have been found to coincide with increased microglial activation [268-271]. The extent of microglial activation can be different depending on different disease types. For example, the inflammation response is much more widespread in MSA compared to PD cases

[272], regions that are affected by microgliosis are different in DLB and AD [273].

Despite many factors that link to PD pathogenesis, intense attention has been taken to the factors of microglia and neuroinflammation, which are supposed to play a regulatory role in the progression of disease [274, 275]. Evidences also have shown that the regular intake of anti-inflammatory medicines like ibuprofen is associated with a lower risk of PD onset [276, 277]. Dopaminergic neurons as the most vulnerable cells population in PD are susceptible under the inflammatory condition no matter if in the *in vivo* animal models or *in vitro* cell culture [278, 279], and the inflammatory response can be induced by microglia activation [280]. Besides, the enhanced activity of microglia in SN of early PD is in correlation with a loss of dopaminergic terminals and the severity state of the disease [269, 281]. Nevertheless, detrimental factors released by the dying dopaminergic neurons can promote the activation of microglia and this overreaction, in turn, exacerbates the neurodegeneration [282, 283]. However, some studies hold the view that removing microglia is beneficial [284]. For example, elimination of microglia by a CSF1R inhibitor PLX5622 can block the interaction between microglia and amyloid plaques. It increases cognition in AD mice, without changing behaviour and memory performance in controls [285].

Activation of microglia is a complicated process and is specifically dependent on the biological substrates. Thus, more detailed studies are still needed to clarify its role in the progression of PD.

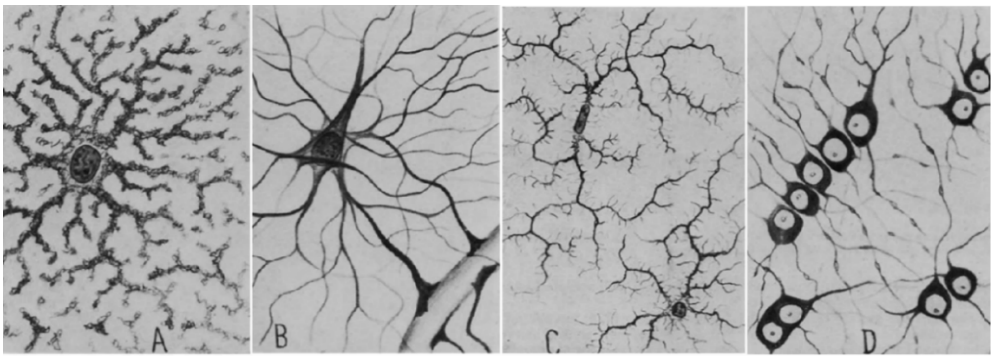

Figure 7. Del Rio-Hortega`s four types of glia (from [286]). **A**, gray matter protoplasmic neuroglia. **B**, white matter fibrous type neuroglia. **C**, microglia. **D**, white matter interfascicular glia (oligodendrocytes).

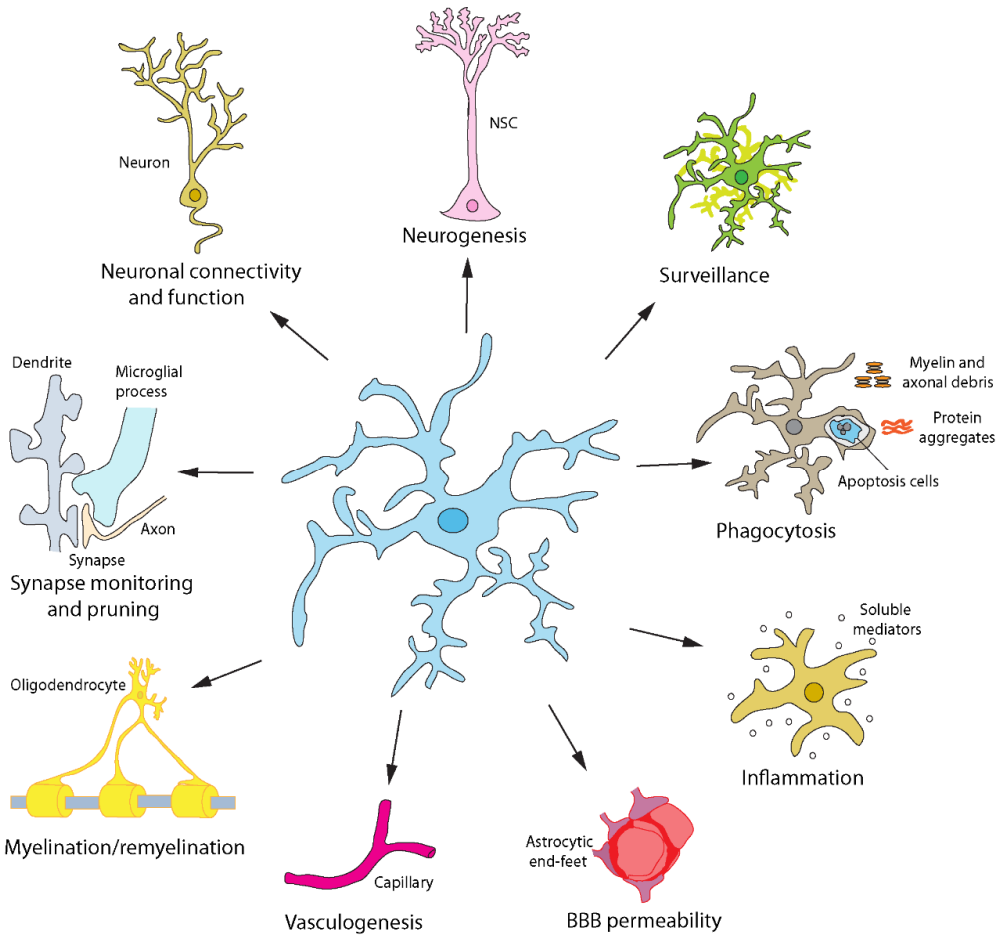

Figure 8. Main functions of microglia. At rest state, microglia is responsible for surveillance. Under the pathological condition, microglia are activated and in the immune state, such as phagocytose of apoptotic cells, myelin and axonal debris, and protein aggregates. To the synapse level, microglia can take actions in monitoring and pruning. Microglia are also able to interact with other cell types in the brain: take part in the neuronal connectivity and function, communicate with neural stem cells (NSCs) and neurogenesis, interact with oligodendrocyte for myelination and remyelination, as well as contribute to the permeability of BBB and vasculogenesis. (adapted from [237])

1.5.2 Interaction between microglia and α-synuclein in PD

The morphology of microglia in PD is supposed to be diverse depending on the disease conditions and is responsible for different functions (Figure 9). Among many factors that induce microglial activation, the interaction between α-synuclein and microglia is intriguing and of great importance to understand the disease pathogenesis and pathophysiology in PD.

Activated microglia have been found to be the most abundant when exposed to fibrillary

α-synuclein [174]. Extracellular LBs and other α-synuclein immuno-reactive aggregates are always accompanied by activated microglia [49]. Injection of α-synuclein monomers or oligomers into SN can induce microgliosis, which suggests that α-synuclein can be the direct stimuli to activate microglia and cause neuroinflammation [287, 288]. LPS injection in the wild type mice and A53T mutation overexpression transgenic mice can also induce acute inflammation. Whereas, the long-lasting neuroinflammation only displays in the transgenic mice after LPS injection. Meanwhile, the progressive degeneration along the nigrostriatal pathway, aggregated α-synuclein and LBs pathology have also been seen in this model [289]. Besides, the extracellular α-synuclein, no matter aggregated or the soluble form can stimulate the phagocytosis state of microglia [290].

Though microglial activation has been observed in various animal models related to α-synuclein toxicity [291-294], the basic mechanism is not completely clear yet. As a vital regulatory factor in immune response, depletion of major histocompatibility complex II (MHCII) has been reported to suppress microglial activation with reduced neurodegeneration [295]. Extracellular α-synuclein is thought to be the endogenous agonist for Toll-like receptor 2 (TLR2) to induce the activation of microglia [296]. Moreover, α-synuclein oligomers are supposed to bind to the heterodimer TLR1/2 on the cellular membrane and induce a myeloid differentiation primary response gene 88 (MyD88)-dependent pro-inflammatory response [297]. The depletion of TLR4 leads to the abnormal clearance activity of microglia in processing recombinant or overexpressed α-synuclein both *in vivo* and *in vitro*, with an aggressive neuronal degeneration [298, 299]. It has also been reported that α-synuclein can act as a chemoattractant to enhance the migration of microglia [300]. Furthermore, α-synuclein-induced microglial pro-inflammatory responses might be mediated by microRNA-155 [301]. In PD cases, the macrophage marker cluster differentiation 68 (CD68), which is expressed by phagocytic microglia, has been found to link to the duration of the disease. Besides, CD68 has a remarkable correlation with the expression level of MHCII and α-synuclein deposition in SN [302].

α-synuclein has been reported to enter microglia by promoting endocytosis activity and micropinocytosis, probably through binding to the ganglioside and gangliosidosis 1 (GM1) dependent lipid rafts [303-305]. TNTs can be another possible way to transfer abnormal α-synuclein into microglia. Macrophages have been reported to exchange materials with neighbour cells and clear bacterial species through TNTs pathway [306, 307]. Given that microglia and macrophages are similar at the functional level and TNTs exchange pathway exists in the neuron to neuron transfer of α-synuclein, it is possible that neurons can transfer α-synuclein to microglia through TNTs activity. According to an *in vitro* study, microglia can take up exosomes that containing α-synuclein through micropinocytosis but fail to completely degrade the fibrillary α-synuclein [308]. The failure of microglial degradation is usually due to the dysfunction in the lysosomal pathway. In both familial and sporadic PD cases, an impaired lysosomal function has been observed in the neurons [195, 309]. However, among neurons, microglia and astrocytes, microglia exert the most efficient effects on clearing the extracellular α-synuclein [310]. Besides, the degradation of α-synuclein depends on microglial activation phenotype and the conformation of α-synuclein [290, 310], though the clear mechanism is not known yet. Thus, the interaction between microglia and α-synuclein is still an interesting topic to understand the pathogenesis of PD.

Considering that the majority population of patients with PD are aged people, senescence itself is already a problematic factor regarding the activity of cells. The normal ageing is featured with slowly accumulated metabolic elements and slightly chronic sterile inflammation with undetectable microorganism pathogen [311, 312]. With senescence, microglia suffer from morphology alteration, decreased activity in phagocytosis and a slight increase of pro-inflammatory reaction [313, 314]. Their morphology in the dystrophic state is featured with de-ramified, spheroid conformation, short and twist cytoplasmic as well as fragmented processes [315]. Compared to the young mice, microglia isolated from the adult mice present several detrimental features. For example, the impaired phagocytosis of exosome-dependent or free-mobile α-

synuclein oligomers and an enhanced secretion level of pro-inflammatory factors [316]. Moreover, the total number of microglia is also decreased with age [317]. The expression of MHCII and IL-1 have been reported to increase in the normally senescent microglia [318, 319]. Due to its senescence limitation, age-related alterations of microglia are very likely to account for a role in the disease progression. Therefore, investigating the relationship among pathology spreading, neuroinflammation related microglial activation and functional alterations is very important to understand the pathogenesis of PD and might also help to establish reliable treatments.

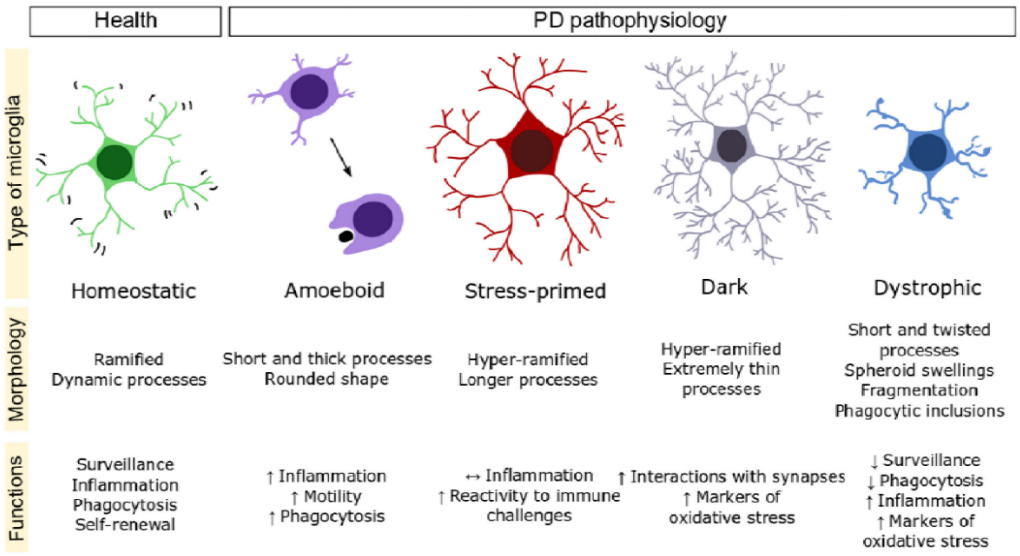

Figure 9. Different microglia phenotypes in Parkinson`s diseases. Demonstration and description of different microglia phenotypes, morphology and their corresponding functions. In the diagram, arrowhead-up symbols mean increase; arrowhead-down symbols mean decrease; bipolar arrowhead mean unchanged. (adapted from [320])

2. Hypothesis and aims of the study

To investigate the fundamental causes of the pathogenesis and progression of PD, I focus my study on the spreading of α-synuclein aggregates and its interaction with ageing, dopamine neurotransmission and neuroinflammation. Evidence in the literature shows dysfunctional striatal dopamine release in both overexpression and knock-out of α-synuclein animal models [145, 321, 322], but the effect of inoculation of exogenous α-synuclein along the nigrostriatal dopaminergic signalling pathway is not reported in the literature. Experimental seeding models are mainly used for studying pathological α-synuclein spreading in the brain, but it remains unknown how seeding of α-synuclein in the PD-vulnerable region SNpc would affect the dopamine release function in striatum over time. Also, there are no studies about how young brains differ from adult brains in dealing with acute inoculation of exogenous α-synuclein PFFs, especially when it is related to α-synuclein aggregation, spreading and neurotransmission.

At last, neuroinflammation is another important non-cell-autonomous risk factor in PD that I would like to consider in my study. In particular, microglia have been reported to be involved in the progression of PD through uncontrolled neuroinflammation [302, 323]. It has also been shown that microglia can interact with α-synuclein [280], affect dopaminergic terminals [269] and change their properties depending on age [318]. The effects of detectable inflammation through microglia plasticity at different stages of the progression is a topic still under debate, since it can be double-sided [324], either protecting the normal physiology of neuronal activity but also drive disease progression when uncontrolled. Therefore, to stress the role of microglia in the pathology spreading along nigrostriatal dopaminergic pathway, especially under the impact of age, is an interesting and important aspect for a better understanding of PD pathogenesis.

In the present study, I aim to investigate the striatal dopamine release function following the exogenously inoculated α-synuclein PFFs in SNpc, its pathological spreading pattern, the alteration of dopaminergic innervation and the dynamic changes of microglia in an age-dependent manner. I would like to answer the following questions:

- Is the striatal dopamine release impaired after the inoculation of PFFs in SNpc?
- How α-synuclein aggregates develop and propagate from the midbrain (the injection site) to the striatum (projecting site), in young and adult brains respectively?
- If any, do the dopaminergic physiological dysfunctions precede or follow the formation of pathological α-synuclein aggregates?
- What is the impact of PFFs inoculation on the dopaminergic network in terms of neuronal loss and altered innervation?
- Does the alteration of function and morphology coincide with neuroinflammation differently depending on age?

3. Methods and materials

3.1 Animals

The first mouse line used in this study is TH-IRES-Cre animals characterized by Lindeberg and colleagues [325]. Briefly, they are knock-in mice expressing Cre-recombinase from the 3'-untranslated region of the endogenous TH gene using an internal ribosomal entry sequence (IRES). The resulting Cre expression matches the normal pattern of TH expression, while the pattern and level of TH are not altered in the knock-in mice. Crossings with two different LacZ reporter mice demonstrated Cre-mediated genomic recombination in TH expressing tissues. Besides, LacZ was found in some unexpected cell populations (including oocytes), indicating recombination due to transient developmental TH expression. Moreover, Trem2 KO mouse line was also used, which was generated by Colonna lab [326], a portion of the transmembrane cytoplasmic domains encoded by exon 3 and 4 of Trem2 was replaced by a floxed NeoR cassette, which was subsequently excised by Cre. The Trem2 mutation was backcrossed to C57BL/6 until >98% of the loci were derived from the B6 strains; additional backcrossing to B6J has been done. Trem2 $^{-/+}$ mice were intercrossed to generate Trem2 $^{-/-}$ mice. Furthermore, C57Bl/6 wild type (Jackson Laboratory, Bar Harbor, ME, USA) mice were also used. All animals were housed in groups under pathogen-free conditions and bred in the animal housing facility at the German Center of Neurodegenerative Diseases and Center for Neuropathology and Prion Research of Ludwig-Maximilians-University Munich, with food and water provided ad libitum (21 ± 2 °C, at 12/12 hour light/dark cycle). After stereotactic injection, mice were housed separately for surgery recovery. All experiments were approved by the Bavarian government (Az 55.2-1-54-2532-214-2016) and performed according to the animal protection law.

3.2 Genotyping

All mouse lines were genotyped by regular polymerase chain reaction (PCR) assay. Tissue from each mouse was collected for DNA extraction (Invisorb® DNA Tissue HTS 96 Kit/C, Stratec molecular). Briefly, tissues were incubated with Lysis Buffer G for overnight under 52°C with shaking, the supernatant was collected and transferred into collection plate after centrifuge, then further incubated with binding buffer A. The filtrated fraction was discarded after centrifuge, two times of centrifugation was followed after washing the pellet fraction with washing buffer. Finally, DNA extractions were collected by warm (52°C) elution buffer. Then, DNA extractions were applied to PCR for identifying genotype. Primers details are listed in Table 2. PCR products were further analyzed by gel electrophoresis for the final identification.

Table 2. Mouse lines and primers for genotyping.

Mouse line	Primer sequence (5`-3`)	Primer type	Positive result
TH-IRES-Cre	GAT ACC TGG CCT GGT CTG	forward	290bp +
	CAC CCT GAC CCA AGC ACT	reverse	430bp +
	CTT TCC TTC CTT TAT TGA GAT	reverse	
Trem2 KO	CCC TAG GAA TTC CTG GAT TCT CCC	forward	231bp -
	TTA CAC AAG ACT GGA GCC CTG AGG A	forward	316bp +
	TCT GAC CAC AGG TGT TCC CG	reverse	

3.3 Preparation of α-synuclein PFFs

The α-synuclein monomers were kindly provided by my previous colleague S. Blumenstock. Monomers were produced as previously described [177]. Briefly, the recombinant wild type mouse α-synuclein was expressed in BL21 (DE3) E.coli using a pRK172 plasmid (kind gift of Kelvin Luk and Virginia Lee, University of Pennsylvania, USA) as previously described in other works [327, 328]. Escherichia coli BL21 (DE3) (Invitrogen, MA, USA) were transformed with the plasmid and expression was induced

with isopropylß-D-thiogalactopyranose (IPTG, Peqlab, Erlangen, Germany). Cells were lysed by boiling after heat-inactivation of proteases. After centrifugation, the supernatant was filtered through Filtropur S 0.2 filters (Sarstedt, Nümbrecht, Germany), loaded on a HiTrap Q HP anion-exchange column (5ml, GE Healthcare, Munich, Germany) and eluted with a linear 25 mM to 500 mM NaCl-gradient. Synuclein containing fractions were concentrated using VivaSpin 2-columns (Sartorius, Göttingen, Germany). Protein concentration was assessed to 5 mg/ml in 50 mM Tris-HCl, pH=7.0. After freezing in liquid nitrogen the protein was stored at -80 °C.

PFFs were assembled from purified α-synuclein monomer (5 mg/ml) by incubation at 37°C and 1400 rpm for 96 hours and stored at -80 °C [165, 329]. For fluorescent labelling, purified α-synuclein monomer (3.75 mg/ml, containing 100 mM $NaHCO_3$) was incubated with 0.34 mg/ml Alexa Fluor® 647 NHS Ester (Life Technologies, Darmstadt, Germany) for 18 hours at 4°C. The remaining free fluorophore was removed from the solution using PD-10 Columns (GE Healthcare, PA, USA) according to the manufacturer's recommendations before fibril assembly as described above. Directly before injection, an aliquot of PFFs was sonicated four times with a handheld probe (SonoPuls Mini 20, MS1.5, Bandelin, Berlin, Germany) according to the following protocol: Amplitude 30%; Time 15 s (pulse on 3 s, pulse off 6 s).

3.4 Western blotting

Before injection, the composition of PFFs resembled from α-synuclein monomers was evaluated by Western blot (Fig. 10 B). Samples of α-synuclein PFFs and monomers (0.5 µg, 1 µg and 2 µg, respectively) were prepared and separated on Mini-PROTEAN® TGX Stain-Free™ gels (Bio-Rad Laboratories, Inc., CA USA). Then they were further transferred onto PVDF membranes (Immobilon®-P, Merck Millipore, Darmstadt, Germany). The blots were incubated with the primary antibody of mouse monoclonal α-synuclein (1:500, Santa Cruz, Dallas, TX USA) and followed by the secondary antibody of goat anti-mouse HRP conjugated (1:3000, Promega, Madison, WI USA). The blots were developed using

GE ECL reagent mix (GE Healthcare, PA USA). Finally, protein bands were detected by the ChemiDoc^{TM} MP Imaging System (Bio-Rad Laboratories, Inc., CA USA).

3.5 Stereotactic injection of α-synuclein PFFs

Two- and five-month-old TH-IRES-Cre mice were anaesthetized with ketamine/xylazine (0.13/0.01 mg/g body weight; WDT/Bayer Health Care, Garbsen/Leverkusen, Germany) and stereotactically injected with 1 µl (5 µg) of PFFs into the SNpc (coordinates relative to the bregma: -3.0 mm anterior, +1.5 mm from the midline, +4.2 mm beneath the dura) [330] of the right hemisphere using a 5 µl Hamilton syringe. Injections were performed at 100 nl/min with the needle in place after injection for at least 5 min. The left hemisphere as the control part was received 1 µl sterile phosphate-buffered saline (PBS). To verify the injection coordinates, TH-IRES-Cre mice were also bilaterally injected PFFs and sterile PBS mixed with AAV1.CAG.FLEX.tdTomato.WPRE.bGH (AllenInstitute864, titer $1x10^{13}$ vg/ml, dilution 1:10).

Two-month-old C57BL/6 wild type mice and Trem2 KO mice were anaesthetized as above, and stereotactically injected with 5 µl (25 µg) of PFFs into the dorsal striatum (coordinates relative to the bregma: +0.2 mm anterior, +2.2 mm from the midline, +2.6 mm beneath the dura) of the right hemisphere using a 5 µl Hamilton syringe. Injections were performed at 400 nl/min with the needle in place after injection for at least 5 min.

TH-IRES-Cre animals were monitored regularly after the surgery and sacrificed at different predetermined time points (1 and 2 months after injection) by cervical dislocation and further conducted the detection of evoked dopamine release on brain slices by fast-scan cyclic voltammetry; or transcardiac perfused (firstly with cold saline and then 4% paraformaldehyde (PFA)) at the indicated time points, brain tissues were further post-fixed with 4% PFA.

3.6 Fast-scan cyclic voltammetry

Fast-scan cyclic voltammetry (FSCV) assay was used *ex vivo* to investigate dopamine release evoked by electrical stimulation in corpus callosum and record in dorsolateral quadrant of the sliced striatum. Five TH-IRES-Cre mice from each of the experimental groups were considered in this analysis, and for each mouse, PBS injected left hemisphere was considered as an internal control of the PFFs injected right hemisphere. Coronal brain slices (250 μm) containing dorsal striatum from mice were prepared as described previously [331, 332]. Slices were kept in oxygenated modified Kreb's buffer as follows (in mM): NaCl 126, KCl 2.5, NaH_2PO_4 1.2, $CaCl_2$ 2.4, $MgCl_2$ 1.2, $NaHCO_3$ 25, glucose 11, HEPES 20, L-ascorbic acid 0.4; at room temperature until required. Recordings were made at 32 °C in a chamber perfused at a rate of 1.5 ml/min. Cylindrical carbon-fibre microelectrodes (~75 μm exposed fibre) were prepared with T650 fibers (7 μm diameter, Goodfellow, Huntingdon, England) and inserted into a glass pipette. The carbon-fibre electrode was held at −0.4 V, and the potential was ramped to +1.2 V and back at 400 V/s every 100 ms. Dopamine release was evoked by a rectangular, electrical pulse stimulation (if not specified otherwise: 400 μA, 1.2 ms, monophasic) generated by a DS3 Constant Current Stimulator (Digitimer, Hertfordshire, UK). Delivery of electrical stimulation was applied every 4 min by a bipolar electrode placed ~100 μm from the recording electrode and always within the dorsolateral striatum area. Data collection was done using DEMON software [333]. Ten cyclic voltammograms of charging currents were recorded as a baseline before stimulation, and the average was subtracted from data collected during and after stimulation. Seeded/control part ratio of DA peak amplitude responses was obtained from four to eight control-seeded paired recordings across the rostral-caudal extent of the dorsolateral striatum and averaged for every single mouse. The time constant (τ) of the evoked DA response was used as an index of DA uptake. Two to four of the most representative seeded/control pairs were chosen for each mouse.

3.7 Drug treatment after α-synuclein PFFs injection

C57BL/6 wild type mice that were injected with preformed fibrils α-synuclein into dorsal striatum were further subjected to PLX5622 (formulated at 1200mg/kg in chow) or control food pellets treatment three days after surgery, lasted for a consecutive 6 weeks. PLX5622, a CSF1R inhibitor, was provided by Plexxikon (Berkeley, CA) and formulated in AIN-76A standard food pellet by Research Diets (New Brunswick, NJ), control mice were treated with AIN-76A food pellet without PLX5622. Animals were monitored regularly after the surgery and sacrificed after 6 weeks of special food treatment, via transcardiac perfusion (firstly with cold saline and then 4% PFA) at the indicated time point, brain tissues were further post-fixed with 4% PFA.

3.8 Immunohistochenmistry

Mice were sacrificed by transcardiac perfusion at each time points as mentioned above, firstly with PBS followed by 4% PFA (w/v) in deep ketamine/xylazine anaesthesia. Brains were removed and post-fixed in PBS containing 4% PFA overnight before cutting 50-µm-thick coronal sections with a vibratome (VT 1000 S from Leica, Wetzlar, Germany). Floating sections were permeabilized with 2% Triton X-100 in PBS overnight at room temperature and blocked with 5% normal goat serum (Sigma-Aldrich) and 4% BSA (bovine serum albumin, VWR) for 6 h on a shaker at room temperature. Primary antibodies (Anti-α-synuclein phospho S129, rabbit polyclonal, Abcam, Cambridge, UK; Anti-Tyrosine Hydroxylase, mouse monoclonal, Merck Millipore, Darmstadt, Germany; Anti-IBA1, Guinea Pig polyclonal, SYSY, Goettingen, Germany; Anti- α-synuclein Phospho (Ser129), mouse monoclonal, Biolegend, San Diego, CA; Anti-IBA1, rabbit, FUJIFILM Wako Chemicals, U.S.A) were incubated for 48 h at 4 °C in a 1:500 dilution, according to the manufacturer's recommendations. Slices were washed 3 × 10 min with PBS and then incubated with the secondary antibodies (1:500; goat anti-rabbit Alexa Fluor 488, goat anti-mouse Alexa Fluor 568, goat anti-guinea pig Alexa Fluor 647, goat anti-mouse Fluor

488, goat anti-rabbit Alexa Fluor 647, Invitrogen, Life Technologies GmbH) for overnight at 4 °C. After 3 × 10 min washing in PBS, sections were incubated for 1 h with NeuroTrace 530/615 Red Fluorescent Nissl Stain (1:500, ThermoFisher Scientific) on a shaker at room temperature. Sections were finally washed for 3 × 10 min with PBS before mounting them on glass coverslips with Dako fluorescence conserving medium (Dako, Hamburg, Germany).

Table 3. List of primary and secondary antibodies used in IHC.

Antibody	Manufacturer	Host species	IHC working dilution
α-synuclein Phospho (Ser129)	abcam	rabbit	1:500
α-synuclein Phospho (Ser129)	Biolegend	mouse	1:500
Tyrosine Hydroxylase	Merck Millipore	mouse	1:500
IBA1	SYSY	guinea pig	1:500
IBA1	Wako	rabbit	1:500
Alexa Fluor 488	Invitrogen	goat anti-rabbit	1:500
Alexa Fluor 488	Invitrogen	goat anti-mouse	1:500
Alexa Fluor 568	Invitrogen	goat anti-mouse	1:500
Alexa Fluor 647	Invitrogen	goat anti-rabbit	1:500
Alexa Fluor 647	Invitrogen	goat anti-guinea pig	1:500

3.9 Confocal microscopy

Images were acquired by using an LSM 780 microscopy. Laser wavelengths used for excitation and collection range of emitted signals were as follows: Alexa fluor® 488- 488 nm/500-550 nm; Alexa fluor® 568- 568 nm/ 578-603 nm; Alexa fluor® 647- 633 nm/ long-pass 670 nm, under the 40x oil objective (Plan-Apochromat 40x/1.4 oil DIC M27). For imaging of the midbrain, 3-dimensional 16-bit data stacks of 1024 x 1024 x 12 pixels with tile scans were acquired for the whole SNpc area of each hemisphere. For imaging of the striatum, three consecutively different positions along the dorsolateral striatum were acquired from 3-dimensional 16-bit data stacks of 1024 x 1024 x 20 pixels were acquired of each hemisphere. For cortex imaging, three consecutively different positions

along the primary somatosensory area were acquired from 3-dimensional 16-bit data stacks of 1024 x 1024 x 20 pixels were acquired from the seeding side (right hemisphere), under the 20x objective (Plan-Apochromat 20x/0.8 M27).

3.10 Stereology

Brain sections outlines were carried out using a Zeiss fluorescent microscope (Imager.M2, ZEISS, Oberkochen, Germany) fully motorized and interfacing to a Dell computer running StereoInvestigator® (MBF Bioscience, Williston, Vermont, USA) and cells labelled with corresponding markers were quantified in 8 serial coronal sections spanning the entire brain hemisphere in the coronal plane, for SNpc counting spaced 150 µm (section interval is 3) apart. Outline and fiduciary marks were drawn at 2.5x magnification (EC-Plan-NEOFLUAR 2.5X/0.075, ZEISS, Oberkochen, Germany) to delineate reference points. Limits for areas of interest were drawn following a mouse brain Atlas [334] as well as their positive markers presented in the region. Cells were identified as positive for a marker if they expressed immune-reactivity visually deemed to be above background, even if it was very weak, which means cells exhibiting varying levels of immune-labelling from very weakly to very strongly stained were all identified as marker positive. All cell counting was done by an investigator blind to genotype and treatment, at 63x magnification (Plan/APOCHROMAT 63X/1.4 Oil DIC, ZEISS, Oberkochen, Germany) using a 3D counting frame in a sampling grid size 130 µm x 130 µm, and the counting frame sized 50 µm x 50 µm, with the counting probe height 12 µm.

3.11 Imaris image processing

The z-stack fluorescent images acquired by confocal microscopy were used to create detailed surfaces rendering TH-positive dopaminergic neurons and striatal terminals, IBA1-positive microglia cells, as well as pS129-positive α-synuclein aggregates. The z-stack images were loaded in Imaris software (version 9.3.1), which was displaying as 3-

colour channels fluorescence in a 3-dimensional isometric view.

For midbrain images processing, the SNpc brain area was drawn following atlas hallmarks [330] and created a surface according to the distribution of TH-positive neurons, and was masked by selecting the “mask all” function with the voxels inside surface as 1.0 and outside as 0.0 value, which indicates this area is the region of interest as channel 4; for creating surfaces, the surface detail value was set as 0.415 µm for all three channels, and in thresholding, background subtraction was set as 1.56 µm for all channels; the threshold intensity value was adjusted manually for pS129 channel, kept the same ratio of adjusted intensity to maximum intensity between control and seeded side, the TH and IBA1 channels threshold intensity was used as defaulted; for adding filter, pS129 channel was filtered by volume with 2 μm^3; then the colocalization between different channels was processed with the surface-coloc command by MATLab under “no smoothing” mode; when subtracting data of each value, filtered with “Intensity Max Ch=4” to guarantee these values were within the SNpc area.

For processing the striatum images, 12 stacks were analyzed for each sample. The surface detail value was set as 0.05 µm for all three channels, and thresholding background subtraction was set as 0.05 µm for channel TH and pS129, and IBA1 channel used the absolute background; threshold intensity was set as 90% of maximum intensity value for all channels; for filter adding, pS129 channel was filtered by volume above 0.5 μm^3, and IBA1 channel was filtered by volume above 5 μm^3; then the colocalization between each channel was processed as mentioned above and subtracted data from each sector after then.

For the cortex images processing, custom-written MATLAB scripts were used. 20-stacks images were analyzed for each sample. Briefly, local background subtraction was used to diminish intensity variations between different stacks. Microglia were identified by applying the 90th percentile as a minimal-intensity threshold. The noise was excluded by applying a connected component analysis excluding patches of contiguous voxels smaller than 1 μm^3. α-synuclein aggregates were identified by applying the 95th percentile as a

minimal-intensity threshold. The noise was excluded by applying a connected component analysis excluding patches of contiguous voxels smaller than 40 μm^3.

3.12 Isolation of microglia

C57Bl/6 wild type mice at postnatal day 3-7 (P3-P7) were used for immunomagnetic microglia isolation by MACS® neural dissociation kit, according to the manufacture`s instruction (Miltenyi Biotec, Germany). Briefly, cortices were dissected on ice from P3-P7 pups, meninges were removed in cold DPBS, tissue was further minced and added to the pre-prepared enzyme solution for an automatic homogenization procedure by gentleMACs Octo Dissociator with heaters. Debris and red blood cells were removed with the kit reagents by several cycles of incubation and centrifugation according to the manufacture`s description. CD11b (microglia) Microbeads were added to the prepared cell suspension to label microglial cell population, microglia were further separated from the cell suspension by flushing through MACs LS columns on the QuadroMacs Separator. All the reagents and tools used in this method were purchased from Miltenyi Biotec.

3.13 Primary microglia culture and immunostaining

The CD11b-positive microglia cell pellets were suspended in Dulbecco`s Modified Eagle Medium (DMEM), containing 10% fetal bovine serum (FBS), 1% Penicillin Streptomycin (Pen Strep), and 10ng/ml recombinant mouse granulocyte-macrophage colony-stimulating factor (GM-CSF), at concentration 10^5/ml. All reagents mentioned above were purchased from gibco®, life technologies™, USA. Cell medium was added into the IbiTreat µ-slide 8 well culture chamber (Ibidi GmbH, Germany), maintained under a regular condition in the incubator. Medium was changed when cells were attached, 10 µg/ml PFFs (labelled with Alexa Fluor™ 647 carboxylic acid, succinimidyl ester, Life technologies, U.S.A) and the same amount of PBS were added to the culture medium, incubated with cells for 3h under a regular condition in the incubator. Cells were further

fixed in 4% PFA after washing with DPBS, then permeated with 0.5 % TritonX 100 (in PBS) for 15 min and blocked with 10% goat serum on a shaker for 2h under room temperature. Primary antibody (Anti-IBA1, rabbit, FUJIFILM Wako Chemicals, U.S.A) was added with dilution 1:200 for incubating overnight under 4°C. Secondary antibody (goat anti-rabbit Alexa 647, Invitrogen, Life Technologies GmbH) was added for 1h incubation at room temperature. After 3 × 10 min washing in PBS, cells were incubated with DAPI for 15 min on a shaker at room temperature. Cells were finally washed for 3 × 10 min with PBS before mounting with Dako fluorescence conserving medium (Dako, Hamburg, Germany), and covered with 8 x 8 mm glass cover clips (H.Saur Laborbedarf, Reutlingen, Germany) in each well.

3.14 Statistical analysis

Graphs were created and statistics were calculated in Prism 8.4.2 (GraphPad Software, San Diego, CA, USA). For dopamine release data from FSCV, two-way ANOVA followed by the Bonferroni *Post Hoc* comparisons was used to compare the percentage of seeded to control dopamine release ratio over different time points after injection. For the assessment of inter-group differences at single time points when ANOVA interaction was not significant, Student's *t*-test (two-sided) or LSD Fisher's test were applied. Statistic for the histological analysis from Imaris was performed using MANOVA within the same brain region (SNpc and Striatum) with the following independent factors: Treatment (Between factor: Control Vs Seeded side), Age (Between Factor: Young vs Adult) and, when shown, Anteroposteriority (Within Factor: 3 levels with different bregma values) or TH Colocalization (TH^+ vs TH^-). Normal distribution was assumed according to the central limit theorem, as values were calculated as the means between mice, each considered as the means of each 3 samples in SNpc and 12 samples in the striatum. For *t*-tests, the variance between groups was tested (F-test) and not found to be significantly different. Data are expressed as mean ± SEM unless otherwise indicated, with $P < 0.05$ defining differences as statistically significant (*$P < 0.05$; **$P < 0.01$; ***$P < 0.001$).

4. Results

4.1 PFFs inoculation in the nigrostriatal pathway confirmed by AAV-driven tdTomato labels in midbrain and striatum

To verify that the PFFs or PBS were injected into SNpc and to navigate the FSCV recording site in the striatum, I combined the AAV1.CAG.FLEX.tdTomato.WPRE.bGH (AAV-tdTomato) together with the seeding materials in the stereotactic surgery (Fig.10 A). The composition of α-synuclein PFFs resembled from monomers was evaluated by Western blot (Fig.10 B). As expected, it showed several high molecular weight species in the α-synuclein PFFs samples, while the high bands were absent in the monomer samples. Based on the Cre-lox system, dopaminergic neurons in SNpc were successfully labelled with the tdTomato fluorescent protein after 1 month of injection (Fig.10 C), indicating that the seeding materials were inoculated in the SNpc. Before each FSCV recording, I checked the striatum slices under an epifluorescent stereoscope (Fig.10 E-F). The TH terminals of contralateral as well as the ipsilateral sides in the striatum were also successfully labelled, which allowed me to record dopamine release in the dorsolateral striatum that was tdTomato-positive (Fig.10 D-F).

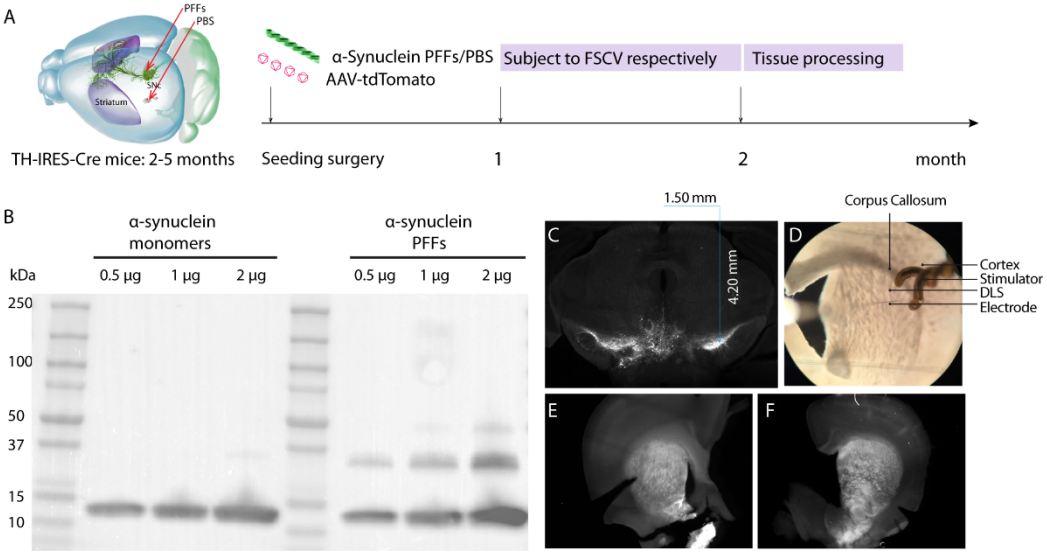

Figure 10. Experimental scheme and validation of injection material and sites. A, experimental scheme. B, Western blot detecting α-synuclein PFFs used for injection. **C**, the labelled fluorescent tdTomato in the midbrain. **D,** the FSCV setup and recording site on one side of the brain slice. **E-F**, the labelled fluorescent tdTomato in contralateral and ipsilateral striatum, respectively.

4.2 Unilateral PFFs inoculation in SNpc affected ipsilateral striatal dopamine release in adult mice

Young (2-month-old) and adult (5-month-old) mice were subjected to the bilateral injection of α-synuclein PFFs in the right hemisphere and the same volume of sterile PBS in the left hemisphere as the internal control in the SNpc. As described previously, the injection materials were mixed with AAV-tdTomato respectively for the validation of injection and navigation of recording. Next, I investigated whether the striatal dopamine release would change at different time points after injection in both young and adult mice.

After 1 and 2 months of injection, I conducted the measurements of dopamine release in the striatum on *ex vivo* brain slices by FSCV. The results were presented as the percentage of dopamine release in the PFFs seeded side to the PBS control side. For the young mice, the function of striatal dopamine release did not alter obviously after 1 and 2 months of injection (Fig.11 E, $P>0.05$) compared to the internal control. For the adult mice, dopamine release stayed unchanged after 1 month of injection (Fig.11 E, $P>0.05$), however, displayed a significant reduction after 2 months compared to the control side (Fig.11 E, [DA]e: Control = 1.852 ± 0.2573, Seeded = 1.424 ± 0.2448, paired Student *t*-test: $t(6) = 4.56$, $P < 0.01$). Besides, the kinetics of dopamine uptake (τ) were also analyzed in both young and adult mice, which showed a tendency of slightly increased kinetic in the adult mice after normalization of the values to the control side (Fig.11 F, $P > 0.05$).

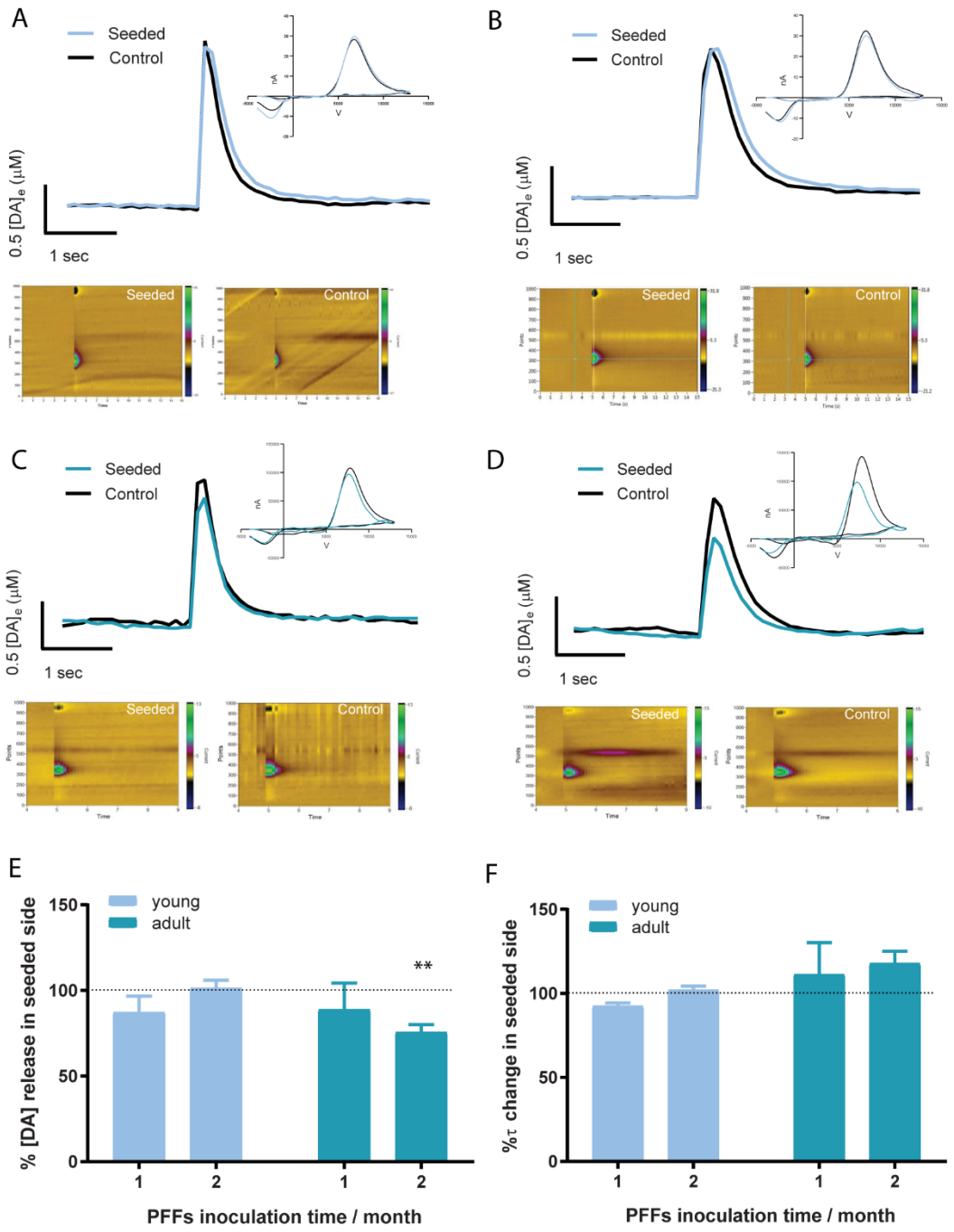

Figure 11. The function of evoked striatal dopamine release in both young and adult mice at different time points after injection. A-D, upper curves are the concentration-time plots, lower are the colour plots, smaller insets are the cyclic voltammograms at 1 month after injection in young (A) and adult mice (C), and 2 months after injection in young (B) and adult mice (D). **E**, the evoked dopamine release concentration in the seeded side at different post-seeding time points in young and adult mice (***P* < 0.01), values are shown as the percentage in the seeded side normalized by their internal control side. **F**. the rate of dopamine uptake following the evoked release, values are shown as the percentage in the seeded side normalized by their internal control side; no significant alterations are shown in dopamine uptake rate at each time point after injection in both young and adult mice (*P* > 0.05).

4.3 Effects of unilateral PFFs inoculation in α-synuclein aggregation and spreading within the nigrostriatal dopaminergic pathway

4.3.1 From SNpc to striatum, phospho-α-synuclein pathology following PFFs inoculation developed differently in young and adult mice overtime without neurodegeneration or evident interhemispheric spreading

To investigate the underlying mechanism of the different patterns of striatal dopamine release in young and adult mice, I first analyzed the distribution of α-synuclein aggregates from SNpc to striatum including the injection site (-3.0 µm from bregma) through the anteroposterior window between -3.5 µm to 1.4 µm from bregma, at different time points after injection in both young and adult mice (Fig.12 A-D).

After 1 month of PFFs injection in SNpc, pathological α-synuclein developed and accumulated in the midbrain in both young (Fig.12 A, Fig.13 A-C) and adult mice (Fig.12 C, Fig.14 A-C). However, in SNpc, the aggregation was more pronounced in the young compared to the adult mice, especially in the areas around the injection site. While in the striatum, the aggregates accumulated more in the adult (Fig.12 C, Fig.14 D-F) compared to the young mice (Fig.12 A, Fig.13 D-F). After 2 months of injection, the formation of aggregates in SNpc grew even more in both young (Fig.12 B, Fig.13 G-I) and adult mice (Fig.12 D, Fig.14 G-I) when compared to the 1 month after injection. Whereas, at 2 months after injection, the aggregates accumulated in the SNpc of young mice were still significantly more than that in the adult mice. While in the striatum, the formation of aggregates in the young mice did not change obviously after 1 and 2 months of injection but decreased in the adult mice (Fig.12 D, Fig.14 J-L) to a comparable level with the young mice (Fig.12 D, Fig.13 J-L) at 2 months after injection. (MANOVA significance in SNpc. Interaction Treatment x Inoculation time: $F(1, 1) = 5.17$, $^{*}P < 0.05$; Interaction Treatment x Age: $F(1, 1) = 16.41$, $^{**}P < 0.001$. In the figures, LSD test: ## $P < 0.01$ for comparison between different inoculation time of same age; ** $P < 0.01$, *** $P < 0.001$ for comparison between different age of same inoculation time. MANOVA significance in

Striatum. Interaction Treatment x Anteroposteriorly: F (1, 2) = 5.26, *P < 0.01; Interaction Treatment x Age: F (1, 1) = 12.21, **P < 0.001. In the figures, LSD test: # P < 0.05, ### P < 0.001 for comparison between different inoculation of same age; * P < 0.05, *** P < 0.001 for comparison between different age of same inoculation time)

Additionally, I also quantified the number of aggregates in each group as shown in Figure S1. The number of aggregates in young mice (Fig.S1 A-B) was much lower compared to the adult mice (Fig.S1 C-D) after 1 and 2 months of injection. This suggests that the adult mice are supposed to have less capability to aggregate with misfolded α-synuclein, leading to more prominent spreading of pathological α-synuclein from SNpc to the striatum. (MANOVA significance in SNpc. Main Factor Treatment: F (1) = 66.96, **P < 0.001. MANOVA significance in Striatum. Interaction Treatment x Age x Anteroposteriorly: F (1, 1, 2) = 4.9, *P < 0.05; Interaction Treatment x Age x Seeding Time: F (1, 1, 1) = 6.9, P < 0.05. In the figures, LSD test: ### P < 0.001 for comparison between different inoculation of same age; *** P < 0.001 for comparison between different age of same inoculation time)

To understand if the decreased striatal dopamine release in adult mice at 2 months after injection was linked to the neuronal degeneration in SNpc, I further determined the TH-positive dopaminergic neurons number according to the basic principles of the stereological method by the Stereo Investigator software. Results showed that TH-positive dopaminergic neurons and the total neuronal cells of SNpc in the seeded site were not significantly decreased compared to the control side (Fig.12 E, P > 0.05). The number of total neuron in SNpc (Fig.12 F, P > 0.05), as well as the estimated SNpc volume (Fig.12 G, P > 0.05), were also statistically comparable to the control side. Table 4 displays the parameters that I used for cell counting. Sampling principles and details of stereology counting were displayed in Figure S2.

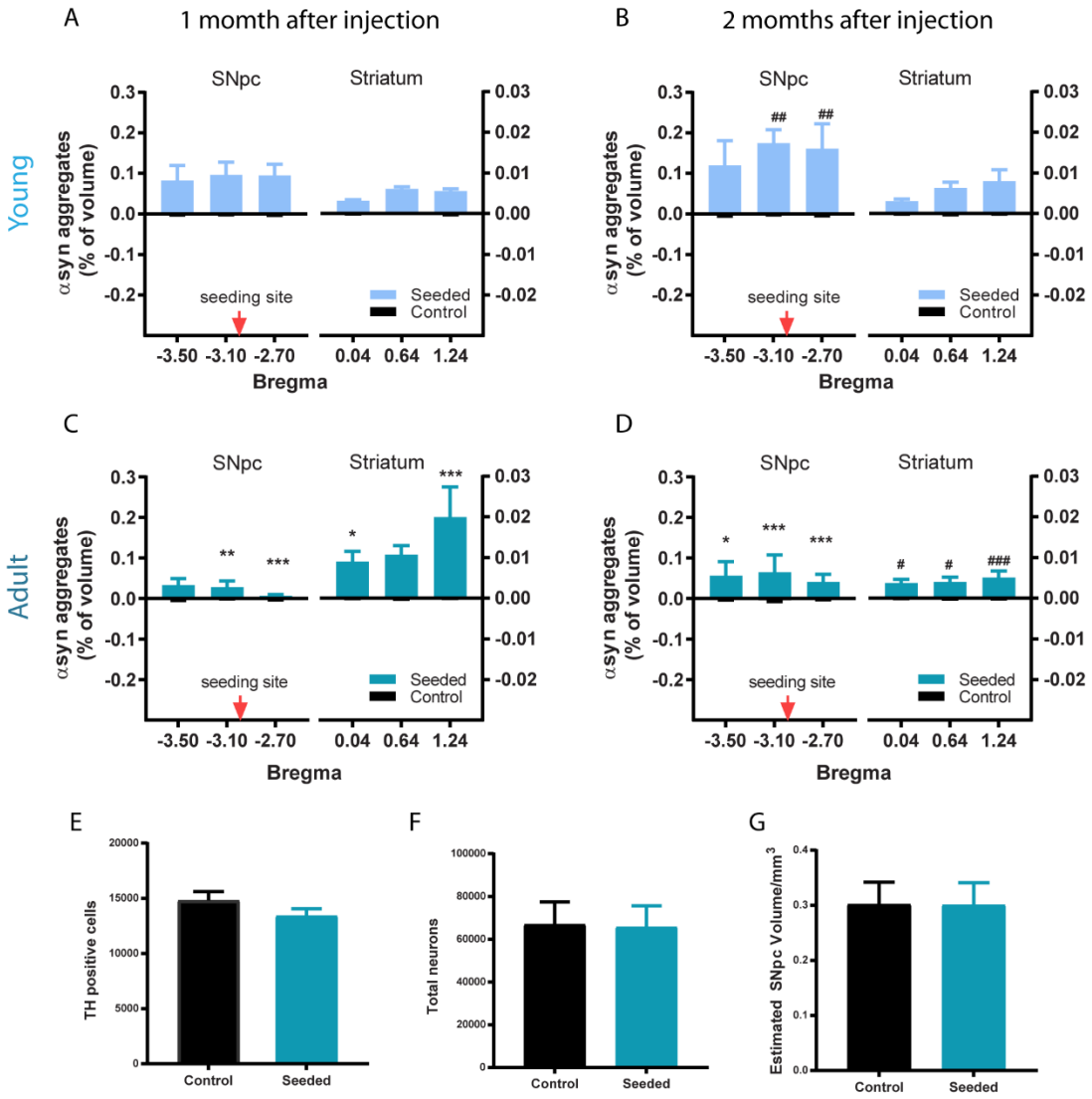

Figure 12. Distribution of phospho-α-synuclein aggregates from SNpc to striatum and stereological counting of the dopaminergic neurons. A-D, the volume covered by α-synuclein aggregates in SNpc and striatum between -3.5 µm and 2.4 µm from bregma including the seeding site, at different time points after injection in both young (A-B) and adult mice(C-D). #comparison between different time points within the same region of the same age (# $P < 0.05$, ## $P < 0.01$; ### $P < 0.001$); *comparison between different ages within the same region of the same inoculation time (* $P < 0.05$, ** $P < 0.01$, *** $P < 0.001$). **E-G**, the stereological cell counting after 2 months of injection in adult mice. **E**, the number of TH-positive cells. **F**, the total neuronal cells. **G**, the estimated volume of SNpc.

Table 4. Parameters for stereological cell counting in the SNpc. Counting frame size is 50 µm x 50 µm, probe height is 12 µm, the sampling grid size is 130 µm x 130 µm, as well as coefficient error and the average cell count per sampling site for each marker, are shown in the table.

SNpc		Counting frame	Sampling grid size	Coefficient of error (Gundersen), m=1	Average cell counts/sampling site
TH	Control	50x50x12 µm	130x130 µm	0.12	1.08
	Seeded	50x50x12 µm	130x130 µm	0.11	0.98
Neurotrace	Control	50x50x12 µm	130x130 µm	0.04	4.77
	Seeded	50x50x12 µm	130x130 µm	0.04	4.86

4.3.2 From SNpc to striatum, phospho-α-synuclein positive aggregates mostly accumulated in the TH-positive dopaminergic neurons or terminals

To better understand the pathology distribution, I further determined the percentage of phospho-α-synuclein positive aggregates in TH-positive (TH^+) neurons of SNpc and striatal terminals, in both young and adult mice. Representative images of phospho-α-synuclein and TH staining in both SNpc and striatum of young and adult mice were shown in Figure 15.

After 1 month of injection, there were approximately 87% of aggregates located in the cell body and axons of TH^+ neurons in the SNpc of young mice and increased significantly after 2 months (Fig.16 A) to a co-localization level of about 92% within TH^+ area. While in the adult mice, about 88% of the aggregates developed in TH^+ structures in SNpc after 1 month of injection and dropped to about 36% after 2 months (Fig.16 C), with a non-significant increase of overall aggregates volume. (MANOVA significance in SNpc. Interaction Age x TH Co-localization x Seeding time: $F(1, 1, 1) = 8.71$, $^*P < 0.01$. In the figures, Bonferroni *post hoc* test: ## $P < 0.01$, ### $P < 0.001$ for comparison of aggregates in TH^+ volume coverage between different inoculation of same age; *** $P < 0.001$ for comparison of aggregates in TH^+ volume coverage between different age of same inoculation time)

Regarding the striatum, in young mice, an approximate 99% co-localization of aggregates

and TH terminals after 1 month of injection was observed and around 92% after 2 months (Fig.16 B), with no significant change in overall aggregates volume. While in adult mice, the TH^+ area co-localized with aggregates was much higher compared to the young mice, with a co-localization of about 91% (Fig.16 D) after 1 month of injection. At 2 months after injection, the TH^+ area covered by aggregates was significantly reduced in adult mice, although with a similar co-localization of 92%, which was comparable to the level in young mice. (MANOVA significance in Striatum. Interaction TH Co-localization x Seeding time: $F(1, 1) = 4.37$, $P < 0.05$. In the figures, LSD test: ### $P < 0.001$ for comparison of aggregates in TH^+ volume coverage between different inoculation of the same age; ** $P < 0.01$ for comparison of aggregates in TH^+ volume coverage between different age of same inoculation time)

4.3.3 In striatum, coverage volume and conformation of TH-positive terminals response to aggregates spreading differently with age

Given that the phospho-α-synuclein aggregates were mainly located in the TH-positive structures and a decrease of DA release after 2 months of injection was observed in adult mice, I further analyzed the volume covered by the TH-positive dopaminergic terminals in dorsolateral striatum in both young and adult mice.

By comparing the volume covered by striatal TH^+ terminals between hemisphere ipsilateral (seeded side) and contralateral (PBS injected control side) to the PFFs injection, I found out that in the young mice, there was a non-significant tendency of TH^+ axonal coverage reduction in the striatum after 1 month of injection (Fig. 17 A, $P > 0.05$), which became significant after 2 months (Fig. 17 B, unpaired *t*-test $T(8) = 4.199$, $^{**}P < 0.01$). In the adult mice, it showed a non-significant tendency of reduced TH^+ axonal coverage (Fig. 17 C, $P > 0.05$) after 1 month of injection, but this reduced tendency did not become significant after 2 months (Fig. 17 D, $P > 0.05$).

To understand if there is heterogeneity in the terminal populations affected by the injection, I further analyzed the cumulative frequency distribution (CFD) of the size (μm^3)

of the puncta using 3D reconstruction of the Imaris software. In the young mice, the CFD curve of the ipsilateral seeded side was left-shifted compared to the contralateral control side after 1 and 2 months of injection, indicating that the proportion of small-sized terminals was significantly higher in the hemisphere ipsilateral to the PFFs injection after 1 month (Fig. 17 E, two-way ANOVA Main Factor Treatment F (1, 160008) = 18960, $P < 0.001$; In the figure LSD test: * $P < 0.05$, ** $P < 0.01$, *** $P < 0.001$) and also after 2 months (Fig. 17 F, two-way ANOVA Main Factor Treatment F (1, 160008) = 38852, P < 0.001; In the figure LSD test: * $P < 0.05$, ** $P < 0.01$, *** $P < 0.001$).

However, the adult mice displayed a different profile of the CFD pattern in TH^+ terminals. It showed a smaller range of significant difference of terminal size in the ipsilateral PFFs injected side (Fig. 17 G, two-way ANOVA Main Factor Treatment F (1, 160008) = 9780, $P < 0.001$; in the figure LSD test: * $P < 0.05$, ** $P < 0.01$), compared to the control side after 1 month of injection. While at 2 months after injection, there was no significantly changed terminal pattern in adult mice (Fig.17 H, $P>0.05$).

These results indicate that an intensifying reduction of the striatal terminals is in progress from 1 month to 2 months after injection in the young mice, and the reduced terminals are more likely to be the larger portion since the small-sized terminals showed an increasing proportion. Whereas, in adult mice, this process gradually disappears from 1 month to 2 months after injection.

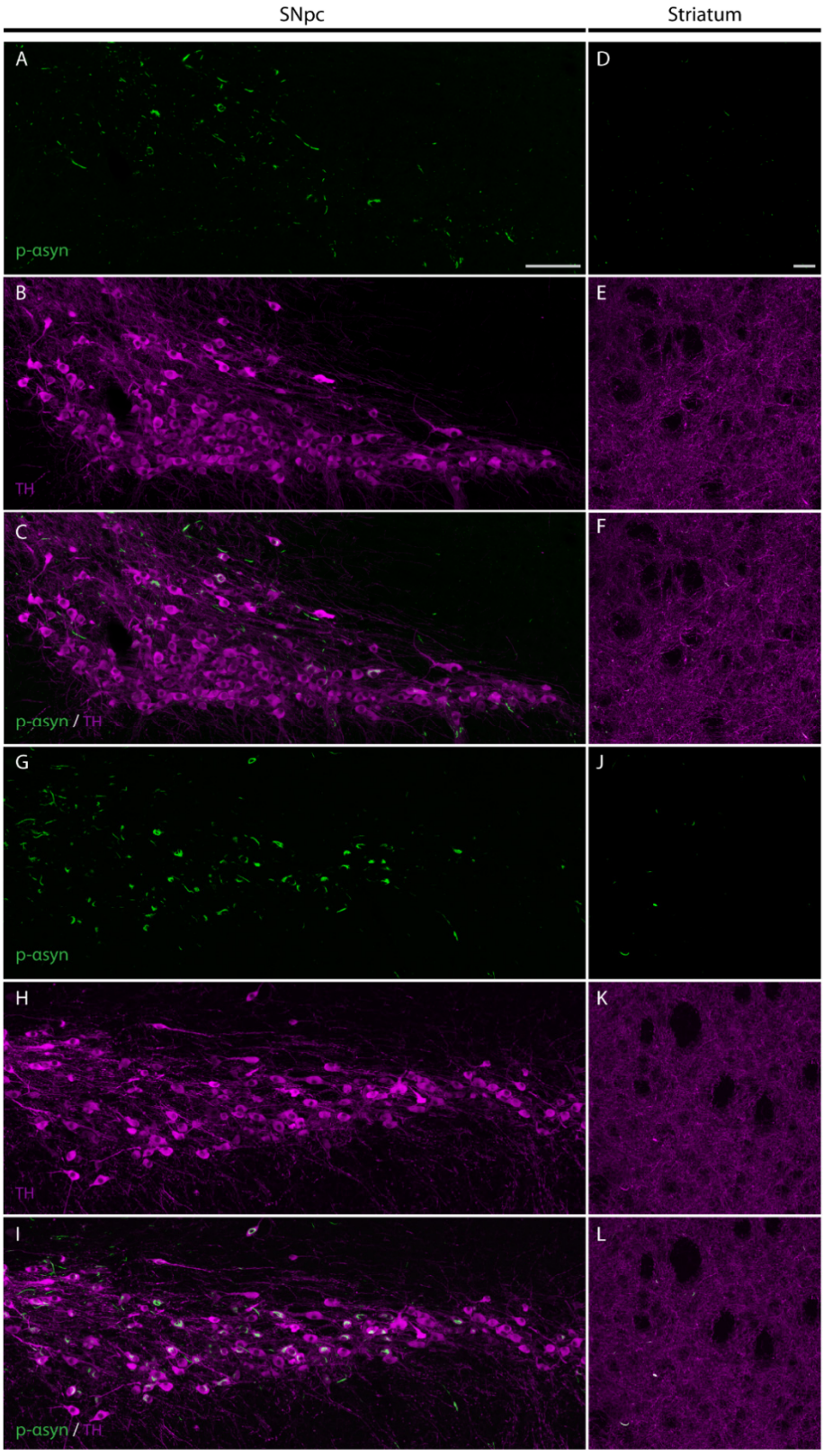

Figure 13. Representative images of phospho-α-synuclein and TH IHC staining in SNpc and striatum at different time points after injection in young mice. Green: phospho-α-synuclein (p-αsyn), Magenta: TH. **A-F**, 1 month after injection in SNc (A-C) and dorsolateral striatum (D-F). **G-L**, 2 months after injection in SNpc (G-I) and dorsolateral striatum (J-L). Scale bars: A-C and G-I, 100 µm; D-F and J-L, 20 µm.

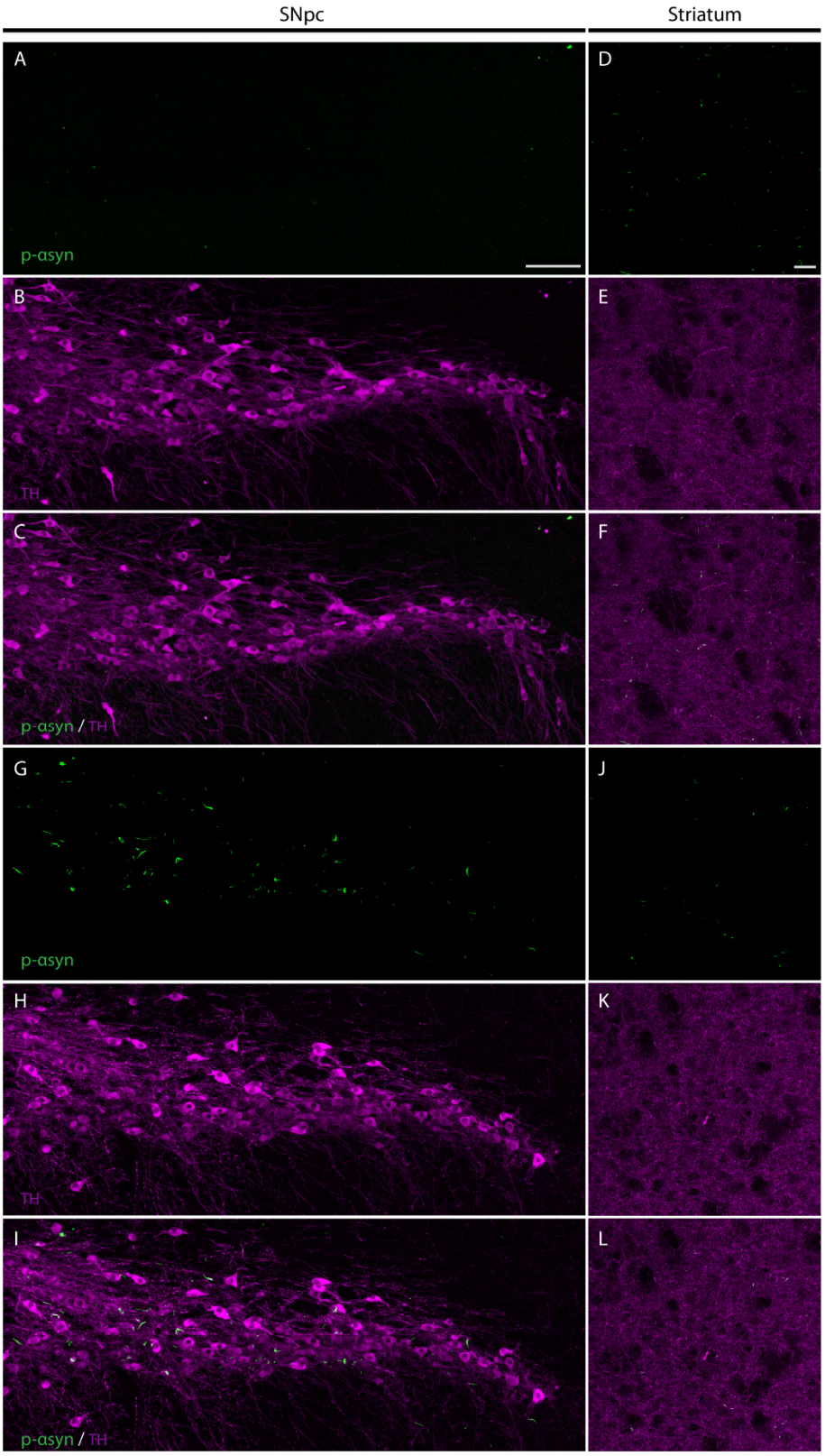

Figure 14. Representative images of phospho-α-synuclein and TH IHC staining in SNpc and striatum at different time points after injection in adult mice. Green: phospho-α-synuclein (p-αsyn), Magenta: TH. **A-F**, 1 month after injection in SNpc (A-C) and dorsolateral striatum (D-F). **G-L**, 2 months after injection in SNpc (G-I) and dorsolateral striatum (J-L). Scale bars: A-C and G-I, 100 µm; D-F and J-L, 20 µm.

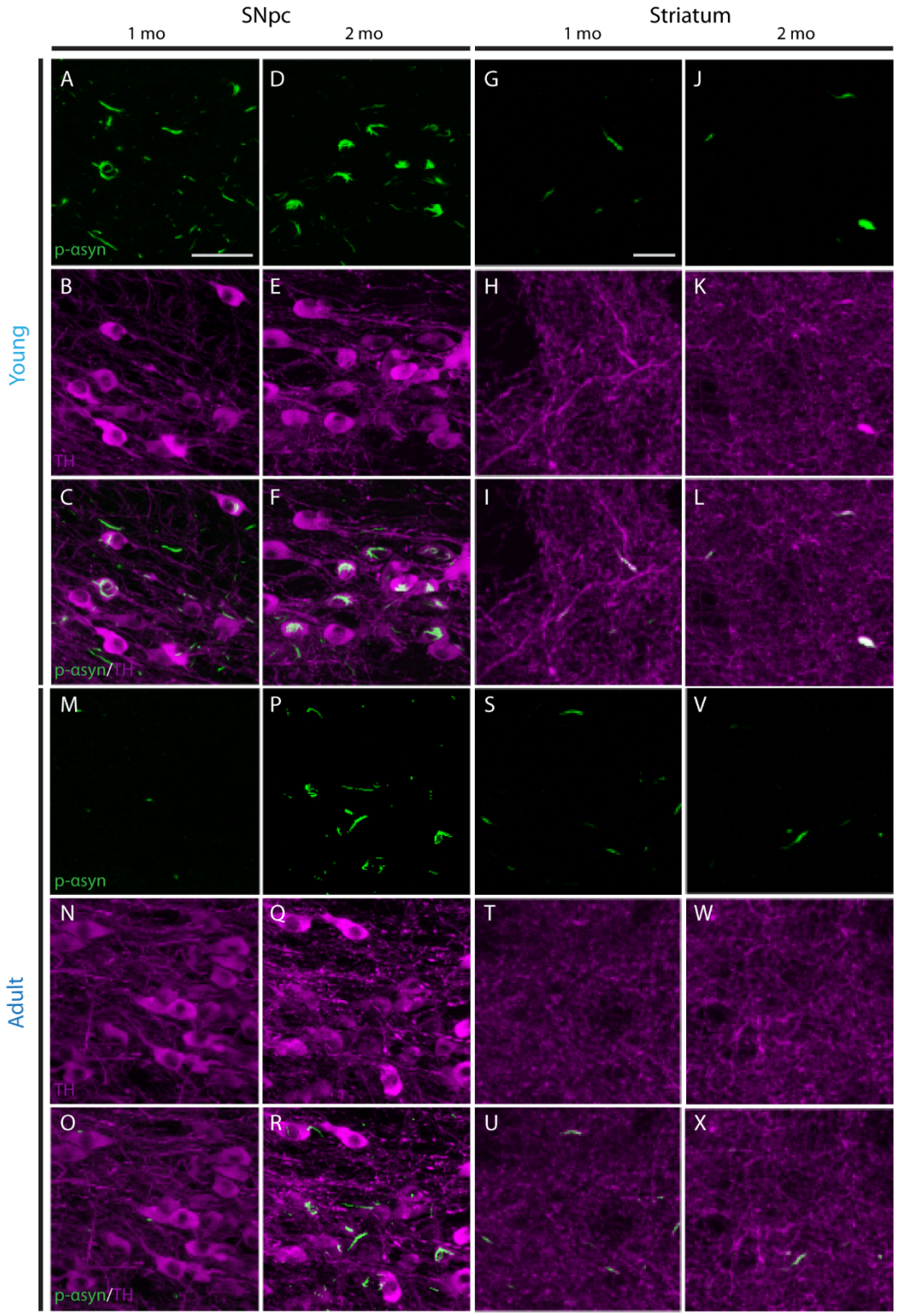

Figure 15. Representative images of phospho-α-synuclein and TH IHC staining in SNpc and striatum at different time points after injection in young and adult mice. Green: phospho-α-synuclein (p-αsyn), Magenta: TH. Scale bars: A-F and M-R, 100 µm; G-L and S-X, 20 µm.

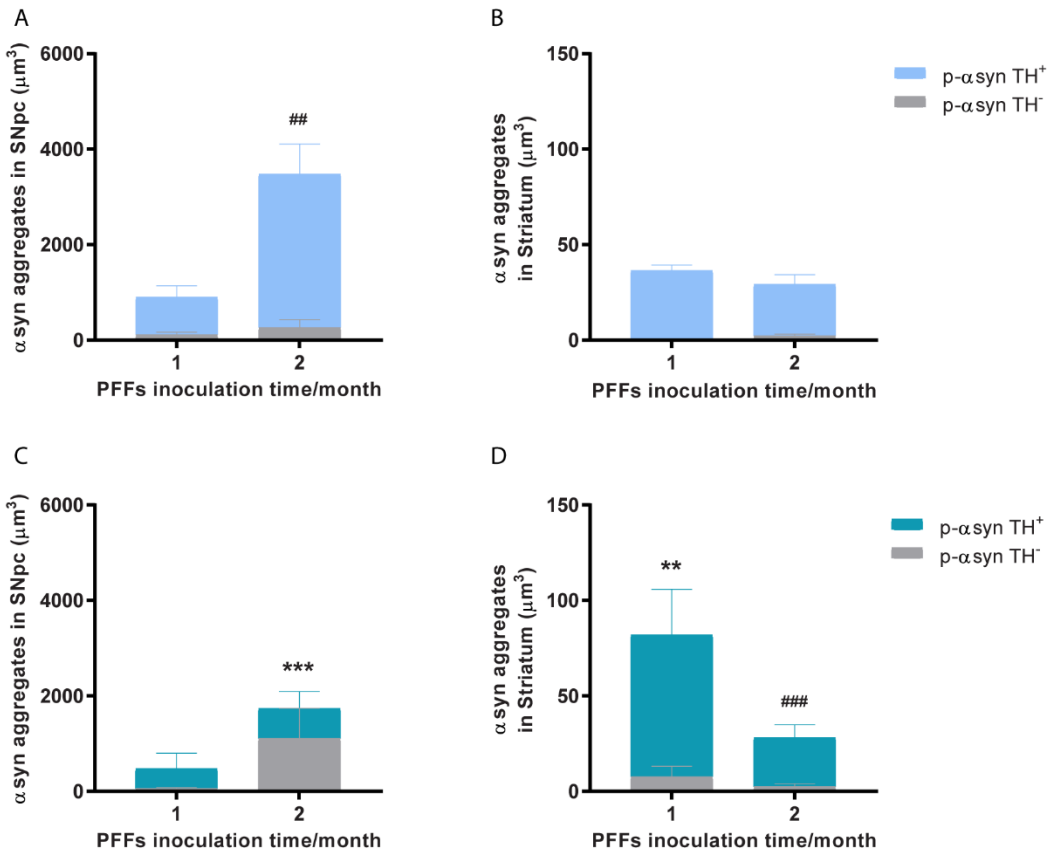

Figure 16. The co-localization of phospho-α-synuclein positive aggregates with TH-positive structures in SNpc and striatum at different time points after injection in young and adult mice. **A-B**, co-localization in SNpc (A) and striatum (B) of young mice after 1 and 2 months of injection, respectively. **C-D**, co-localization in SNpc (C) and striatum (D) of adult mice after 1 and 2 months of injection, respectively. #comparison between different time points within the same region of same age (## $P < 0.01$; ### $P < 0.010$); *comparison between different age within the same region of same inoculation time (** $P < 0.01$, *** $P < 0.001$).

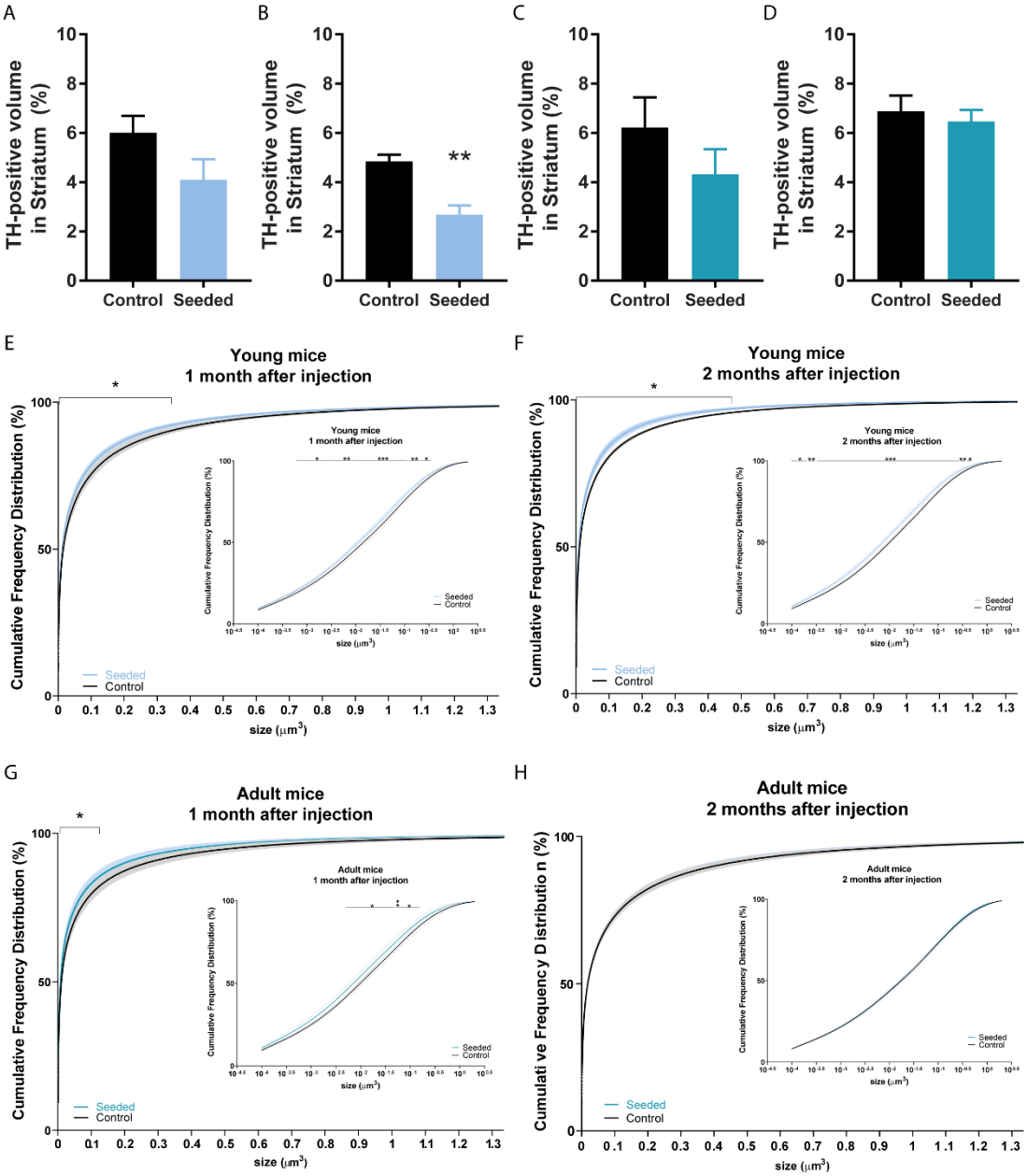

Figure 17. Profile of striatal TH-positive terminals at different time points after injection in young and adult mice. A-D, the volume covered by TH-positive terminals in the estimated dorsolateral striatum area after 1 month (A) and 2 months (B) of injection in young mice, and after 1 month (C) and 2 months (D) of injection in adult mice. Only after 2 months of injection in the young mice, the volume covered by TH-positive terminals is significantly reduced when compared with the contralateral control (***P* < 0.01)**. E-H**, the cumulative frequency distribution of TH-positive terminals in the striatum after 1 and 2 months of injection in young (E-F) and adult mice (G-H). (**P* < 0.05, ***P* < 0.01).

4.4 Neuroinflammation response upon α-synuclein spreading after unilateral PFFs inoculation

4.4.1 In SNpc, the volume proportion of microglia increased after α-synuclein PFFs inoculation in young mice and kept activation overtime

As reported previously, elevated microglial activation was found in PD brains [269, 335] and it can be induced by exposing the brain tissue to misfolded forms of α-synuclein, such as the fibrillary forms [174]. The activated microglia were also found to cluster with the extracellular LBs or other aggregates that are positive to α-synuclein [49]. In my current mouse model, I used microglial coverage volume after PFFs injection to evaluate the activation of microglia. Thus, to better understand the relationship between the alterations along the nigrostriatal pathway and microglial activation in an age-dependent manner, I further quantified the volume covered by IBA1-positive microglia in SNpc at each time point after injection in both young and adult mice. Values were presented as the percentage of coverage volume in the seeded side to the control side.

In the young mice, the microglial coverage volume was higher after 1 month of injection and kept the high level after 2 months compared to the control side (Fig.18 U, A-D). While in the adult mice, microglial coverage volume was slightly increased after 1 month of injection and became less active after 2 months (Fig.18 U, E-H). Consider the different patterns of aggregates formation in SNpc between young and adult mice, the high level of microglial activation coincided with the efficient formation of aggregates in the young mice. While in adult mice, the lower level of activated microglia coincided with the less efficient formation of aggregates compared to the young mice.

Collectively, in SNpc, microglial activation was increased in both young and adult mice after 1 month of injection, although the activation level was always higher than the control side in the young mice (Fig.18 U, two-way ANOVA Main Factor Age $F(1, 16) = 6.366$; $*P < 0.05$). And the level of microglial activation was positively related to the efficiency of aggregates formation.

4.4.2 In striatum, the volume proportion of microglia varied differently in young and adult mice, the proliferation decreased in adult mice overtime

From the above results, I observed a decreased TH-positive terminals in the striatum. Consider the property of microglial activation in SNpc upon α-synuclein aggregates formation, I speculated that the decrease of TH terminals may link to the level of microglial activation in the striatum. Therefore, I further analyzed the microglial coverage volume in the dorsolateral striatum at each time point after injection in both young and adult mice.

In the young mice, the volume covered by microglia in the striatum was increased after 1 month of injection and kept the constant high level after 2 months compared to the control side (Fig.18 V, I-N). While in the adult mice, the microglial coverage volume was increased at 1 month after injection and became comparable to its control side after 2 months (Fig.18 V, O-T). Consider the different patterns of TH-positive terminal distribution in striatum between young and adult mice, the high level of microglial activation coincided with the decreased terminals in the young mice. While in the adult mice, the lower level of activated microglia coincided with the unchanged TH terminal volume compared to the young mice.

To summarize, microglial activation in the striatum was increased in both young and adult mice after 1 month of injection, although the activation level was always higher than the control side in the young mice (Fig. 18 V, two-way ANOVA Main Factor Age $F(1, 16) = 6.366$; $*P < 0.05$). And the level of microglial activation in the striatum was positively related to the declination of striatal TH terminals.

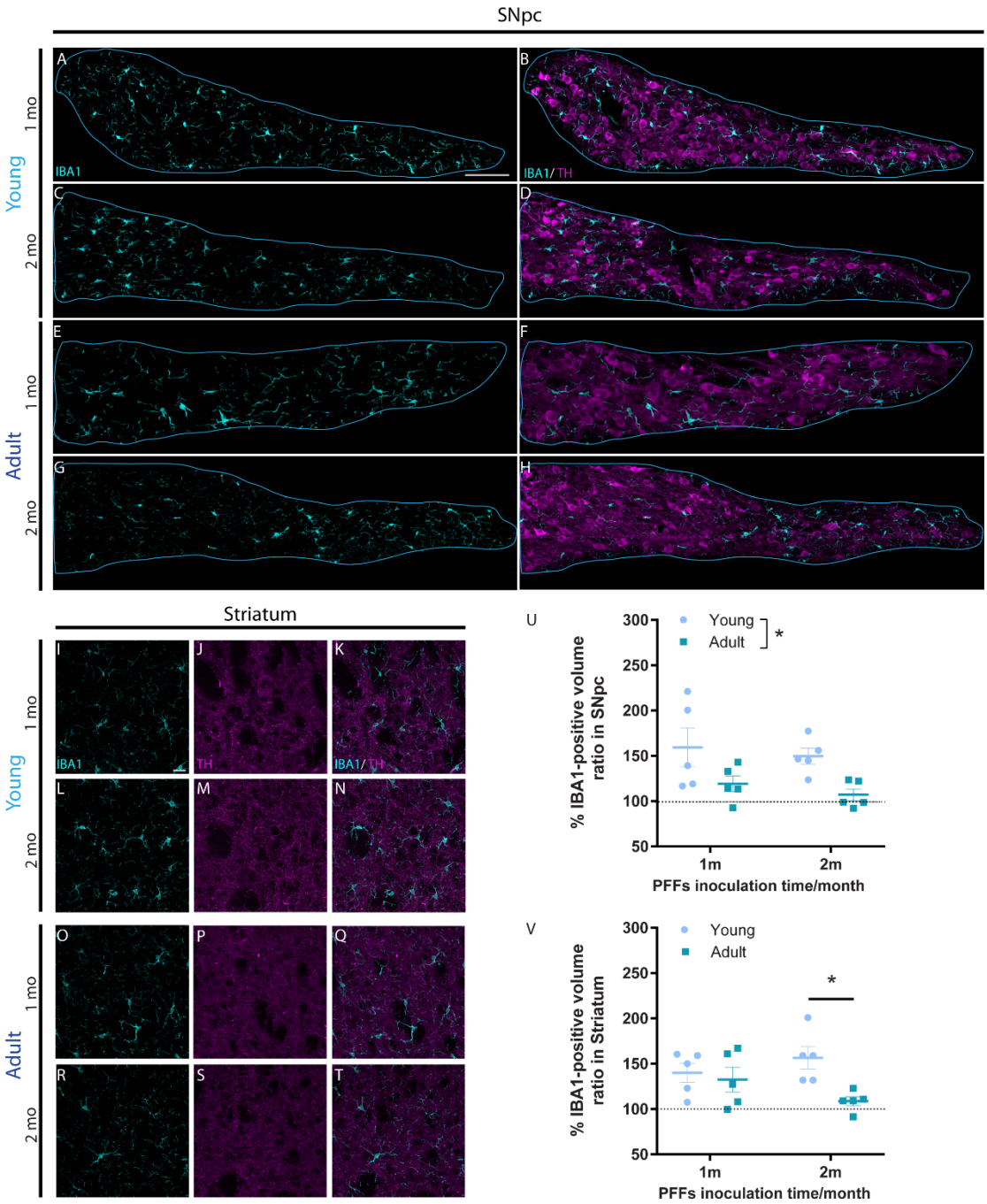

Figure 18. Representative images of IBA1 and TH IHC staining and quantification of IBA1-positive microglia at different time points after injection in SNpc and striatum of young and adult mice. A-H, representative images of IBA1 and TH IHC staining in SNpc at different time points after injection in young and adult mice. **I-T**, representative images of IBA1 and TH IHC staining in the striatum at different time points after injection in young and adult mice. **U-V**, the coverage volume of microglia in SNpc (U) and striatum (V) after 1 and 2 months of PFFs injection in young and old mice (*P<0.05). Values are expressed as the ratio of the microglia coverage volume of the seeded side normalized by the microglia coverage volume of the internal control side. Scale bars, A-H, 100 µm; I-T, 20 µm.

4.5 Microglia repopulation or loss of Trem2 function augmented α-synuclein PFFs induced spreading from striatum to cortex

When PFFs were seeded in the midbrain, I observed relatively limited spreading phenomena to the connected projecting areas in the striatum. As reported in the literature, seeds are more prone to be transferred toward the retrograde route at the early time points [336]. To test the role of microglia in the pathology spreading after PFFs inoculation, I moved to another model that shows more prominent spreading effect. Instead of focusing on the nigrostriatal pathway, I injected α-synuclein PFFs into the dorsal striatum, in which model the α-synuclein pathology spreads more obviously and retrogradely along the cortico-striatal pathway [177].

In this mouse model, α-synuclein PFFs were injection into the dorsal striatum of C57BL/6 wild type mice and Trem2 KO transgenic mice at two months of age. Wild type mice then started to receive PLX5622 (1200 mg/kg chow), which is a CSF1R inhibitor that eliminating microglia from the brain [284, 285]. The wild type mice were administered with the food pellet without PLX5622 as control. Treatment lasted for consecutive six weeks, then all the mice were anaesthetized and subjected to transcardial perfusion for tissue collection (Fig.19). After six weeks of PFFs inoculation in the striatum, α-synuclein aggregates developed into the somatosensory cortex and mainly condensed in the layer IV-V (Fig.20). The proportion of coverage volume of both phospho-α-synuclein positive aggregates and IBA1-positive microglia were quantified in each group.

In PLX5622 treated mice, microglia were mostly depleted in the cortex compared to the control (Fig.21 J, unpaired *t*-test, ****$P<0.0001$). Upon microglia depletion, the coverage volume of aggregates developed in cortex increased significantly compared to the control mice (Fig.21 K, unpaired *t*-test, *$P<0.05$), which indicates that microglia takes an important part in pathological α-synuclein spreading. To investigate the potential mechanism underlying the role of microglia in pathology spreading, aggregates were also quantified in the cortex of Trem2 KO mice after six weeks of PFFs seeding. Upon

knocking out of Trem2 receptor, α-synuclein aggregates accumulate significantly more in the cortex compared to the normal mice (Fig.21 K, unpaired *t*-test, **P* <0.05), while the coverage volume of microglia also increased significantly (Fig.21 J, unpaired *t*-test, **P*<0.05). Considering that Trem2 is an important receptor for regulating the phagocytosis function of microglia, the increase of microglia coverage volume may act as a compensation to the loss of Trem2 function.

Besides, *ex vivo* cell culture of primary microglia isolated from the postnatal mouse pups was also conducted. After microglia cells recovered from isolation procedure and attached to the well surface, Alexa 647 labelled α-synuclein PFFs were added to the cells and the same volume of PBS addition as control. According to the IHC staining results, microglia were able to take up and process PFFs after exposure to the materials and the morphology of microglia also changed obviously compared to the ones exposed to PBS as control (Fig. S3). This result suggests that microglia can internalize α-synuclein materials, which supports the potential role of microglia in affecting the pathology spreading by interacting with α-synuclein.

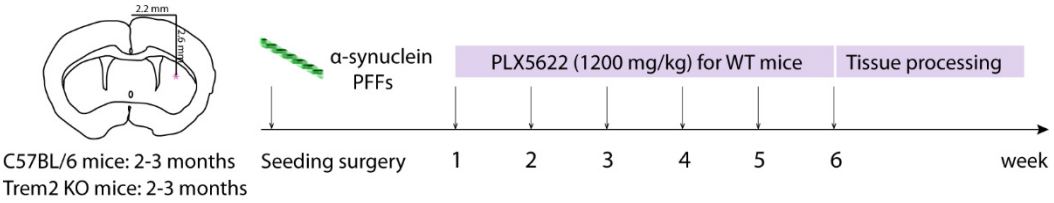

Figure 19. General experimental scheme for intrastriatal PFFs injection and mice treatment.

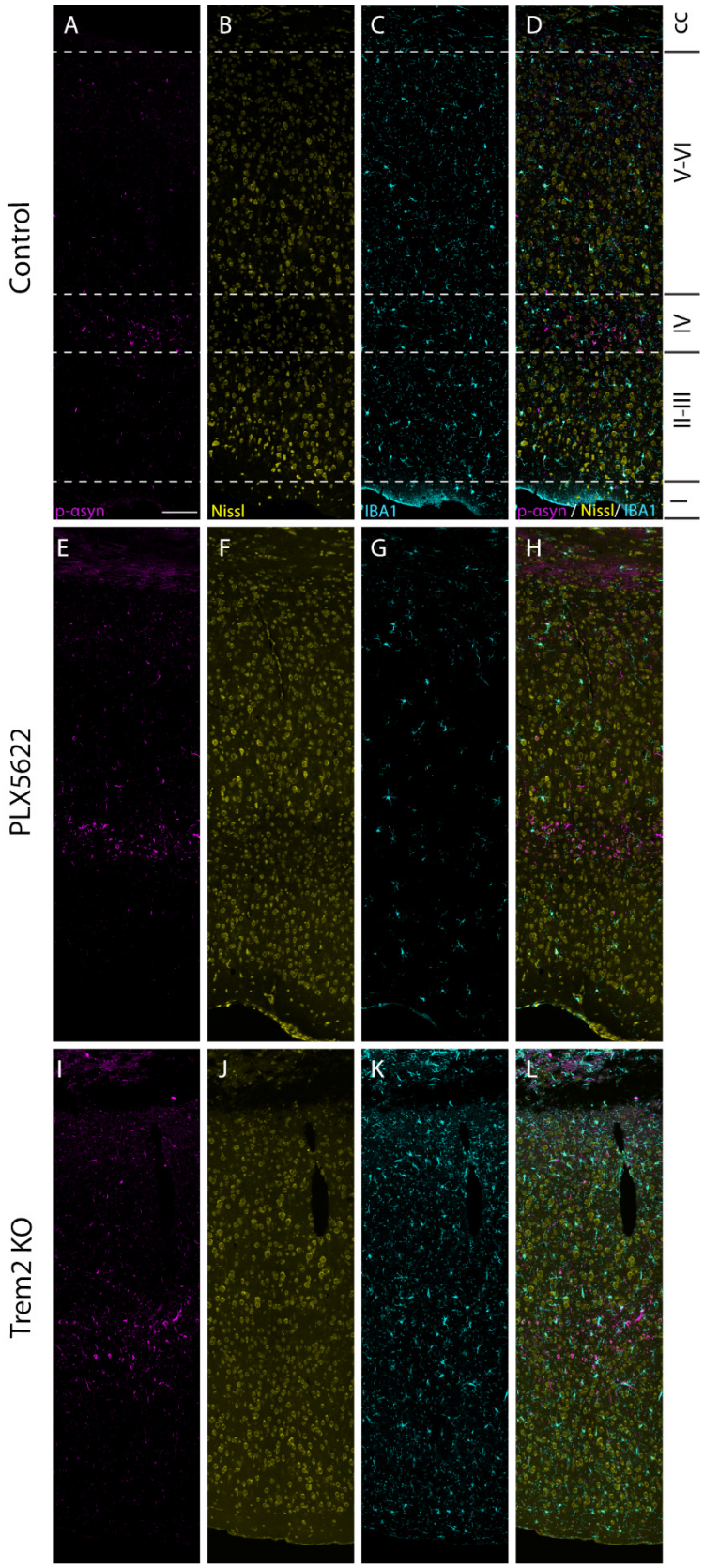

Figure 20. Representative images of phospho-α-synuclein, Nissl and IBA1 IHC staining in somatosensory cortex through all layers. Magenta**:** phospho-α-synuclein (p-αsyn). Yellow: Nissl stain. Cyan: IBA1. I-VI, layer I-VI. cc, corpus callosum. Scale bar, 100 µm.

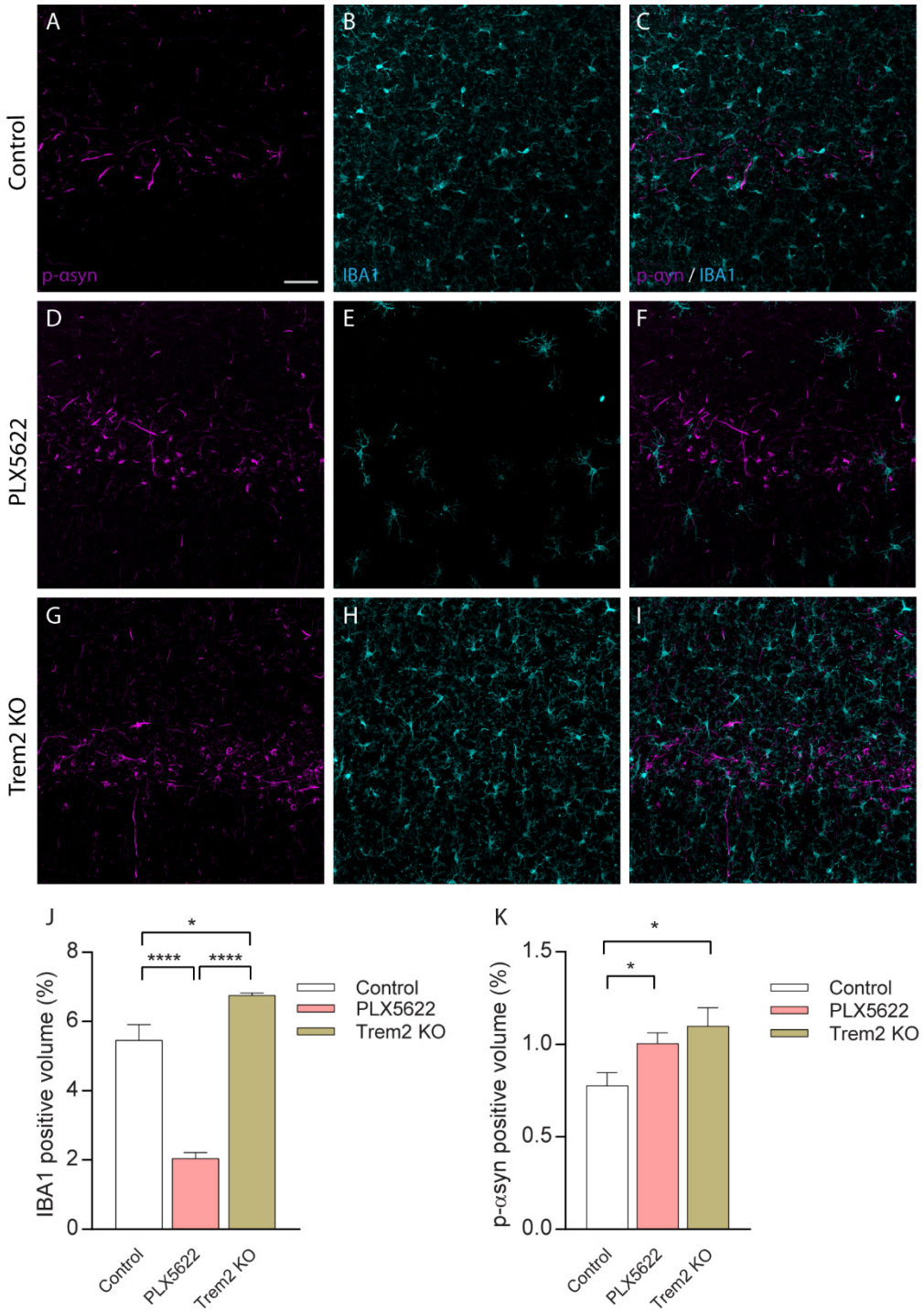

Figure 21. Representative images of phospho-α-synuclein and IBA1 IHC staining and the quantification of microglia and α-synuclein aggregates in somatosensory cortex. Magenta: phospho-α-synuclein (p-αsyn). Cyan: IBA1. Scale bar, 50 µm. (**P*<0.05, *****P*<0.0001)

5. Supplementary figures

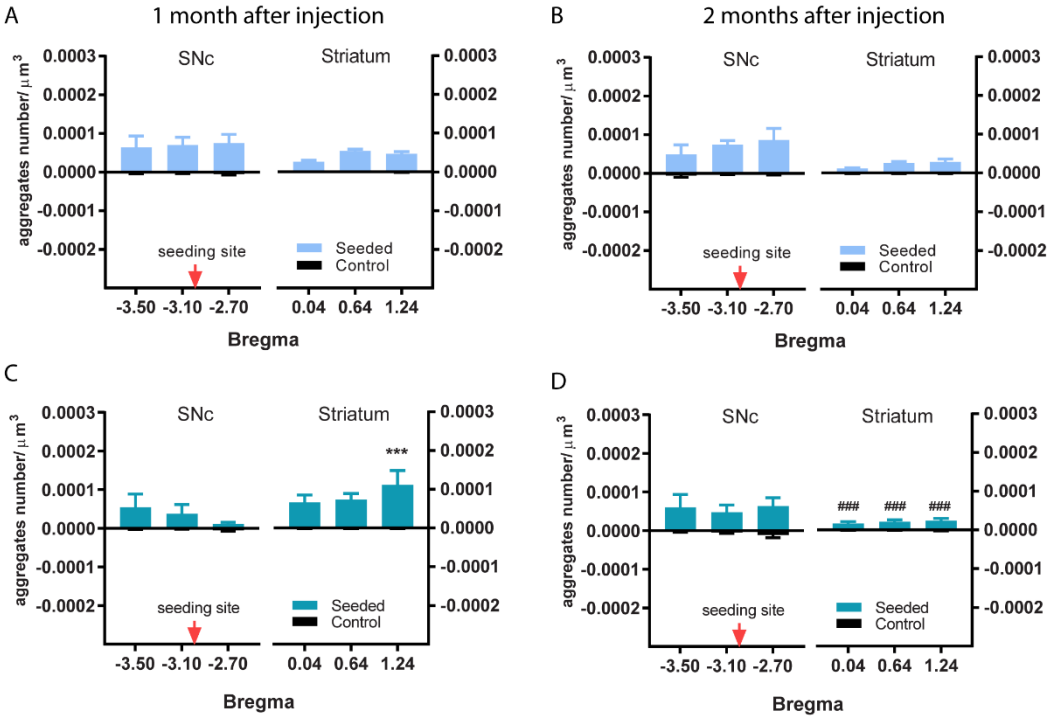

Figure S1. Distribution of phospho-α-synuclein aggregates numbers from SNpc to striatum at different time points after injection in young and adult mice. #comparison between different time points within the same region of the same age (### $P < 0.010$); *comparison between different ages within the same region of the same inoculation time (*** $P < 0.001$).

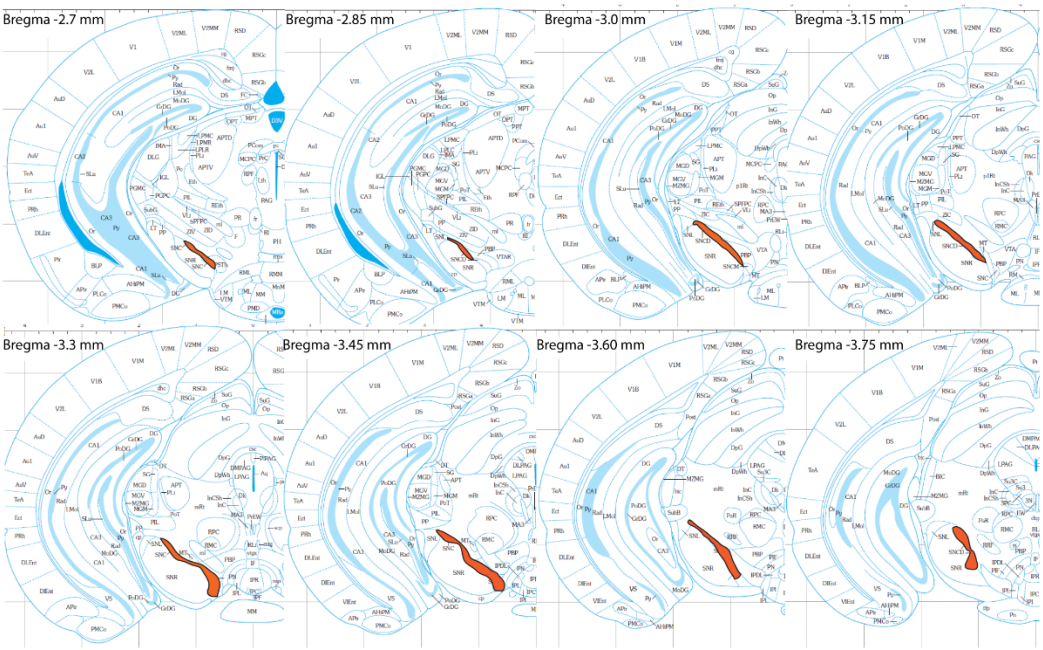

Figure S2. The sampling of stereological cell counting in SNpc. Eight serial brain slices containing SNpc brain region were selected by bregma according to the Mouse Brain Atlas [334] for stereological quantification. Brian slices were cut in 50 μm thickness and picked up with an interval of three, spacing 150 μm from each other.

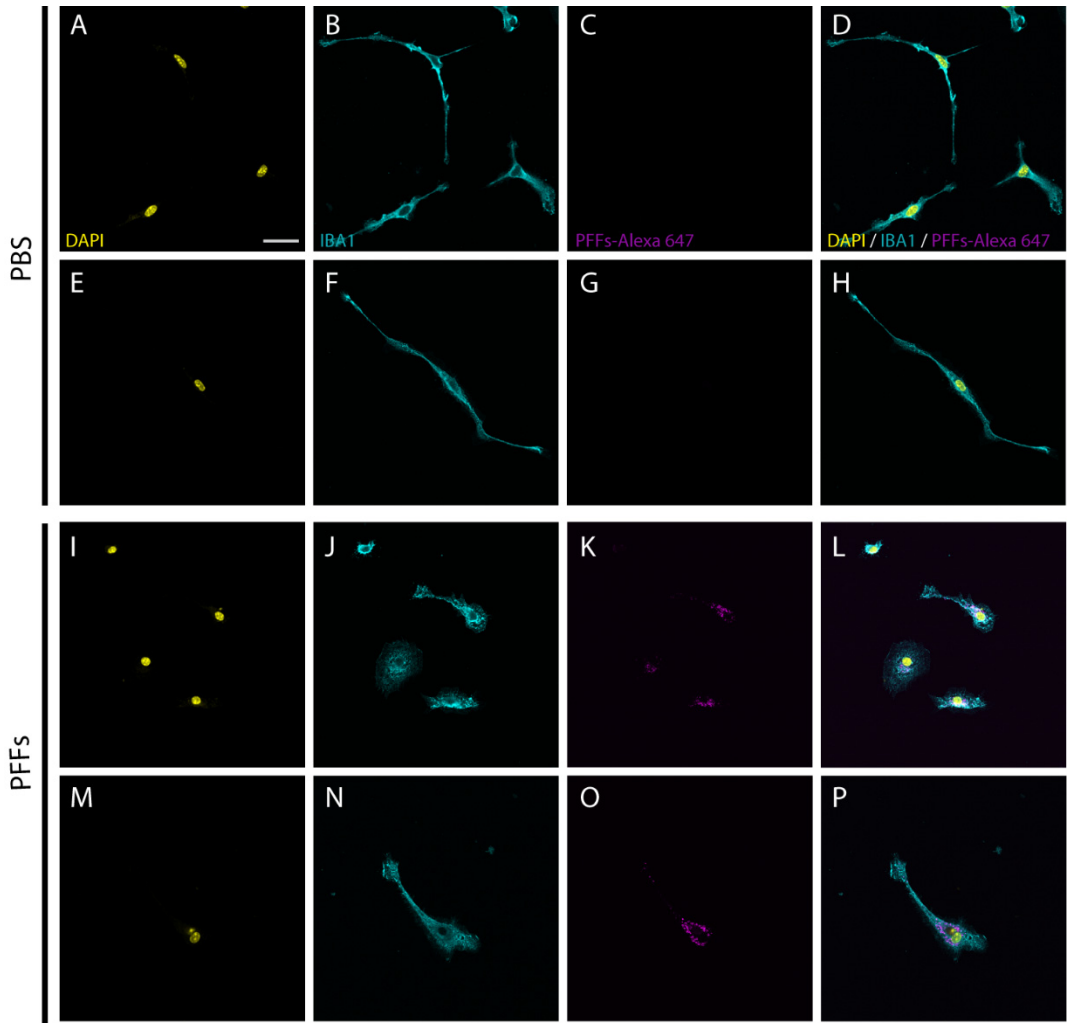

Figure S3. Representative immunofluorescent images of IBA1-positive primary microglia and Alexa 647 tagged α-synuclein PFFs. **A-H**, images of PBS treated primary microglia; **I-P**, images of PFFs treated primary microglia. Yellow: DAPI. Cyan: IBA1. Magenta: PFFs-Alexa 647. Scale bar, 30 µm.

6. Discussion

6.1 Age impact on pathology development triggered by PFFs seeding

As reported in several *in vitro* biophysical studies, the formation of α-synuclein fibrils is nucleation-dependent. Following a rapid consumption of monomers, fibrils get formed. This is thought to be the potential mechanism of the spreading of α-synuclein pathology along interconnected brain regions [165-167]. Therefore, exploring the process of template misfolding, aggregates formation and propagation of α-synuclein is of great importance to understand the pathogenesis of PD and other α-synucleinopathies. Spreading of α-synuclein pathology has been intensively studied via *in vitro* or *in vivo*, by introducing the brain homogenates from patients or recombinant α-synuclein PFFs in cell culture and experimental animals [83, 85, 209, 210, 213, 230].

However, it is still not clear how misfolded species conduct spreading from cell to cell throughout the brain. Several studies have reported the possible ways of α-synuclein transmission. For example, α-synuclein aggregates can be released directly from dead cells or may penetrate membranes by other means [337]. Alternatively, they can be transported through retrograde axonal trafficking [215]. Also, being conveyed and released by calcium-dependent exosomes [224], α-synuclein can enter the neighbouring cells through endocytosis [218, 219]. Besides, TNTs-dependent lysosomal vesicles transport has also been considered as a way to spread [220].

As a newly important tool in PD research, a mouse model focusing on the misfolded and aggregated α-synuclein has received high attention. In this model, an intracerebral injection of recombinant α-synuclein PFFs can trigger LBs-like pathology. However, the different sources of α-synuclein have also been debated regarding the efficiency in triggering consistent pathology. By seeding in the mouse brain, wild type mouse α-synuclein PFFs can induce the pathology within weeks, while the human source PFFs can take months [83, 85, 181]. In previous studies, seeding models are mostly used to explore the pathology development within one age group. Whereas, functional changes and the age impact are remained to be investigated. To close this gap, my study was

using the recombinant mouse α-synuclein PFFs to inoculate with the dopaminergic neurons in SNpc. With this model, I aimed to explore the effects of α-synuclein spreading on the functional and morphological alterations along the nigrostriatal dopaminergic pathway in an age-dependent manner. To validate the site of injection, I mixed the tdTomato-tagged AAVs with seeding materials to inject into different aged TH-IRES-Cre mice brains. As shown in Figure 10 C-F, the dopaminergic neuron population in SNpc and their terminals in the striatum were well labelled with the fluorescent protein. This confirmed that the coordinates I used for the stereotactic injection were the target SNpc region.

After 1 month of PFFs inoculation in SNpc, I observed that the phospho-α-synuclein (pS129) positive aggregates already formed around the seeding site in both young and adult mice. However, according to the quantification, the young mice developed a significantly higher volume of aggregates in SNpc compared to the adult mice (Fig.12 A and C). This indicates that the younger mice tend to conduct a more efficient aggregation process than the adult mice once the template seeding is triggered. Interestingly, I found that in the striatum, the volume of aggregates was not similar to the phenomena in SNpc between the two age groups. In the striatum, the volume of aggregates is much higher in the adult mice compared to the young mice (Fig.12 A and C). Considering the aggregation pattern in SNpc, it is very likely that the young mice have a higher ability to convert the misfolded α-synuclein into highly condensed aggregates within a short time window. This efficient formation of aggregates might contribute to the reduced propagation of misfolded α-synuclein from SNpc to the striatum.

After 2 months of PFFs inoculation, the volume of aggregates in SNpc showed a significant increase in both young and adult mice compared to the volume at 1 month (Fig.12 B and D). Whereas, the volume of aggregates in SNpc was still significantly higher in the young mice compared to the adult mice. While in the striatum, the volume of α-synuclein aggregates in both young and adult group became comparable (Fig.12 B and D). The above observations also coincided with the diffusion pattern of pathology as

displayed in Figure S1. In the striatum, the number of aggregates was much higher in the adult mice after 1 month of inoculation, while in the young mice the number was always lower after injection. This result also supports the notion that the young mice tended to possess a stronger ability to form aggregates in SNpc when PFFs were introduced, and this process was significantly more efficient than that in the adult mice. Moreover, the higher efficient formation of aggregates within the SNpc, in turn, results in a lower quantity of α-synuclein pathology propagating into the striatum.

6.2 DA neurotransmission and exogenous α-synuclein seeding

The native α-synuclein is a small, soluble and mostly presynaptic protein, which plays an essential role in the presynaptic functions. For example, α-synuclein can bind to tubulin and promote the formation of microtubules, regulating the fusion and clustering of presynaptic vesicles. It is also involved in the exocytosis process as well as the presynaptic dopamine release [205]. As a critical protein in PD, the level of α-synuclein expression can affect dopamine release. Under physiological α-synuclein expression levels, the function of dopamine release is maintained. Whereas, overexpression or mutations of α-synuclein leads to decreased dopamine release. Furthermore, depletion of α-synuclein results in the enhanced level of dopamine release. As reported in the previous studies, the corresponding changes of neurotransmission under different levels of α-synuclein are probably due to the dysfunction of related factors in dopamine release, such as VMAT2, DAT or the alteration of synaptic vesicle pools [126, 140, 147, 148, 150, 338].

However, these conclusions are based on studies using transgenic animal models or *in vitro* experiments. It is still not known how the dopamine release function would change in the context of exogenous α-synuclein inoculation along the dopaminergic pathway. Though some of the research measured the DA contents and DA release based on seeding models, they mainly used HPLC-based methods for analyzing brain tissue homogenates [83], which are less sensitive tools compared to the sub-second resolution

FSCV and less relevant for PD research compared to the seeding model in the midbrain.

In my study, I injected the α-synuclein PFFs into the midbrain and measured the dopamine release in dorsolateral striatum after two different inoculation time points, in two cohorts of mice with different ages (2 months old, defined as the young cohort; and 5 months old defined as the adult cohort). Interestingly, I found exclusively in the adult mice, the electrically evoked dopamine release significantly decreased by about 25% compared to its control side after 2 months of PFFs injection (Fig.11 E). Similar to the distribution of aggregates in the striatum, the dopamine release did not change significantly in the young mice.

In the young mice, unchanged dopamine release coincided with the low volume of striatal aggregates retaining after 1 and 2 months of PFFs inoculation. While in the adult mice, the volume of aggregated α-synuclein in the striatum was significantly higher after 1 month of PFFs inoculation. However, the aggregates volume became comparable to that observed in the young mice after 2 months. It seems that the striatal neuronal network in the adult mice underwent a substantial compensatory activity to recover from the higher volume of aggregates at 1 month, and eventually resulted in a neurotransmitter release dysfunction at 2 months after injection.

Moreover, the uptake rate of dopamine in each group did not change significantly compared to their control side (Fig.11 F). The unchanged uptake rate of dopamine suggests that the decreased striatal dopamine release in the adult mice is not likely to be related to the function of dopamine transporters. I considered the different patterns of dopamine release in each group might be linked to the potential loss of dopaminergic neuron population in SNpc. Alternatively, it is related to the morphological or functional alterations of these striatal terminals themselves.

6.3 Degeneration along the dopaminergic pathway in the seeding model

In PD, as the disease progresses, neuronal loss commonly explains the cause of decreased dopamine level in the striatum, which further contributes to the onset of motor dysfunctions. Translated into animal models, phenotypical neuronal loss and terminal degeneration have been observed. For example, in mice overexpressing wild type and mutant α-synuclein, chemical reagents induced PD models, viral-vector-driven and PFFs or other pathological α-synuclein materials injected animal models [67-86].

In my current study, I observed that dopamine release function was impaired after 2 months of PFFs inoculation in the adult mice. To verify whether this declination was related to the nigral degeneration, I further estimated the number of dopaminergic neuron population in SNpc of this group. Results from unbiased stereological counting showed that the total number of TH-positive dopaminergic neurons and the total neuronal cells in SNpc did not change significantly compared to its control side. Therefore, the inoculation of α-synuclein PFFs in SNpc did not cause a neuronal loss after 2 months of injection. Moreover, it also indicated that the decreased striatal dopamine release was not due to the loss of dopaminergic neurons in SNpc, which is consistent with the observations from other groups [85].

Thus, I speculate that the alteration of striatal dopamine release might be linked to a specific mechanism in the local striatal network. Therefore, I focused the further analysis on the striatal network. Interestingly, I observed a specific distribution of the pattern of dopaminergic terminals that correlated with the pathophysiological phenotype of dopamine release. From the quantification of the volume covered by TH-positive terminals in the dorsolateral striatum (Fig.17 A-D), a slight but not significant decline occurred in both young and adult mice after 1 month of PFFs inoculation. More importantly, a significant decrease of the volume covered by terminals was observed in the young mice after 2 months of PFFs inoculation. Whereas, in the adult mice, the

volume covered by striatal terminals did not change obviously in the ipsilateral seeded side compared to the control side.

Upon the significant decrease of the dopaminergic terminals in the young mice, I was curious about whether the terminal profile also changed correspondingly. Therefore, I further analyzed the cumulative frequency distribution of terminal sizes in the dorsolateral striatum of each age group. Interestingly, in the groups that sustained a normal dopamine release capability, the cumulative frequency distribution curves of TH-positive terminals upon size (μm^3) displayed a significant left-shifted profile in the seeded side compared to the control side (Fig.17 E-G). While in the adult mice that suffered from dopamine release declination, the terminal distribution pattern did not change compared to the control side (Fig.17 H), as was also seen in the total volume of terminals (Fig.17 D). The left-shifted profile indicates that the portion of small-sized terminals is significantly higher. It, in turn, reveals that the decreased terminals are very likely to be the portion of large-sized terminals. Considering the preserved dopamine release, the higher proportion of small terminals may help to maintain a normal function of dopamine release once being interfered by α-synuclein pathology.

Taken together, the altered pattern of striatal terminals in the young brains suggests that the striatal neuronal network can preserve the function of dopamine release by removing a certain type of terminals. Large-sized terminals are very likely to decrease since the smaller ones displayed an increased portion. Considering that the aggregates are probably prone to form in the larger terminals, as a response, the local neuronal network (for example the glial activation) might be activated. As a result, the defective larger terminals that contain aggregates are probably removed, and the total volume covered by dopaminergic terminals decreases accordingly. Whereas, the portion of small terminals is increased, and the function of dopamine release is spared.

6.4 Participation of microglia in the progression of α-synuclein pathology

In PD cases and other α-synucleinopathies like MSA, microglial activation has been found to play a role during the progression of the disease [269, 335]. Studies based on experimental animal models of PD also have shown the participation of neuroinflammation in several critical physiological processes during disease. For example, the relationship with different α-synuclein species and organelles like mitochondria [288, 308, 339]. Besides, the inflammatory responses can induce intrinsic vulnerability of dopaminergic neurons in SNpc. This susceptibility may relate to the metabolism of dopamine, high iron content, calcium signalling and deficient antioxidant activity [340]. As the immune cells of the brain, microglia behave differently depending on the different states: in surveillance or activation. Once becoming activated, microglia can phagocytose apoptotic cells, myelin or axonal debris and protein aggregates [237]. At the synaptic level, microglia are responsible for monitoring and pruning dendritic spines. Microglial activation can be triggered by many factors. For instance, α-synuclein has been reported to induce the activation of microglia, which is mediated by different factors like MHCII [295], TLR2 [296] and TLR4 [298, 299]. The number of phagocytic microglia have been found to be linked to the duration of PD, the coincidence with α-synuclein depositions and the expression level of MCHII [302]. Besides, among many factors that are important for microglial proliferation and phagocytosis, Trem2 has been newly found to be a risk factor in PD [250, 255-257]. However, the role of Trem2 is not clearly established in PD, especially in terms of microglia affecting the spreading of α-synuclein pathology.

6.4.1 Microglia and neurotransmission: from the SNpc to the striatum

In my current study, I injected α-synuclein PFFs into SNpc of mice with different ages and measured dopamine release after 1 and 2 months, respectively. I found that pathological α-synuclein aggregated and propagated differently in young and adult mice. Moreover, the function of dopamine release also changed differently depending on age. By analyzing TH-positive terminals in the striatum, I noticed the coincidence between the alteration of dopaminergic terminals and the function of dopamine release. Decreased volume covered by TH terminals coincides with a spared function of dopamine release and vice versa. This phenomenon is reminiscent of the speculation that a certain mechanism or function might reduce TH terminals and further maintain the normal function of dopamine release. Considering the strong link between neuroinflammation and PD, I speculate that the alteration of TH terminals does involve microglial activation, which may be mediated by the misfolded α-synuclein. Thus, to find out the potential correlation, I determined the coverage volume of microglia in SNpc (Fig.18 U) and striatum (Fig.18 V) after 1 and 2 months of injection in both young and adult mice.

After 1 month of injection, the volume covered by microglia in SNpc was increased in both young and adult mice compared to the control side. However, the young mice displayed a significantly higher level of microglial coverage than the adult mice. Similarly, after 2 months of injection, the volume covered by microglia in SNpc was still higher in the young mice. Considering the formation of aggregates in SNpc, it seems that the high level of microglial coverage goes along with the efficient formation of aggregates in the young mice. Whereas, it is to the contrary of what I observed in the adult mice. This suggests that the formation process of aggregates correlates with the induction of microglial activation.

In the striatum, the volume covered by microglia was higher in both young and adult mice after 1 month of injection compared to their control sides. However, the high level of microglial coverage was constantly enhanced only in the young mice after 2 months. Combined with the observation of TH terminal distribution, it seems that the high

volume of microglial coverage goes along with the decreased coverage volume of terminals. It suggests that the reduced coverage volume of TH terminals is very likely to result from the high level of microglial activation. The interaction between TH terminals and microglia might contribute to the regulation of dopamine release, which is mediated by the α-synuclein pathology. Note that the volume of α-synuclein aggregates was significantly higher in the striatum of adult mice after 1 month of injection, while the coverage volume of microglia was decreased from 1 to 2 months after injection. This indicates that microglia in the striatum of adult mice probably compromise a lot from the overloaded aggregates at 1 month. Nevertheless, microglia in the adult mice seem not as active as that in the young mice when the pathogens have been introduced. Taken together, it suggests that the ability to have microglia activated is to some extent age-dependent. Compared to the "old microglia", the "young microglia" can react appropriately to the changes in the brain environment to preserve its normal function in neurotransmission.

6.4.2 Microglia and pathology spreading: from the striatum to the cerebral cortex

Since I observed that the distribution of α-synuclein pathology and the activation of microglia were different depending on age, it is of great interest to know how microglia affects the development of pathology, especially on the spreading process. Thus, I further moved on to another seeding model that shows more prominent spreading effect. As to the striato-cortical seeding, the spreading of α-synuclein species follows retrograde transportation. This model displays more pronounced aggregates compared with the nigrostriatal spreading model used so far. In this set of experiments, I injected α-synuclein PFFs into the dorsal striatum of wild type mice aged two months, followed by a consecutive six-week of PLX5622 treatment. PLX5622 is a CSF1R inhibitor that depletes microglia from the brain. Following the depletion of microglia, the amount of α-synuclein aggregates was significantly higher in the somatosensory cortex compared to

the control mice. It suggests an essential role of microglia upon the spreading of pathology from the striatum to the cerebral cortex. Besides, from my *in vitro* experiments, I observed cultured primary microglia was able to engulf and uptake α-synuclein contents (Fig. S3). Therefore, I speculate that microglia may restrict the pathological spreading by uptake and probably further degradation of misfolded proteins.

One of the important functions of microglia is phagocytosis, which helps to scavenge dead cells, debris and other pathogens [237]. According to the literature, Trem2 is specifically expressed in microglia, which can modulate the microglial activation and regulate its phagocytosis function, proliferation and survival [341-344]. Apart from its strong link in AD, Trem2 is also a newly identified risk factor for PD and plays a vital role in α-synuclein related neuroinflammation [345-347]. Therefore, I further injected PFFs into the dorsal striatum of two months old Trem2 KO mice and measured the volume of aggregates in the somatosensory cortex. Interestingly, similar to the PLX5622 treated mice, the amount of α-synuclein aggregates in the somatosensory cortex of Trem2 KO mice was significantly higher compared to the control mice after six weeks of PFFs inoculation. It suggests an intriguing role of Trem2 in the spreading of α-synuclein pathology. Upon the loss of Trem2 function, the misfolded α-synuclein might become more prone to propagate into the cortex when the template seeding has been introduced in the striatum. Besides, compared to the control mice, I also observed a higher coverage volume of microglia in the cortex of Trem2 KO mice. The increased volume covered by microglia might be a compensatory response to the loss of Trem2 function.

In summary, during α-synuclein spreading from the striatum to the cerebral cortex, microglia may act as a barrier probably by uptake and degradation of misfolded protein species. This restrictive role of microglia in α-synuclein spreading is (perhaps not only) dependent on the function of Trem2.

6.5 Potential mechanisms and future directions

In this current study, two types of PFFs injections into the mouse brains were used. To clarify the role of ageing and neuroinflammation in neurotransmission along α-synuclein PFFs inoculated nigrostriatal dopaminergic pathway, I injected PFFs into the midbrain of mice with different ages. Misfolded α-synuclein is transported in an anterograde direction from the SNpc to the striatum. Striatal dopamine release and detailed morphological measurements were analyzed at each predetermined time points in both young and adult mouse groups. To further investigate the role of microglia in the spreading of α-synuclein pathology, I injected PFFs into the dorsal striatum of mice and measured morphological alterations in the somatosensory cortex. In this model, the transmission of misfolded α-synuclein follows a retrograde transport along the cortico-striatal pathway from the striatum to the cerebral cortex.

Along the nigrostriatal pathway, a very efficient formation process of aggregates was observed in the young mouse midbrain, and the pathology propagation into striatum always stayed at a low level. However, this low level of striatal aggregates was enough to activate microglia. Microglial activation further maintained the homeostasis of striatal neuronal network. During maintaining of the local physiological function, a portion of TH terminals was probably removed. It is very likely that the large-sized terminals were removed since the system was prone to have more small-sized terminals according to the cumulative frequency distribution analysis of the terminal sizes. Moreover, aggregates were more commonly found to form in the large terminals, which may activate microglia. It suggests a role of microglia in removing large terminals containing misfolded proteins, by which the normal function of dopamine release in the striatum is preserved. Whereas, the adult mice were not able to efficiently form such aggregates, which led to a much stronger propagation into the striatum. This large amount of aggregates also triggered the activation of microglia, though not as strong as in the young mice. In the adult mice, the microglial activation coincided with the preserved DA neurotransmission at the early stage (1 month after PFFs injection) and secured the

striatal pathology under a low level later on. However, due to the overloaded striatal pathology and the different microglia age in the adult mice, microglial activation might be compromised. As a result, the terminals containing aggregates in the adult mice were preserved but do not function properly anymore, which eventually led to the observed dysfunction of dopamine release in the striatum. This study particularly stressed the impact of age on α-synuclein propagation, which further affects the neuroinflammatory activity as well as the dopaminergic neurotransmission.

As to the spreading of pathology along the cortico-striatal pathway, Trem2-dependent microglia function plays a crucial role in acting as a barrier during spreading. PLX5622 is a CSF1R inhibitor that can globally eliminate microglia from the brain. Upon the depletion of microglia, there was significantly more α-synuclein spreading into the cerebral cortex following a retrograde transmission from the striatum. Similarly, mice lacking Trem2 also displayed a much higher amount of α-synuclein aggregates in the cerebral cortex. Meanwhile, the coverage volume of microglia was statistically increased in the Trem2 KO mice compared to the control mice. It indicates that the presence of microglia is not enough to prevent the insults unless they are fully functional. With this observation, my study highlights the role of microglia in restricting the retrograde transmission of misfolded α-synuclein from the striatum to the cerebral cortex, probably in a Trem2-dependent manner.

Although more experiments might be needed to further confirm the role of Trem2 in microglia-involved alleviation of α-synuclein spreading throughout the brain. For example, the knock-in of Trem2 might provide more information about the modulation mechanism. Besides, it also arouses much interest to explore the role of Trem2 in neurotransmission along the dopaminergic pathway for the future study. For example, α-synuclein PFFs could be injected into the midbrain of Trem2 KO mice at different ages. Furthermore, the injected Trem2 KO mice would be subjected to the measurements of striatal DA release, to explore the pathology spreading along the nigrostriatal pathway as well as other morphological analysis at different inoculation time points.

In conclusion, my current study addressed the role of ageing in pathological α-synuclein spreading, dopaminergic neurotransmission, microglial activation, and their potential interactions. The young mouse brain shows very little α-synuclein spreading through an efficient way to promote local aggregation of the seeded material at the injection side, which involves a robust microglial activation differently to the adult mouse brain. The highly activated microglia might help to preserve a normal striatal dopamine release, which is probably through removing aggregates from affected large terminals. Furthermore, loss of Trem2 in microglia shows a significant effect on pathological α-synuclein spreading.

Bibliography

1. Heemels, M.-T., Neurodegenerative diseases. Nature, 2016. **539**(7628): p. 179-180.
2. Wyss-Coray, T., Ageing, neurodegeneration and brain rejuvenation. Nature, 2016. **539**(7628): p. 180-186.
3. Dugger, B.N. and D.W. Dickson, Pathology of neurodegenerative diseases. Cold Spring Harbor perspectives in biology, 2017. **9**(7): p. a028035.
4. Stopschinski, B.E. and M.I. Diamond, The prion model for progression and diversity of neurodegenerative diseases. The Lancet Neurology, 2017. **16**(4): p. 323-332.
5. Spires-Jones, T.L., J. Attems, and D.R. Thal, Interactions of pathological proteins in neurodegenerative diseases. Acta Neuropathol, 2017. **134**(2): p. 187-205.
6. De Lau, L.M. and M.M. Breteler, Epidemiology of Parkinson's disease. The Lancet Neurology, 2006. **5**(6): p. 525-535.
7. Bear, M.F., B.W. Connors, and M.A. Paradiso, Neuroscience. 2016.
8. Shrimanker, I., P. Tadi, and J.C. Sánchez-Manso, Parkinsonism, in StatPearls [Internet]. 2019, StatPearls Publishing.
9. Pfeiffer, R.F., Non-motor symptoms in Parkinson's disease. Parkinsonism & related disorders, 2016. **22**: p. S119-S122.
10. Aarsland, D., et al., Prevalence and characteristics of dementia in Parkinson disease: an 8-year prospective study. Archives of neurology, 2003. **60**(3): p. 387-392.
11. Halliday, G., et al., The progression of pathology in longitudinally followed patients with Parkinson’s disease. Acta neuropathologica, 2008. **115**(4): p. 409-415.
12. Dauer, W. and S. Przedborski, Parkinson's disease: mechanisms and models. Neuron, 2003. **39**(6): p. 889-909.
13. Polymeropoulos, M.H., et al., Mutation in the α-synuclein gene identified in families with Parkinson's disease. science, 1997. **276**(5321): p. 2045-2047.
14. Spatola, M. and C. Wider, Genetics of Parkinson's disease: the yield. Parkinsonism & related disorders, 2014. **20**: p. S35-S38.
15. Sidransky, E., et al., Multicenter analysis of glucocerebrosidase mutations in Parkinson's disease. New England Journal of Medicine, 2009. **361**(17): p. 1651-1661.
16. Klein, C. and A. Westenberger, Genetics of Parkinson’s disease. Cold Spring Harbor perspectives in medicine, 2012. **2**(1): p. a008888.
17. MacLeod, D.A., et al., RAB7L1 interacts with LRRK2 to modify intraneuronal protein sorting and Parkinson’s disease risk. Neuron, 2013. **77**(3): p. 425-439.
18. Rhodes, S.L., et al., Replication of GWAS associations for GAK and MAPT in Parkinson's disease. Annals of human genetics, 2011. **75**(2): p. 195-200.

19. Mata, I.F., et al., APOE, MAPT, and SNCA genes and cognitive performance in Parkinson disease. JAMA neurology, 2014. **71**(11): p. 1405-1412.

20. Bender, A., et al., High levels of mitochondrial DNA deletions in substantia nigra neurons in aging and Parkinson disease. Nature genetics, 2006. **38**(5): p. 515-517.

21. Vilchez, D., I. Saez, and A. Dillin, The role of protein clearance mechanisms in organismal ageing and age-related diseases. Nature communications, 2014. **5**(1): p. 1-13.

22. Wong, Y.C. and E.L. Holzbaur, Autophagosome dynamics in neurodegeneration at a glance. J Cell Sci, 2015. **128**(7): p. 1259-1267.

23. Finkel, T. and N.J. Holbrook, Oxidants, oxidative stress and the biology of ageing. Nature, 2000. **408**(6809): p. 239.

24. Giasson, B.I., et al., Oxidative damage linked to neurodegeneration by selective α-synuclein nitration in synucleinopathy lesions. Science, 2000. **290**(5493): p. 985-989.

25. Choi, H.K., et al., Purine-rich foods, dairy and protein intake, and the risk of gout in men. New England Journal of Medicine, 2004. **350**(11): p. 1093-1103.

26. Ascherio, A. and M.A. Schwarzschild, The epidemiology of Parkinson's disease: risk factors and prevention. The Lancet Neurology, 2016. **15**(12): p. 1257-1272.

27. Flagmeier, P., et al., Mutations associated with familial Parkinson's disease alter the initiation and amplification steps of α-synuclein aggregation. Proceedings of the National Academy of Sciences, 2016. **113**(37): p. 10328-10333.

28. Holdorff, B., Friedrich Heinrich Lewy (1885–1950) and his work. Journal of the History of the Neurosciences, 2002. **11**(1): p. 19-28.

29. Beal, M.F., Experimental models of Parkinson's disease. Nature reviews neuroscience, 2001. **2**(5): p. 325-332.

30. Volpicelli-Daley, L.A., et al., Formation of α-synuclein Lewy neurite–like aggregates in axons impedes the transport of distinct endosomes. Molecular biology of the cell, 2014. **25**(25): p. 4010-4023.

31. Duda, J.E., et al., Novel antibodies to synuclein show abundant striatal pathology in Lewy body diseases. Annals of neurology, 2002. **52**(2): p. 205-210.

32. Baba, M., et al., Aggregation of alpha-synuclein in Lewy bodies of sporadic Parkinson's disease and dementia with Lewy bodies. The American journal of pathology, 1998. **152**(4): p. 879.

33. Spillantini, M.G., et al., α-Synuclein in Lewy bodies. Nature, 1997. **388**(6645): p. 839-840.

34. Auluck, P.K., G. Caraveo, and S. Lindquist, α-Synuclein: membrane interactions and toxicity in Parkinson's disease. Annual review of cell and developmental biology,

2010. **26**: p. 211-233.

35. Braak, H., et al., Staging of brain pathology related to sporadic Parkinson's disease. Neurobiology of aging, 2003. **24**(2): p. 197-211.

36. Rey, N.L., et al., Transfer of human α-synuclein from the olfactory bulb to interconnected brain regions in mice. Acta neuropathologica, 2013. **126**(4): p. 555-573.

37. Sánchez-Ferro, Á., et al., In vivo gastric detection of α-synuclein inclusions in Parkinson's disease. Movement Disorders, 2015. **30**(4): p. 517-524.

38. Shannon, K.M., et al., Alpha-synuclein in colonic submucosa in early untreated Parkinson's disease. Movement Disorders, 2012. **27**(6): p. 709-715.

39. Hawkes, C.H., K. Del Tredici, and H. Braak, A timeline for Parkinson's disease. Parkinsonism & related disorders, 2010. **16**(2): p. 79-84.

40. Challis, C., et al., Gut-seeded alpha-synuclein fibrils promote gut dysfunction and brain pathology specifically in aged mice. Nat Neurosci, 2020.

41. Makin, S., Pathology: the prion principle. Nature, 2016. **538**(7626): p. S13-S16.

42. González-Hernández, T., et al., Vulnerability of mesostriatal dopaminergic neurons in Parkinson's disease. Frontiers in neuroanatomy, 2010. **4**: p. 140.

43. Fearnley, J.M. and A.J. Lees, Ageing and Parkinson's disease: substantia nigra regional selectivity. Brain, 1991. **114**(5): p. 2283-2301.

44. Bernheimer, H., et al., Brain dopamine and the syndromes of Parkinson and Huntington Clinical, morphological and neurochemical correlations. Journal of the neurological sciences, 1973. **20**(4): p. 415-455.

45. Surmeier, D.J., J.A. Obeso, and G.M. Halliday, Parkinson's disease is not simply a prion disorder. Journal of Neuroscience, 2017. **37**(41): p. 9799-9807.

46. Mosharov, E.V., et al., Interplay between cytosolic dopamine, calcium, and α-synuclein causes selective death of substantia nigra neurons. Neuron, 2009. **62**(2): p. 218-229.

47. Dryanovski, D.I., et al., Calcium entry and α-synuclein inclusions elevate dendritic mitochondrial oxidant stress in dopaminergic neurons. Journal of Neuroscience, 2013. **33**(24): p. 10154-10164.

48. Kordower, J.H., et al., Disease duration and the integrity of the nigrostriatal system in Parkinson's disease. Brain, 2013. **136**(8): p. 2419-2431.

49. McGeer, P.L., et al., Reactive microglia are positive for HLA-DR in the substantia nigra of Parkinson's and Alzheimer's disease brains. Neurology, 1988. **38**(8): p. 1285-1285.

50. McGeer, P.L. and E.G. McGeer, Glial reactions in Parkinson's disease. Movement disorders: official journal of the Movement Disorder Society, 2008. **23**(4): p. 474-483.

51. Colton, C.A. and D.M. Wilcock, Assessing activation states in microglia. CNS & Neurological Disorders-Drug Targets (Formerly Current Drug Targets-CNS & Neurological Disorders), 2010. **9**(2): p. 174-191.

52. Klegeris, A., et al., α-Synuclein activates stress signaling protein kinases in THP-1 cells and microglia. Neurobiology of aging, 2008. **29**(5): p. 739-752.

53. Snyder, S.H., What dopamine does in the brain. Proceedings of the National Academy of Sciences, 2011. **108**(47): p. 18869-18871.

54. Carlsson, A., M. Lindqvist, and T. Magnusson, 3, 4-Dihydroxyphenylalanine and 5-hydroxytryptophan as reserpine antagonists. Nature, 1957. **180**(4596): p. 1200-1200.

55. Carlsson, A., et al., On the presence of 3-hydroxytyramine in brain. Science, 1958. **127**(3296): p. 471-471.

56. Bertler, Å. and E. Rosengren, Occurrence and distribution of dopamine in brain and other tissues. Experientia, 1959. **15**(1): p. 10-11.

57. Ehringer, H. and O. Hornykiewicz, Verteilung von Noradrenalin und Dopamin (3-Hydroxytyramin) im Gehirn des Menschen und ihr Verhalten bei Erkrankungen des extrapyramidalen Systems. Klinische Wochenschrift, 1960. **38**(24): p. 1236-1239.

58. Hornykiewicz, O., Dopamine miracle: from brain homogenate to dopamine replacement. Movement disorders: official journal of the Movement Disorder Society, 2002. **17**(3): p. 501-508.

59. Cotzias, G.C., M.H. Van Woert, and L.M. Schiffer, Aromatic amino acids and modification of parkinsonism. New England Journal of Medicine, 1967. **276**(7): p. 374-379.

60. Björklund, A. and S.B. Dunnett, Fifty years of dopamine research. Trends in neurosciences, 2007. **30**(5): p. 185-187.

61. Sahin, G. and D. Kirik, Efficacy of L-DOPA Therapy in Parkinson’s Disease. and Health, 2012: p. 454.

62. Okun, M.S., Deep-brain stimulation for Parkinson's disease. New England Journal of Medicine, 2012. **367**(16): p. 1529-1538.

63. Wang, L., et al., Delayed delivery of AAV-GDNF prevents nigral neurodegeneration and promotes functional recovery in a rat model of Parkinson's disease. Gene therapy, 2002. **9**(6): p. 381-389.

64. Bartus, R.T., et al., Properly scaled and targeted AAV2-NRTN (neurturin) to the substantia nigra is safe, effective and causes no weight loss: support for nigral targeting in Parkinson's disease. Neurobiology of disease, 2011. **44**(1): p. 38-52.

65. Albert, K., et al., AAV Vector-Mediated Gene Delivery to Substantia Nigra Dopamine Neurons: Implications for Gene Therapy and Disease Models. Genes (Basel), 2017. **8**(2).

66. Poewe, W., et al., Parkinson disease. Nature reviews Disease primers, 2017. **3**(1): p. 1-21.

67. Blesa, J., et al., Classic and new animal models of Parkinson's disease. BioMed Research International, 2012. **2012**.

68. Blesa, J. and S. Przedborski, Parkinson's disease: animal models and dopaminergic cell vulnerability. Frontiers in neuroanatomy, 2014. **8**: p. 155.

69. Forno, L., et al., Similarities and differences between MPTP-induced parkinsonsim and Parkinson's disease. Neuropathologic considerations. Advances in neurology, 1993. **60**: p. 600-608.

70. Halliday, G., et al., No Lewy pathology in monkeys with over 10 years of severe MPTP Parkinsonism. Movement disorders: official journal of the Movement Disorder Society, 2009. **24**(10): p. 1519-1523.

71. Betarbet, R., et al., Chronic systemic pesticide exposure reproduces features of Parkinson's disease. Nature neuroscience, 2000. **3**(12): p. 1301-1306.

72. Feany, M.B. and W.W. Bender, A Drosophila model of Parkinson's disease. Nature, 2000. **404**(6776): p. 394-398.

73. Thiruchelvam, M., et al., Risk factors for dopaminergic neuron loss in human α-synuclein transgenic mice. European Journal of Neuroscience, 2004. **19**(4): p. 845-854.

74. Wakamatsu, M., et al., Selective loss of nigral dopamine neurons induced by overexpression of truncated human α-synuclein in mice. Neurobiology of aging, 2008. **29**(4): p. 574-585.

75. Lin, X., et al., Conditional expression of Parkinson's disease-related mutant α-synuclein in the midbrain dopaminergic neurons causes progressive neurodegeneration and degradation of transcription factor nuclear receptor related 1. Journal of Neuroscience, 2012. **32**(27): p. 9248-9264.

76. Li, Y., et al., Mutant LRRK2 R1441G BAC transgenic mice recapitulate cardinal features of Parkinson's disease. Nature neuroscience, 2009. **12**(7): p. 826-828.

77. Moore, D.J. and T.M. Dawson, Value of genetic models in understanding the cause and mechanisms of Parkinson's disease. Current neurology and neuroscience reports, 2008. **8**(4): p. 288-296.

78. Masliah, E., et al., Dopaminergic loss and inclusion body formation in α-synuclein mice: implications for neurodegenerative disorders. Science, 2000. **287**(5456): p. 1265-1269.

79. Van der Putten, H., et al., Neuropathology in mice expressing human α-synuclein. Journal of Neuroscience, 2000. **20**(16): p. 6021-6029.

80. Klein, R.L., et al., Dopaminergic cell loss induced by human A30P α-synuclein gene transfer to the rat substantia nigra. Human gene therapy, 2002. **13**(5): p. 605-612.

81. Decressac, M., et al., Progressive neurodegenerative and behavioural changes induced by AAV-mediated overexpression of α-synuclein in midbrain dopamine neurons. Neurobiology of disease, 2012. **45**(3): p. 939-953.

82. Kirik, D., et al., Nigrostriatal α-synucleinopathy induced by viral vector-mediated overexpression of human α-synuclein: a new primate model of Parkinson's disease. Proceedings of the National Academy of Sciences, 2003. **100**(5): p. 2884-2889.

83. Luk, K.C., et al., Pathological alpha-synuclein transmission initiates Parkinson-like neurodegeneration in nontransgenic mice. Science, 2012. **338**(6109): p. 949-53.

84. Masuda-Suzukake, M., et al., Pathological alpha-synuclein propagates through neural networks. Acta neuropathologica communications, 2014. **2**(1): p. 88.

85. Masuda-Suzukake, M., et al., Prion-like spreading of pathological alpha-synuclein in brain. Brain, 2013. **136**(Pt 4): p. 1128-38.

86. Thakur, P., et al., Modeling Parkinson's disease pathology by combination of fibril seeds and α-synuclein overexpression in the rat brain. Proceedings of the National Academy of Sciences, 2017. **114**(39): p. E8284-E8293.

87. Volpicelli-Daley, L.A., et al., How can rAAV-alpha-synuclein and the fibril alpha-synuclein models advance our understanding of Parkinson's disease? J Neurochem, 2016. **139 Suppl 1**: p. 131-155.

88. Watabe-Uchida, M., et al., Whole-brain mapping of direct inputs to midbrain dopamine neurons. Neuron, 2012. **74**(5): p. 858-873.

89. Gerfen, C.R., M. Herkenham, and J. Thibault, The neostriatal mosaic: II. Patch-and matrix-directed mesostriatal dopaminergic and non-dopaminergic systems. Journal of Neuroscience, 1987. **7**(12): p. 3915-3934.

90. Cheng, H.C., C.M. Ulane, and R.E. Burke, Clinical progression in Parkinson disease and the neurobiology of axons. Annals of neurology, 2010. **67**(6): p. 715-725.

91. Fernstrom, J.D. and M.H. Fernstrom, Tyrosine, phenylalanine, and catecholamine synthesis and function in the brain. The Journal of nutrition, 2007. **137**(6): p. 1539S-1547S.

92. Christenson, J.G., W. Dairman, and S. Udenfriend, Preparation and properties of a homogeneous aromatic L-amino acid decarboxylase from hog kidney. Archives of biochemistry and biophysics, 1970. **141**(1): p. 356-367.

93. Guillot, T.S. and G.W. Miller, Protective actions of the vesicular monoamine transporter 2 (VMAT2) in monoaminergic neurons. Molecular neurobiology, 2009.

39(2): p. 149-170.

94. Harrington, K., et al., Dopamine transporter (Dat) and synaptic vesicle amine transporter (VMAT2) gene expression in the substantia nigra of control and Parkinson's disease. Molecular brain research, 1996. **36**(1): p. 157-162.

95. Klein, M.O., et al., Dopamine: functions, signaling, and association with neurological diseases. Cellular and molecular neurobiology, 2019. **39**(1): p. 31-59.

96. Missale, C., et al., Dopamine receptors: from structure to function. Physiological reviews, 1998. **78**(1): p. 189-225.

97. Contreras, F., et al., Dopamine, hypertension and obesity. Journal of human hypertension, 2002. **16**(1): p. S13-S17.

98. Wamsley, J., et al., Comparison of the distribution of D-1 and D-2 dopamine receptors in the rat brain. Journal of chemical neuroanatomy, 1989. **2**(3): p. 119-137.

99. Hurley, M. and P. Jenner, What has been learnt from study of dopamine receptors in Parkinson's disease? Pharmacology & therapeutics, 2006. **111**(3): p. 715-728.

100. Alcaro, A., R. Huber, and J. Panksepp, Behavioral functions of the mesolimbic dopaminergic system: an affective neuroethological perspective. Brain research reviews, 2007. **56**(2): p. 283-321.

101. Swanson, L., The projections of the ventral tegmental area and adjacent regions: a combined fluorescent retrograde tracer and immunofluorescence study in the rat. Brain research bulletin, 1982. **9**(1-6): p. 321-353.

102. Lee, H.J., et al., Activation of direct and indirect pathway medium spiny neurons drives distinct brain-wide responses. Neuron, 2016. **91**(2): p. 412-424.

103. Obeso, J.A., et al., The basal ganglia in Parkinson's disease: current concepts and unexplained observations. Annals of Neurology: Official Journal of the American Neurological Association and the Child Neurology Society, 2008. **64**(S2): p. S30-S46.

104. Kemp, J.M. and T.P.S. Powell, The structure of the caudate nucleus of the cat: light and electron microscopy. Philosophical Transactions of the Royal Society of London. B, Biological Sciences, 1971. **262**(845): p. 383-401.

105. Dudman, J.T. and C.R. Gerfen, The basal ganglia, in The rat nervous system. 2015, Elsevier. p. 391-440.

106. Gerfen, C.R. and D.J. Surmeier, Modulation of striatal projection systems by dopamine. Annual review of neuroscience, 2011. **34**: p. 441-466.

107. Freund, T., J. Powell, and A. Smith, Tyrosine hydroxylase-immunoreactive boutons in synaptic contact with identified striatonigral neurons, with particular reference to dendritic spines. Neuroscience, 1984. **13**(4): p. 1189-1215.

108. Ferré, S., et al., Adenosine–cannabinoid receptor interactions. Implications for striatal function. British journal of pharmacology, 2010. **160**(3): p. 443-453.

109. Yager, L.M., et al., The ins and outs of the striatum: role in drug addiction. Neuroscience, 2015. **301**: p. 529-541.

110. Everitt, B.J. and T.W. Robbins, Neural systems of reinforcement for drug addiction: from actions to habits to compulsion. Nature neuroscience, 2005. **8**(11): p. 1481-1489.

111. Pennartz, C., et al., The hippocampal–striatal axis in learning, prediction and goal-directed behavior. Trends in neurosciences, 2011. **34**(10): p. 548-559.

112. Juárez Olguín, H., et al., The role of dopamine and its dysfunction as a consequence of oxidative stress. Oxidative medicine and cellular longevity, 2016. **2016**.

113. Mori, F., et al., Immunohistochemical comparison of α-and β-synuclein in adult rat central nervous system. Brain research, 2002. **941**(1-2): p. 118-126.

114. Maroteaux, L., J.T. Campanelli, and R.H. Scheller, Synuclein: a neuron-specific protein localized to the nucleus and presynaptic nerve terminal. Journal of Neuroscience, 1988. **8**(8): p. 2804-2815.

115. Maroteaux, L. and R. Scheller, The rat brain synucleins; family of proteins transiently associated with neuronal membrane. Molecular brain research, 1991. **11**(3-4): p. 335-343.

116. Lavedan, C., The synuclein family. Genome research, 1998. **8**(9): p. 871-880.

117. Pinho, R., et al., Nuclear localization and phosphorylation modulate pathological effects of alpha-synuclein. Human molecular genetics, 2019. **28**(1): p. 31-50.

118. Devi, L., et al., Mitochondrial import and accumulation of α-synuclein impair complex I in human dopaminergic neuronal cultures and Parkinson disease brain. Journal of Biological Chemistry, 2008. **283**(14): p. 9089-9100.

119. Goers, J., et al., Nuclear localization of α-synuclein and its interaction with histones. Biochemistry, 2003. **42**(28): p. 8465-8471.

120. Bendor, J.T., T.P. Logan, and R.H. Edwards, The function of alpha-synuclein. Neuron, 2013. **79**(6): p. 1044-66.

121. Ahn, M., et al., Chaperone-like activities of α-synuclein: α-synuclein assists enzyme activities of esterases. Biochemical and biophysical research communications, 2006. **346**(4): p. 1142-1149.

122. Appel-Cresswell, S., et al., Alpha-synuclein p. H50Q, a novel pathogenic mutation for Parkinson's disease. Movement disorders, 2013. **28**(6): p. 811-813.

123. Lesage, S., et al., G51D α-synuclein mutation causes a novel Parkinsonian–pyramidal syndrome. Annals of neurology, 2013. **73**(4): p. 459-471.

124. Zarranz, J.J., et al., The new mutation, E46K, of α-synuclein causes parkinson and Lewy body dementia. Annals of Neurology: Official Journal of the American Neurological Association and the Child Neurology Society, 2004. **55**(2): p. 164-173.

125. Fusco, G., et al., Direct observation of the three regions in α-synuclein that determine its membrane-bound behaviour. Nature communications, 2014. **5**(1): p. 1-8.

126. Burre, J., The Synaptic Function of alpha-Synuclein. J Parkinsons Dis, 2015. **5**(4): p. 699-713.

127. Mor, D.E., et al., Dynamic structural flexibility of α-synuclein. Neurobiology of disease, 2016. **88**: p. 66-74.

128. Stefanis, L., α-Synuclein in Parkinson's disease. Cold Spring Harbor perspectives in medicine, 2012. **2**(2): p. a009399.

129. Ulmer, T.S. and A. Bax, Comparison of structure and dynamics of micelle-bound human α-synuclein and Parkinson disease variants. Journal of Biological Chemistry, 2005. **280**(52): p. 43179-43187.

130. Bertoncini, C.W., et al., Familial mutants of α-synuclein with increased neurotoxicity have a destabilized conformation. Journal of Biological Chemistry, 2005. **280**(35): p. 30649-30652.

131. Sevcsik, E., et al., Allostery in a disordered protein: oxidative modifications to α-synuclein act distally to regulate membrane binding. Journal of the American Chemical Society, 2011. **133**(18): p. 7152-7158.

132. Li, W., et al., Aggregation promoting C-terminal truncation of α-synuclein is a normal cellular process and is enhanced by the familial Parkinson's disease-linked mutations. Proceedings of the National Academy of Sciences, 2005. **102**(6): p. 2162-2167.

133. van der Wateren, I.M., et al., C-terminal truncation of alpha-synuclein promotes amyloid fibril amplification at physiological pH. Chem Sci, 2018. **9**(25): p. 5506-5516.

134. Venda, L.L., et al., alpha-Synuclein and dopamine at the crossroads of Parkinson's disease. Trends Neurosci, 2010. **33**(12): p. 559-68.

135. Davidson, W.S., et al., Stabilization of α-synuclein secondary structure upon binding to synthetic membranes. Journal of Biological Chemistry, 1998. **273**(16): p. 9443-9449.

136. Bertoncini, C.W., et al., Release of long-range tertiary interactions potentiates aggregation of natively unstructured α-synuclein. Proceedings of the National Academy of Sciences, 2005. **102**(5): p. 1430-1435.

137. Calo, L., et al., Synaptic failure and α-synuclein. Movement Disorders, 2016. **31**(2): p. 169-177.

138. Burré, J., M. Sharma, and T.C. Südhof, Cell biology and pathophysiology of α-synuclein. Cold Spring Harbor perspectives in medicine, 2018. **8**(3): p. a024091.

139. Zhu, M. and A.L. Fink, Lipid binding inhibits α-synuclein fibril formation. Journal of Biological Chemistry, 2003. **278**(19): p. 16873-16877.

140. Burré, J., et al., α-Synuclein promotes SNARE-complex assembly in vivo and in vitro. Science, 2010. **329**(5999): p. 1663-1667.

141. Bellucci, A., et al., Alpha-synuclein aggregation and cell death triggered by energy deprivation and dopamine overload are counteracted by D2/D3 receptor activation. Journal of neurochemistry, 2008. **106**(2): p. 560-577.

142. Lee, F.J., et al., Direct binding and functional coupling of α-synuclein to the dopamine transporters accelerate dopamine-induced apoptosis. The FASEB Journal, 2001. **15**(6): p. 916-926.

143. Wersinger, C., et al., Modulation of dopamine transporter function by α-synuclein is altered by impairment of cell adhesion and by induction of oxidative stress. The FASEB journal, 2003. **17**(14): p. 2151-2153.

144. Bellucci, A., et al., Redistribution of DAT/α-synuclein complexes visualized by “in situ” proximity ligation assay in transgenic mice modelling early Parkinson's disease. PloS one, 2011. **6**(12).

145. Chadchankar, H., et al., Decreased reuptake of dopamine in the dorsal striatum in the absence of alpha-synuclein. Brain research, 2011. **1382**: p. 37-44.

146. Al-Wandi, A., et al., Absence of α-synuclein affects dopamine metabolism and synaptic markers in the striatum of aging mice. Neurobiology of aging, 2010. **31**(5): p. 796-804.

147. Garcia-Reitboeck, P., et al., Endogenous alpha-synuclein influences the number of dopaminergic neurons in mouse substantia nigra. Experimental neurology, 2013. **248**: p. 541-545.

148. Robertson, D.C., et al., Developmental loss and resistance to MPTP toxicity of dopaminergic neurones in substantia nigra pars compacta of γ-synuclein, α-synuclein and double α/γ-synuclein null mutant mice. Journal of neurochemistry, 2004. **89**(5): p. 1126-1136.

149. Yavich, L., et al., Role of α-synuclein in presynaptic dopamine recruitment. Journal of Neuroscience, 2004. **24**(49): p. 11165-11170.

150. Guo, J.T., et al., Inhibition of vesicular monoamine transporter-2 activity in α-synuclein stably transfected SH-SY5Y cells. Cellular and molecular neurobiology, 2008. **28**(1): p. 35-47.

151. Mor, D.E., et al., Dopamine induces soluble alpha-synuclein oligomers and nigrostriatal degeneration. Nat Neurosci, 2017. **20**(11): p. 1560-1568.

152. Roy, S., Synuclein and dopamine: the Bonnie and Clyde of Parkinson's disease. nature neuroscience, 2017. **20**(11): p. 1514-1515.

153. Perez, R.G., et al., A role for α-synuclein in the regulation of dopamine biosynthesis. Journal of Neuroscience, 2002. **22**(8): p. 3090-3099.

154. Wu, B., et al., Phosphorylation of α-synuclein upregulates tyrosine hydroxylase activity in MN9D cells. Acta histochemica, 2011. **113**(1): p. 32-35.

155. Lou, H., et al., Serine 129 phosphorylation reduces the ability of α-synuclein to regulate tyrosine hydroxylase and protein phosphatase 2A in vitro and in vivo. Journal of Biological Chemistry, 2010. **285**(23): p. 17648-17661.

156. Chu, Y. and J.H. Kordower, Age-associated increases of α-synuclein in monkeys and humans are associated with nigrostriatal dopamine depletion: is this the target for Parkinson's disease? Neurobiology of disease, 2007. **25**(1): p. 134-149.

157. Spillantini, M.G., et al., α-Synuclein in filamentous inclusions of Lewy bodies from Parkinson's disease and dementia with Lewy bodies. Proceedings of the National Academy of Sciences, 1998. **95**(11): p. 6469-6473.

158. Gould, N., et al., Evidence of native α-synuclein conformers in the human brain. Journal of Biological Chemistry, 2014. **289**(11): p. 7929-7934.

159. Wang, W., et al., A soluble α-synuclein construct forms a dynamic tetramer. Proceedings of the National Academy of Sciences, 2011. **108**(43): p. 17797-17802.

160. Dettmer, U., et al., KTKEGV repeat motifs are key mediators of normal α-synuclein tetramerization: Their mutation causes excess monomers and neurotoxicity. Proceedings of the National Academy of Sciences, 2015. **112**(31): p. 9596-9601.

161. Burré, J., et al., Properties of native brain α-synuclein. Nature, 2013. **498**(7453): p. E4-E6.

162. Fauvet, B., et al., α-Synuclein in central nervous system and from erythrocytes, mammalian cells, and Escherichia coli exists predominantly as disordered monomer. Journal of Biological Chemistry, 2012. **287**(19): p. 15345-15364.

163. Munishkina, L.A., et al., Conformational behavior and aggregation of α-synuclein in organic solvents: modeling the effects of membranes. Biochemistry, 2003. **42**(9): p. 2720-2730.

164. Mehra, S., S. Sahay, and S.K. Maji, α-Synuclein misfolding and aggregation: Implications in Parkinson's disease pathogenesis. Biochimica et Biophysica Acta (BBA)-Proteins and Proteomics, 2019.

165. Conway, K.A., et al., Acceleration of oligomerization, not fibrillization, is a shared property of both α-synuclein mutations linked to early-onset Parkinson's disease: implications for pathogenesis and therapy. Proceedings of the National Academy of Sciences, 2000. **97**(2): p. 571-576.

166. Buell, A.K., et al., Solution conditions determine the relative importance of nucleation and growth processes in α-synuclein aggregation. Proceedings of the National Academy of Sciences, 2014. **111**(21): p. 7671-7676.

167. Uchihara, T. and B.I. Giasson, Propagation of alpha-synuclein pathology: hypotheses, discoveries, and yet unresolved questions from experimental and human brain studies. Acta neuropathologica, 2016. **131**(1): p. 49-73.

168. Sharon, R., et al., The formation of highly soluble oligomers of α-synuclein is regulated by fatty acids and enhanced in Parkinson's disease. Neuron, 2003. **37**(4): p. 583-595.

169. Danzer, K.M., et al., Different species of α-synuclein oligomers induce calcium influx and seeding. Journal of Neuroscience, 2007. **27**(34): p. 9220-9232.

170. Winner, B., et al., In vivo demonstration that α-synuclein oligomers are toxic. Proceedings of the National Academy of Sciences, 2011. **108**(10): p. 4194-4199.

171. Cremades, N., et al., Direct observation of the interconversion of normal and toxic forms of α-synuclein. Cell, 2012. **149**(5): p. 1048-1059.

172. Stöckl, M.T., N. Zijlstra, and V. Subramaniam, α-Synuclein oligomers: an amyloid pore? Molecular neurobiology, 2013. **47**(2): p. 613-621.

173. Tsigelny, I.F., et al., Role of α-synuclein penetration into the membrane in the mechanisms of oligomer pore formation. The FEBS journal, 2012. **279**(6): p. 1000-1013.

174. Peelaerts, W., et al., α-Synuclein strains cause distinct synucleinopathies after local and systemic administration. Nature, 2015. **522**(7556): p. 340-344.

175. Greenbaum, E.A., et al., The E46K mutation in α-synuclein increases amyloid fibril formation. Journal of Biological Chemistry, 2005. **280**(9): p. 7800-7807.

176. Tanik, S.A., et al., Lewy body-like α-synuclein aggregates resist degradation and impair macroautophagy. Journal of Biological Chemistry, 2013. **288**(21): p. 15194-15210.

177. Blumenstock, S., et al., Seeding and transgenic overexpression of alpha-synuclein triggers dendritic spine pathology in the neocortex. EMBO Mol Med, 2017. **9**(5): p. 716-731.

178. Prusiner, S.B., et al., Evidence for α-synuclein prions causing multiple system atrophy in humans with parkinsonism. Proceedings of the National Academy of Sciences, 2015. **112**(38): p. E5308-E5317.

179. Woerman, A.L., et al., Propagation of prions causing synucleinopathies in cultured cells. Proceedings of the National Academy of Sciences, 2015. **112**(35): p. E4949-E4958.

180. Fares, M.-B., et al., Induction of de novo α-synuclein fibrillization in a neuronal model for Parkinson's disease. Proceedings of the National Academy of Sciences, 2016. **113**(7): p. E912-E921.

181. Luk, K.C., et al., Molecular and biological compatibility with host alpha-synuclein influences fibril pathogenicity. Cell reports, 2016. **16**(12): p. 3373-3387.

182. Przedborski, S. and V. Jackson-Lewis, ROS and Parkinson's disease: a view to a kill. In free Radicals in Brain Pathophysiology, G. Poli, E. Cadenas and L. Packer, eds. 2000, New York: Marcel Dekker, Inc.

183. Beckman, K.B. and B.N. Ames, The free radical theory of aging matures. Physiological reviews, 1998. **78**(2): p. 547-581.

184. Freeman, D., et al., Alpha-synuclein induces lysosomal rupture and cathepsin dependent reactive oxygen species following endocytosis. PloS one, 2013. **8**(4).

185. Ghavami, S., et al., Autophagy and apoptosis dysfunction in neurodegenerative disorders. Progress in neurobiology, 2014. **112**: p. 24-49.

186. Nakamura, K., α-Synuclein and mitochondria: partners in crime? Neurotherapeutics, 2013. **10**(3): p. 391-399.

187. Parihar, M., et al., Mitochondrial association of alpha-synuclein causes oxidative stress. Cellular and Molecular Life Sciences, 2008. **65**(7-8): p. 1272-1284.

188. Winslow, A.R., et al., α-Synuclein impairs macroautophagy: implications for Parkinson's disease. Journal of Cell Biology, 2010. **190**(6): p. 1023-1037.

189. Winslow, A.R. and D.C. Rubinsztein, The Parkinson disease protein α-synuclein inhibits autophagy. Autophagy, 2011. **7**(4): p. 429-431.

190. Smith, W.W., et al., Endoplasmic reticulum stress and mitochondrial cell death pathways mediate A53T mutant alpha-synuclein-induced toxicity. Human molecular genetics, 2005. **14**(24): p. 3801-3811.

191. Parihar, M.S., et al., Alpha-synuclein overexpression and aggregation exacerbates impairment of mitochondrial functions by augmenting oxidative stress in human neuroblastoma cells. The international journal of biochemistry & cell biology, 2009. **41**(10): p. 2015-2024.

192. Cuervo, A.M., et al., Impaired degradation of mutant α-synuclein by chaperone-mediated autophagy. Science, 2004. **305**(5688): p. 1292-1295.

193. Emmanouilidou, E., L. Stefanis, and K. Vekrellis, Cell-produced α-synuclein oligomers are targeted to, and impair, the 26S proteasome. Neurobiology of aging, 2010. **31**(6): p. 953-968.

194. Martinez-Vicente, M., et al., Dopamine-modified α-synuclein blocks chaperone-mediated autophagy. The Journal of clinical investigation, 2008. **118**(2): p. 777-788.

195. Alvarez-Erviti, L., et al., Lysosomal dysfunction increases exosome-mediated alpha-synuclein release and transmission. Neurobiology of disease, 2011. **42**(3): p. 360-367.

196. Lewis, J., et al., In vivo silencing of alpha-synuclein using naked siRNA. Molecular neurodegeneration, 2008. **3**(1): p. 19.

197. Cooper, J.M., et al., Systemic exosomal siRNA delivery reduced alpha-synuclein aggregates in brains of transgenic mice. Movement Disorders, 2014. **29**(12): p. 1476-1485.

198. Decressac, M., et al., TFEB-mediated autophagy rescues midbrain dopamine neurons from α-synuclein toxicity. Proceedings of the National Academy of Sciences, 2013. **110**(19): p. E1817-E1826.

199. Rothaug, M., et al., LIMP-2 expression is critical for β-glucocerebrosidase activity and α-synuclein clearance. Proceedings of the National Academy of Sciences, 2014. **111**(43): p. 15573-15578.

200. Gitler, A.D., et al., α-Synuclein is part of a diverse and highly conserved interaction network that includes PARK9 and manganese toxicity. Nature genetics, 2009. **41**(3): p. 308.

201. Tsunemi, T. and D. Krainc, Zn2+ dyshomeostasis caused by loss of ATP13A2/PARK9 leads to lysosomal dysfunction and alpha-synuclein accumulation. Human molecular genetics, 2014. **23**(11): p. 2791-2801.

202. Fonseca-Ornelas, L., et al., Small molecule-mediated stabilization of vesicle-associated helical α-synuclein inhibits pathogenic misfolding and aggregation. Nature communications, 2014. **5**(1): p. 1-11.

203. Games, D., et al., Reducing C-terminal-truncated alpha-synuclein by immunotherapy attenuates neurodegeneration and propagation in Parkinson's disease-like models. Journal of Neuroscience, 2014. **34**(28): p. 9441-9454.

204. Tran, H.T., et al., α-Synuclein immunotherapy blocks uptake and templated propagation of misfolded α-synuclein and neurodegeneration. Cell reports, 2014. **7**(6): p. 2054-2065.

205. Koprich, J.B., L.V. Kalia, and J.M. Brotchie, Animal models of α-synucleinopathy for Parkinson disease drug development. Nature Reviews Neuroscience, 2017. **18**(9): p. 515.

206. Kordower, J.H., et al., Lewy body–like pathology in long-term embryonic nigral transplants in Parkinson's disease. Nature medicine, 2008. **14**(5): p. 504-506.

207. Li, J.-Y., et al., Lewy bodies in grafted neurons in subjects with Parkinson's disease suggest host-to-graft disease propagation. Nature medicine, 2008. **14**(5): p. 501-503.

208. Desplats, P., et al., Inclusion formation and neuronal cell death through neuron-to-neuron transmission of α-synuclein. Proceedings of the National Academy of Sciences, 2009. **106**(31): p. 13010-13015.

209. Luk, K.C., et al., Exogenous α-synuclein fibrils seed the formation of Lewy body-like intracellular inclusions in cultured cells. Proceedings of the National Academy of Sciences, 2009. **106**(47): p. 20051-20056.

210. Volpicelli-Daley, L.A., et al., Exogenous alpha-synuclein fibrils induce Lewy body pathology leading to synaptic dysfunction and neuron death. Neuron, 2011. **72**(1): p. 57-71.

211. Rey, N.L., et al., Widespread transneuronal propagation of α-synucleinopathy triggered in olfactory bulb mimics prodromal Parkinson's disease. Journal of Experimental Medicine, 2016. **213**(9): p. 1759-1778.

212. Sacino, A.N., et al., Intramuscular injection of α-synuclein induces CNS α-synuclein pathology and a rapid-onset motor phenotype in transgenic mice. Proceedings of the National Academy of Sciences, 2014. **111**(29): p. 10732-10737.

213. Recasens, A., et al., Lewy body extracts from Parkinson disease brains trigger α-synuclein pathology and neurodegeneration in mice and monkeys. Annals of neurology, 2014. **75**(3): p. 351-362.

214. Freundt, E.C., et al., Neuron-to-neuron transmission of α-synuclein fibrils through axonal transport. Annals of neurology, 2012. **72**(4): p. 517-524.

215. Danzer, K.M., et al., Heat-shock protein 70 modulates toxic extracellular α-synuclein oligomers and rescues trans-synaptic toxicity. The FASEB journal, 2011. **25**(1): p. 326-336.

216. Tsunemi, T., K. Hamada, and D. Krainc, ATP13A2/PARK9 regulates secretion of exosomes and α-synuclein. Journal of Neuroscience, 2014. **34**(46): p. 15281-15287.

217. Kong, S.M., et al., Parkinson's disease-linked human PARK9/ATP13A2 maintains zinc homeostasis and promotes α-Synuclein externalization via exosomes. Human molecular genetics, 2014. **23**(11): p. 2816-2833.

218. Oh, S.H., et al., Mesenchymal stem cells inhibit transmission of α-synuclein by modulating clathrin-mediated endocytosis in a parkinsonian model. Cell reports, 2016. **14**(4): p. 835-849.

219. Mao, X., et al., Pathological alpha-synuclein transmission initiated by binding lymphocyte-activation gene 3. Science, 2016. **353**(6307).

220. Abounit, S., et al., Tunneling nanotubes spread fibrillar alpha-synuclein by intercellular trafficking of lysosomes. EMBO J, 2016. **35**(19): p. 2120-2138.

221. Valadi, H., et al., Exosome-mediated transfer of mRNAs and microRNAs is a novel mechanism of genetic exchange between cells. Nature cell biology, 2007. **9**(6): p. 654-659.

222. Gibbings, D.J., et al., Multivesicular bodies associate with components of miRNA effector complexes and modulate miRNA activity. Nature cell biology, 2009. **11**(9): p. 1143-1149.

223. Lancaster, G.I. and M.A. Febbraio, Exosome-dependent trafficking of HSP70 A novel secretory pathway for cellular stress proteins. Journal of Biological Chemistry, 2005. **280**(24): p. 23349-23355.

224. Danzer, K.M., et al., Exosomal cell-to-cell transmission of alpha synuclein oligomers. Molecular neurodegeneration, 2012. **7**(1): p. 42.

225. Reyes, J.F., et al., Alpha-synuclein transfers from neurons to oligodendrocytes. Glia, 2014. **62**(3): p. 387-398.

226. Konno, M., et al., Suppression of dynamin GTPase decreases α-synuclein uptake by neuronal and oligodendroglial cells: a potent therapeutic target for synucleinopathy. Molecular neurodegeneration, 2012. **7**(1): p. 38.

227. Angot, E. and P. Brundin, Dissecting the potential molecular mechanisms underlying α-synuclein cell-to-cell transfer in Parkinson's disease. Parkinsonism & related disorders, 2009. **15**: p. S143-S147.

228. Agnati, L.F. and K. Fuxe, Extracellular-vesicle type of volume transmission and tunnelling-nanotube type of wiring transmission add a new dimension to brain neuro-glial networks. Philosophical Transactions of the Royal Society B: Biological Sciences, 2014. **369**(1652): p. 20130505.

229. Costanzo, M. and C. Zurzolo, The cell biology of prion-like spread of protein aggregates: mechanisms and implication in neurodegeneration. Biochemical Journal, 2013. **452**(1): p. 1-17.

230. Cavaliere, F., et al., In vitro alpha-synuclein neurotoxicity and spreading among neurons and astrocytes using Lewy body extracts from Parkinson disease brains. Neurobiol Dis, 2017. **103**: p. 101-112.

231. Wang, X., N.V. Bukoreshtliev, and H.-H. Gerdes, Developing neurons form transient nanotubes facilitating electrical coupling and calcium signaling with distant astrocytes. PloS one, 2012. **7**(10).

232. Sun, X., et al., Tunneling-nanotube direction determination in neurons and astrocytes. Cell death & disease, 2012. **3**(12): p. e438-e438.

233. Rostami, J., et al., Human astrocytes transfer aggregated alpha-synuclein via tunneling nanotubes. Journal of Neuroscience, 2017. **37**(49): p. 11835-11853.

234. Aulic, S., et al., alpha-Synuclein Amyloids Hijack Prion Protein to Gain Cell Entry, Facilitate Cell-to-Cell Spreading and Block Prion Replication. Sci Rep, 2017. **7**(1): p. 10050.

235. Walsh, D.M. and D.J. Selkoe, A critical appraisal of the pathogenic protein spread hypothesis of neurodegeneration. Nat Rev Neurosci, 2016. **17**(4): p. 251-60.

236. Orihuela, R., C.A. McPherson, and G.J. Harry, Microglial M1/M2 polarization and metabolic states. British journal of pharmacology, 2016. **173**(4): p. 649-665.

237. Sierra, A., R.C. Paolicelli, and H. Kettenmann, Cien años de microglía: milestones in a century of microglial research. Trends in neurosciences, 2019.

238. Alliot, F., I. Godin, and B. Pessac, Microglia derive from progenitors, originating from the yolk sac, and which proliferate in the brain. Developmental Brain Research, 1999. **117**(2): p. 145-152.

239. Ginhoux, F., et al., Fate mapping analysis reveals that adult microglia derive from primitive macrophages. Science, 2010. **330**(6005): p. 841-845.

240. Carson, M.J., et al., CNS immune privilege: hiding in plain sight. Immunological reviews, 2006. **213**(1): p. 48-65.

241. Lawson, L.J., et al., Heterogeneity in the distribution and morphology of microglia in the normal adult mouse brain. Neuroscience, 1990. **39**(1): p. 151-170.

242. Nimmerjahn, A., F. Kirchhoff, and F. Helmchen, Resting microglial cells are highly dynamic surveillants of brain parenchyma in vivo. Science, 2005. **308**(5726): p. 1314-1318.

243. Eugenín, E.A., et al., Microglia at brain stab wounds express connexin 43 and in vitro form functional gap junctions after treatment with interferon-γ and tumor necrosis factor-α. Proceedings of the National Academy of Sciences, 2001. **98**(7): p. 4190-4195.

244. Bruce-Keller, A.J., Microglial–neuronal interactions in synaptic damage and recovery. Journal of neuroscience research, 1999. **58**(1): p. 191-201.

245. Stevens, B., et al., The classical complement cascade mediates CNS synapse elimination. Cell, 2007. **131**(6): p. 1164-1178.

246. Paolicelli, R.C., et al., Synaptic pruning by microglia is necessary for normal brain development. science, 2011. **333**(6048): p. 1456-1458.

247. Glanzer, J.G., et al., Genomic and proteomic microglial profiling: pathways for neuroprotective inflammatory responses following nerve fragment clearance and activation. Journal of neurochemistry, 2007. **102**(3): p. 627-645.

248. Wright, G.J., et al., Characterization of the CD200 receptor family in mice and humans and their interactions with CD200. The Journal of Immunology, 2003. **171**(6): p. 3034-3046.

249. Kierdorf, K. and M. Prinz, Factors regulating microglia activation. Frontiers in cellular neuroscience, 2013. **7**: p. 44.

250. Rayaprolu, S., et al., TREM2 in neurodegeneration: evidence for association of the p. R47H variant with frontotemporal dementia and Parkinson's disease. Molecular neurodegeneration, 2013. **8**(1): p. 19.

251. Zheng, H., et al., TREM2 promotes microglial survival by activating Wnt/β-catenin pathway. Journal of Neuroscience, 2017. **37**(7): p. 1772-1784.

252. Cantoni, C., et al., TREM2 regulates microglial cell activation in response to demyelination in vivo. Acta neuropathologica, 2015. **129**(3): p. 429-447.

253. Ulrich, J.D., et al., Elucidating the Role of TREM2 in Alzheimer's Disease. Neuron, 2017. **94**(2): p. 237-248.

254. Ulland, T.K., et al., TREM2 Maintains Microglial Metabolic Fitness in Alzheimer's Disease. Cell, 2017. **170**(4): p. 649-663 e13.

255. Zhang, Y., et al., TREM2 modulates microglia phenotypes in the neuroinflammation of Parkinson's disease. Biochem Biophys Res Commun, 2018. **499**(4): p. 797-802.

256. Ren, M., et al., TREM2 overexpression attenuates neuroinflammation and protects dopaminergic neurons in experimental models of Parkinson's disease. Exp Neurol, 2018. **302**: p. 205-213.

257. Guo, Y., et al., TREM2 deficiency aggravates α-synuclein–induced neurodegeneration and neuroinflammation in Parkinson's disease models. The FASEB Journal, 2019. **33**(11): p. 12164-12174.

258. Gordon, S. and P.R. Taylor, Monocyte and macrophage heterogeneity. Nature Reviews Immunology, 2005. **5**(12): p. 953-964.

259. Hanisch, U.-K. and H. Kettenmann, Microglia: active sensor and versatile effector cells in the normal and pathologic brain. Nature neuroscience, 2007. **10**(11): p. 1387-1394.

260. Henkel, J.S., et al., Microglia in ALS: the good, the bad, and the resting. Journal of Neuroimmune Pharmacology, 2009. **4**(4): p. 389-398.

261. Ransohoff, R.M. and V.H. Perry, Microglial physiology: unique stimuli, specialized responses. Annual review of immunology, 2009. **27**: p. 119-145.

262. Boche, D., V. Perry, and J. Nicoll, Activation patterns of microglia and their identification in the human brain. Neuropathology and applied neurobiology, 2013. **39**(1): p. 3-18.

263. Cherry, J.D., J.A. Olschowka, and M.K. O'Banion, Neuroinflammation and M2 microglia: the good, the bad, and the inflamed. Journal of neuroinflammation, 2014. **11**(1): p. 98.

264. Long-Smith, C.M., A.M. Sullivan, and Y.M. Nolan, The influence of microglia on the pathogenesis of Parkinson's disease. Progress in neurobiology, 2009. **89**(3): p. 277-287.

265. Halliday, G.M. and C.H. Stevens, Glia: initiators and progressors of pathology in Parkinson's disease. Movement Disorders, 2011. **26**(1): p. 6-17.

266. Ferrari, C.C., et al., Progressive neurodegeneration and motor disabilities induced by chronic expression of IL-1β in the substantia nigra. Neurobiology of disease, 2006. **24**(1): p. 183-193.

267. McCoy, M.K., et al., Blocking soluble tumor necrosis factor signaling with dominant-negative tumor necrosis factor inhibitor attenuates loss of dopaminergic neurons in models of Parkinson's disease. Journal of Neuroscience, 2006. **26**(37): p. 9365-9375.

268. Fellner, L. and N. Stefanova, The role of glia in alpha-synucleinopathies. Molecular neurobiology, 2013. **47**(2): p. 575-586.

269. Ouchi, Y., et al., Microglial activation and dopamine terminal loss in early Parkinson's disease. Annals of neurology, 2005. **57**(2): p. 168-175.

270. Bartels, A., et al., [11C]-PK11195 PET: quantification of neuroinflammation and a monitor of anti-inflammatory treatment in Parkinson's disease? Parkinsonism & related disorders, 2010. **16**(1): p. 57-59.

271. Gerhard, A., et al., In vivo imaging of microglial activation with [11C](R)-PK11195 PET in idiopathic Parkinson's disease. Neurobiology of disease, 2006. **21**(2): p. 404-412.

272. Nagatsu, T. and M. Sawada, Inflammatory process in Parkinson's disease: role for cytokines. Current pharmaceutical design, 2005. **11**(8): p. 999-1016.

273. Higuchi, M., et al., Glucose hypometabolism and neuropathological correlates in brains of dementia with Lewy bodies. Experimental neurology, 2000. **162**(2): p. 247-256.

274. Doorn, K.J., et al., Emerging roles of microglial activation and non-motor symptoms in Parkinson's disease. Progress in neurobiology, 2012. **98**(2): p. 222-238.

275. Blandini, F., Neural and immune mechanisms in the pathogenesis of Parkinson's disease. Journal of Neuroimmune Pharmacology, 2013. **8**(1): p. 189-201.

276. Chen, H., et al., Nonsteroidal antiinflammatory drug use and the risk for Parkinson's disease. Annals of Neurology: Official Journal of the American Neurological Association and the Child Neurology Society, 2005. **58**(6): p. 963-967.

277. Rees, K., et al., Non-steroidal anti-inflammatory drugs as disease-modifying agents for Parkinson's disease: evidence from observational studies. Cochrane Database of Systematic Reviews, 2011(11).

278. Castano, A., et al., Lipopolysaccharide intranigral injection induces inflammatory reaction and damage in nigrostriatal dopaminergic system. Journal of

neurochemistry, 1998. **70**(4): p. 1584-1592.

279. Fernagut, P.-O. and M.-F. Chesselet, Alpha-synuclein and transgenic mouse models. Neurobiology of disease, 2004. **17**(2): p. 123-130.

280. Austin, S.A., et al., α-synuclein expression modulates microglial activation phenotype. Journal of Neuroscience, 2006. **26**(41): p. 10558-10563.

281. Orr, C.F., et al., A possible role for humoral immunity in the pathogenesis of Parkinson's disease. Brain, 2005. **128**(11): p. 2665-2674.

282. Saijo, K., et al., A Nurr1/CoREST pathway in microglia and astrocytes protects dopaminergic neurons from inflammation-induced death. Cell, 2009. **137**(1): p. 47-59.

283. Zhang, W., et al., Aggregated α-synuclein activates microglia: a process leading to disease progression in Parkinson's disease. The FASEB Journal, 2005. **19**(6): p. 533-542.

284. Rice, R.A., et al., Elimination of microglia improves functional outcomes following extensive neuronal loss in the hippocampus. Journal of Neuroscience, 2015. **35**(27): p. 9977-9989.

285. Dagher, N.N., et al., Colony-stimulating factor 1 receptor inhibition prevents microglial plaque association and improves cognition in 3xTg-AD mice. J Neuroinflammation, 2015. **12**: p. 139.

286. Somjen, G.G., Nervenkitt: notes on the history of the concept of neuroglia. Glia, 1988. **1**(1): p. 2-9.

287. Wilms, H., et al., Suppression of MAP kinases inhibits microglial activation and attenuates neuronal cell death induced by α-synuclein protofibrils. International journal of immunopathology and pharmacology, 2009. **22**(4): p. 897-909.

288. Couch, Y., et al., The acute inflammatory response to intranigral α-synuclein differs significantly from intranigral lipopolysaccharide and is exacerbated by peripheral inflammation. Journal of neuroinflammation, 2011. **8**(1): p. 166.

289. Gao, H.-M., et al., Neuroinflammation and α-synuclein dysfunction potentiate each other, driving chronic progression of neurodegeneration in a mouse model of Parkinson's disease. Environmental health perspectives, 2011. **119**(6): p. 807-814.

290. Park, J.Y., et al., Microglial phagocytosis is enhanced by monomeric α-synuclein, not aggregated α-synuclein: Implications for Parkinson's disease. Glia, 2008. **56**(11): p. 1215-1223.

291. Chung, C.Y., et al., Dynamic changes in presynaptic and axonal transport proteins combined with striatal neuroinflammation precede dopaminergic neuronal loss in a rat model of AAV α-synucleinopathy. Journal of Neuroscience, 2009. **29**(11): p. 3365-3373.

292. Theodore, S., et al., Targeted overexpression of human α-synuclein triggers microglial activation and an adaptive immune response in a mouse model of Parkinson disease. Journal of Neuropathology & Experimental Neurology, 2008. **67**(12): p. 1149-1158.

293. Lastres-Becker, I., et al., alpha-Synuclein expression and Nrf2 deficiency cooperate to aggravate protein aggregation, neuronal death and inflammation in early-stage Parkinson's disease. Hum Mol Genet, 2012. **21**(14): p. 3173-92.

294. Gao, H.-M., et al., Neuroinflammation and oxidation/nitration of α-synuclein linked to dopaminergic neurodegeneration. Journal of Neuroscience, 2008. **28**(30): p. 7687-7698.

295. Harms, A.S., et al., MHCII is required for α-synuclein-induced activation of microglia, CD4 T cell proliferation, and dopaminergic neurodegeneration. Journal of Neuroscience, 2013. **33**(23): p. 9592-9600.

296. Kim, C., et al., Neuron-released oligomeric α-synuclein is an endogenous agonist of TLR2 for paracrine activation of microglia. Nature communications, 2013. **4**(1): p. 1-12.

297. Daniele, S.G., et al., Activation of MyD88-dependent TLR1/2 signaling by misfolded α-synuclein, a protein linked to neurodegenerative disorders. Sci. Signal., 2015. **8**(376): p. ra45-ra45.

298. Stefanova, N., et al., Toll-like receptor 4 promotes α-synuclein clearance and survival of nigral dopaminergic neurons. The American journal of pathology, 2011. **179**(2): p. 954-963.

299. Fellner, L., et al., Toll-like receptor 4 is required for α-synuclein dependent activation of microglia and astroglia. Glia, 2013. **61**(3): p. 349-360.

300. Wang, S., et al., α-Synuclein, a chemoattractant, directs microglial migration via H2O2-dependent Lyn phosphorylation. Proceedings of the National Academy of Sciences, 2015. **112**(15): p. E1926-E1935.

301. Thome, A.D., et al., microRNA-155 regulates alpha-synuclein-induced inflammatory responses in models of Parkinson disease. Journal of Neuroscience, 2016. **36**(8): p. 2383-2390.

302. Croisier, E., et al., Microglial inflammation in the parkinsonian substantia nigra: relationship to alpha-synuclein deposition. J Neuroinflammation, 2005. **2**: p. 14.

303. Liu, J., et al., Identification of proteins involved in microglial endocytosis of α-synuclein. Journal of proteome research, 2007. **6**(9): p. 3614-3627.

304. Lee, H.-J., et al., Assembly-dependent endocytosis and clearance of extracellular a-synuclein. The international journal of biochemistry & cell biology, 2008. **40**(9): p. 1835-1849.

305. Park, J.Y., et al., On the mechanism of internalization of α-synuclein into microglia: roles of ganglioside GM1 and lipid raft. Journal of neurochemistry, 2009. **110**(1): p. 400-411.

306. Önfelt, B., et al., Cutting edge: Membrane nanotubes connect immune cells. The Journal of Immunology, 2004. **173**(3): p. 1511-1513.

307. Önfelt, B., et al., Structurally distinct membrane nanotubes between human macrophages support long-distance vesicular traffic or surfing of bacteria. The Journal of Immunology, 2006. **177**(12): p. 8476-8483.

308. Fitzner, D., et al., Selective transfer of exosomes from oligodendrocytes to microglia by macropinocytosis. Journal of cell science, 2011. **124**(3): p. 447-458.

309. Chu, Y., et al., Alterations in lysosomal and proteasomal markers in Parkinson's disease: relationship to alpha-synuclein inclusions. Neurobiology of disease, 2009. **35**(3): p. 385-398.

310. Lee, H.-J., et al., Clearance and deposition of extracellular α-synuclein aggregates in microglia. Biochemical and biophysical research communications, 2008. **372**(3): p. 423-428.

311. Chen, G.Y. and G. Nuñez, Sterile inflammation: sensing and reacting to damage. Nature Reviews Immunology, 2010. **10**(12): p. 826-837.

312. Franceschi, C., et al., Inflammaging and anti-inflammaging: a systemic perspective on aging and longevity emerged from studies in humans. Mechanisms of ageing and development, 2007. **128**(1): p. 92-105.

313. Rawji, K.S., et al., Immunosenescence of microglia and macrophages: impact on the ageing central nervous system. Brain, 2016. **139**(3): p. 653-661.

314. Streit, W.J., et al., Dystrophic (senescent) rather than activated microglial cells are associated with tau pathology and likely precede neurodegeneration in Alzheimer's disease. Acta neuropathologica, 2009. **118**(4): p. 475-485.

315. Streit, W.J., et al., Dystrophic microglia in the aging human brain. Glia, 2004. **45**(2): p. 208-212.

316. Bliederhaeuser, C., et al., Age-dependent defects of alpha-synuclein oligomer uptake in microglia and monocytes. Acta Neuropathol, 2016. **131**(3): p. 379-91.

317. Hayakawa, N., H. Kato, and T. Araki, Age-related changes of astorocytes, oligodendrocytes and microglia in the mouse hippocampal CA1 sector. Mechanisms of ageing and development, 2007. **128**(4): p. 311-316.

318. Conde, J.R. and W.J. Streit, Microglia in the aging brain. Journal of Neuropathology & Experimental Neurology, 2006. **65**(3): p. 199-203.

319. Sheffield, L. and N. Berman, Microglial expression of MHC class II increases in normal aging of nonhuman primates. Neurobiology of aging, 1998. **19**(1): p. 47-55.

320. Lecours, C., et al., Microglial implication in Parkinson's disease: loss of beneficial physiological roles or gain of inflammatory functions? Frontiers in Cellular Neuroscience, 2018. **12**: p. 282.

321. Butler, B., et al., Dopamine transporter activity is modulated by α-synuclein. Journal of Biological Chemistry, 2015. **290**(49): p. 29542-29554.

322. Swant, J., et al., α-Synuclein stimulates a dopamine transporter-dependent chloride current and modulates the activity of the transporter. Journal of Biological Chemistry, 2011. **286**(51): p. 43933-43943.

323. Vila, M., et al., The role of glial cells in Parkinson's disease. Current opinion in neurology, 2001. **14**(4): p. 483-489.

324. Wyss-Coray, T. and L. Mucke, Inflammation in neurodegenerative disease—a double-edged sword. Neuron, 2002. **35**(3): p. 419-432.

325. Lindeberg, J., et al., Transgenic expression of Cre recombinase from the tyrosine hydroxylase locus. Genesis, 2004. **40**(2): p. 67-73.

326. Turnbull, I.R., et al., Cutting edge: TREM-2 attenuates macrophage activation. The Journal of Immunology, 2006. **177**(6): p. 3520-3524.

327. Kostka, M., et al., Single particle characterization of iron-induced pore-forming α-synuclein oligomers. Journal of Biological Chemistry, 2008. **283**(16): p. 10992-11003.

328. Nuscher, B., et al., α-Synuclein has a high affinity for packing defects in a bilayer membrane a thermodynamics study. Journal of Biological Chemistry, 2004. **279**(21): p. 21966-21975.

329. Deeg, A.A., et al., Anle138b and related compounds are aggregation specific fluorescence markers and reveal high affinity binding to α-synuclein aggregates. Biochimica et Biophysica Acta (BBA)-General Subjects, 2015. **1850**(9): p. 1884-1890.

330. Paxinos, G. and K.B. Franklin, Paxinos and Franklin's the mouse brain in stereotaxic coordinates. 2019: Academic press.

331. Sgobio, C., et al., Optogenetic measurement of presynaptic calcium transients using conditional genetically encoded calcium indicator expression in dopaminergic neurons. PLoS One, 2014. **9**(10).

332. Sgobio, C., et al., Aldehyde dehydrogenase 1-positive nigrostriatal dopaminergic fibers exhibit distinct projection pattern and dopamine release dynamics at mouse dorsal striatum. Sci Rep, 2017. **7**(1): p. 5283.

333. Yorgason, J.T., R.A. España, and S.R. Jones, Demon voltammetry and analysis software: analysis of cocaine-induced alterations in dopamine signaling using multiple kinetic measures. Journal of neuroscience methods, 2011. **202**(2): p. 158-164.

334. KBJ, P.G.F., The mouse brain in stereotaxic coordinates. San Diego: Academic Press, 2001. **200**(1): p. 65-69.

335. Stefanova, N., et al., Microglial activation mediates neurodegeneration related to oligodendroglial α-synucleinopathy: Implications for multiple system atrophy. Movement disorders: official journal of the Movement Disorder Society, 2007. **22**(15): p. 2196-2203.

336. Mezias, C., et al., Neural connectivity predicts spreading of alpha-synuclein pathology in fibril-injected mouse models: Involvement of retrograde and anterograde axonal propagation. Neurobiology of disease, 2020. **134**: p. 104623.

337. El-Agnaf, O.M., et al., Detection of oligomeric forms of α-synuclein protein in human plasma as a potential biomarker for Parkinson's disease. The FASEB journal, 2006. **20**(3): p. 419-425.

338. Anwar, S., et al., Functional alterations to the nigrostriatal system in mice lacking all three members of the synuclein family. J Neurosci, 2011. **31**(20): p. 7264-74.

339. Hunter, R.L., et al., Inflammation induces mitochondrial dysfunction and dopaminergic neurodegeneration in the nigrostriatal system. Journal of neurochemistry, 2007. **100**(5): p. 1375-1386.

340. Surmeier, D.J., J.A. Obeso, and G.M. Halliday, Selective neuronal vulnerability in Parkinson disease. Nature Reviews Neuroscience, 2017. **18**(2): p. 101.

Acknowledgements

I would like to thank Prof. Dr Jochen Herms, for providing me with the possibility to work on this interesting project and the useful suggestions, as well as offering the opportunity to present my work on the international conference.

I furthermore would like to thank Prof. Dr Stylianos Michalakis, who readily agreed to represent my dissertation at the faculty of chemistry and pharmacy. Also, many thanks to my committee members Prof. Dr Gerhard Rammes, Prof. Dr Martin Biel, Prof. Dr Franz Paintner, Prof. Dr Gerhard Winter, for the approval and support of my dissertation.

I would also like to thank Dr Carmelo Sgobio for the precious help in the main part of my project and providing constructive suggestions. Thanks to Dr Sonja Blumenstock for kindly providing and teaching me to generate seeding materials. I also appreciate the help from Dr Yuan Shi for talking about problems of my experiments and useful solutions and thank Dr Finn Peters and Mochen Cui for the support regarding image analysis.

I furthermore acknowledge Dr Kaichuan Zhu, Dr. med. Mario Dorostkar, Dr Elena Montagna, Dr Severin Filser, Jose Medina-Luque, Katrin Prasch, Tanja Blume, Katharina Ochs for the useful discussions. Many thanks to the excellent technical support from Dr. med. vet Gerda Mitteregger, Dr. med. vet Meike Miller, Fang Zhang and Nadine Lachner. I would also like to thank Plexxikon for providing PLX5622. And thanks to all the people who proof-read this dissertation.

Special thanks to the China Scholarship Council and my country for providing me with this valuable opportunity to study abroad and financial support.

Last but not least, to the forever and ever love of my life: my beloved parents, siblings and extended family members, who have always been my support and give me strength. And in memory of my grandpa. I deeply am grateful and love you all.